Determinants of Myofilament Length Dependent Activation

BY

RYAN DANIEL MATEJA
B.S., University of Illinois at Chicago, 2005

THESIS

Submitted as partial fulfillment of the requirements
for the degree of Doctor of Philosophy in Physiology and Biophysics
in the Graduate College of the
University of Illinois at Chicago, 2012

Chicago, Illinois

Defense Committee:

Brenda Russell, Chair
Pieter de Tombe, Advisor
R. John Solaro
Sergey Popov
Kerry McDonald, University of Missouri

This thesis is dedicated to my family and friends for your unconditional love and support.

ACKNOWLEDGMENTS

When I first started graduate school, I never imagined the kind of life-altering and challenging endeavor that I had in store. It is truly amazing to be at the end of this journey and to look back at everyone and everything that has made this experience so unique and special. I would like to thank my Thesis Committee: Dr. Brenda Russell (chair), Dr. Kerry McDonald, Dr. Sergey Popov, Dr. R. John Solaro, Dr. Larry Tobacman and Dr. Pieter de Tombe for your assistance and mentoring. It was invaluable to me to have such knowledgeable and generous role models during my academic career.

To my advisor Dr. Pieter de Tombe, I appreciate everything you have taught me and all your advice along the way. Thank you for providing me with many opportunities and giving me room to grow as a scientist and a person. I can never thank you enough for all you have done. To all my lab mates (past and present), thank you for making work fun and enjoyable. It was wonderful to be around such a great group of people who were always willing to help out, whether it was with lab work or simply providing comedic relief after a day of failed experiments. On that note, thank you especially to my UIC friends Sukriti, Ed, Kelly, Aaron, Pom, Nii, Steve, John and Gerrie; and my Loyola friends Zikiar, Jason, Younns, Beth, Namthip, Taya, and Mohit thanks for all your help and friendship.

To the department staff at UIC and Loyola, we students are so lucky to have such considerate people always there to help out when we spend too much time worrying about our data and not enough about the administrative aspects involved. I would also like to acknowledge Dr. Sadayappan and Dr. Henderson for always being willing to talk about work and life, and helping me figure out what I want to do after I graduate. Thanks also to Slim and Pete, who

were always available to help me fix problems and indulge my many questions regardless of how busy they were.

I could never have reached this goal without the care and love of my friends and family; particularly my parents, my sister, my parents-in-law, and my very large and thoughtful extended family. You have all believed in me during this entire process, and always inspired me to try my best at all times. I feel as if we've reached this moment together. Mom, you've helped me believe that I can accomplish anything, as long as I believe in myself; Dad, you've helped me believe that I can accomplish anything, as long as I work hard. I know these values will continue to help me navigate the next chapters of my life. I owe everything to you both. I am very lucky to have such a great sister. Thank you for always being there and seeing the brightest in me even when I didn't. And thanks also to my in-laws for having faith in me and always providing encouragement.

To my wife, thank you for being my partner during this process, and most importantly, in life. You've always been there for the good times and the bad, which can be difficult when your husband has picked single myofibrils as a thesis project. None of this would have been possible if it wasn't for your unwavering love, support and understanding. I love you.

Finally, thank you to all who have supported me that I have not mentioned, there isn't enough space to write about everyone, but know that I have appreciated it all.

RDM

TABLE OF CONTENTS

TABLE OF CONTENTS (continued)

LIST OF TABLES

LIST OF FIGURES

LIST OF FIGURES

LIST OF ABBREVIATIONS

acto-	Actin
ADP	Adenosine Diphosphate
ATP	Adenosine Triphosphate
ATPase	Adenosine Triphosphatase
ANOVA	Analysis of Variance
BDM	2,3-Butanedione monoxime
Ca^{2+}	Calcium
cTnC	Cardiac troponin C
cTnI	Cardiac troponin I
cTnT	Cardiac troponin T
DTT	Dithiothreitol
EDTA	Ethylenediaminetetraacetic acid
EGTA	Ethylene glycol-bis(β-aminoethylether) N',N',N',N'-tetraacetic acid
ELC	Essential light chain
F_{MAX}	Ca^{2+}-saturated maximal force
fn3	Fibronectin type 3
fsTnC	Fast skeletal TnC
fsTnI	Fast skeletal TnI
HM	Homozygous Mutant
Ig	Immunoglobulin
LDA	Length dependent activation
LDH	Lactate dehydrogenase

Mg^{2+}	Magnesium
MHC	Myosin heavy chain
MLC-1	Myosin light chain type 1
MLC-2	Myosin light chain type 2
MOPS	3-morpholinopropanesulfonic acid
MyBP-C	Myosin binding protein-C
NAD+	Nicotinamide adenine dinucleotide
NADH	The Reduced form of NAD+
P_i	Inorganic phosphate
PAGE	Polyacrylamide gel electrophoresis
PKA	Protein kinase A
PKC	Protein kinase C
RLC	Regulatory light chain
S1	Myosin heavy chain subfragment-1
S2	Myosin heavy chain subfragment-2
SDS	Sodium dodecyl sulfate
S.E.M.	Standard error of the mean
SL	Sarcomere length
ssTnI	Slow skeletal TnI
SR	Sarcoplamic Reticulum
TA	Tibialis Anterior
Tm	Tropomyosin

Tn	Troponin
TnC	Troponin C
TnI	Troponin I
TnT	Troponin T
UV	Ultraviolet
WT	Wild-type

Summary

In order to gain a better understanding of how sarcomere length modulates myofilament contraction, we investigated how long it takes a muscle to form length dependent activation (LDA) and the influence of titin isoform LDA. LDA is the underlying mechanism behind the Frank-Starling law of the heart, which regulates cardiac output to meet the demands of the body on a beat-to-beat basis. Therefore, the experiments described herein were based on understanding two unresolved questions regarding LDA. First, what is the delay between a change in a muscles sarcomere length (SL), and the subsequent alteration of cross-bridge cycling? Previously, this delay was estimated at ~100 ms in rabbit myocardium, but those experiments were not designed to specifically measure how long it takes LDA to form. Second, what are the myofilament contractile consequences of expressing a longer isoform of titin? The extent of LDA exhibited in a muscle is related to the titin isoform present; preparations that have increased titin-based stiffness also exhibit increased LDA. Therefore, determining the kinetics of LDA and the influence of titin isoform size will provide insights into the mechanisms underlying the phenomenon by which a change in SL alters cross-bridge cycling.

Accordingly, to measure if there is a delay between a change in SL and subsequent cross-bridge cycling, it was important to insure that the muscle was quickly and homogenously activated immediately following a rapid length change. This was accomplished by quickly activating single cardiac myofibrils following a rapid length change and comparing its force development to a myofibril which did not undergo a rapid length change. To increase our chances of detecting such a small delay we performed experiments at 15°C and used guinea-pig myocardium, which contains almost exclusively the slower β-isoform of myosin. Additionally, by using a photomultiplier tube we were able to time solution switch from low [Ca^{2+}] relaxing

solution to high [Ca^{2+}] activating solution so that it occurred precisely at the completion of the rapid length change. We found there was no measurable delay in activation kinetics and submaximal force for length changes as fast as 5 ms, suggesting that LDA occurs nearly instantaneously.

Next, we determined the effect of titin isoform expression on LDA. Traditionally, when measuring the effect of titin isoform, tissues naturally expressing different isoforms are compared. One caveat to this approach is that in addition to altered titin expression, theses tissues also express different isoforms of other contractile proteins, making it difficult to determine the specific consequences of a longer titin isoform alone. Thus, to measure the impact of titin isoform alone, we utilized a recently developed rat which has a homozygous autosomal mutation (HM) that cause preferential expression of a giant titin isoform and assessed the extent of LDA in these preparations compared to wild-type (WT) preparations. We found that expression of a longer titin isoform in skeletal muscle reduced passive tension, maximal active tension, maximal ATPase, tension cost and Ca^{2+} sensitivity compared to WT preparations. Furthermore, the SL-dependence of these measurements were reduced in HM muscles compared to WT. Single myofibril experiments were performed to assess activation and relaxation kinetics, which showed that expression of a longer titin isoform reduces activation kinetics but did not affect relaxation kinetics. Because LDA is most prominent in cardiac muscle, we also determined the influence of titin isoform expression on force development in trabeculae. Similarly, HM muscles exhibited a decrease in maximal force and Ca^{2+} sensitivity, and the SL-dependence of these parameters were blunted. Therefore, we established that expression of a longer titin isoform attenuates LDA.

Summary (continued)

Thus, these experiments provide evidence that LDA forms nearly instantaneously following a change in muscle length and that the degree of LDA exhibited is dependent on the titin isoform present in the muscle. We hypothesize that LDA arises from titin-strain mediated geometric rearrangement of thick and thin filament contractile proteins.

Determinants of Myofilament Length Dependent Activation

Ryan D. Mateja Ph.D.
Department of Physiology and Biophysics
University of Illinois at Chicago
Chicago, Illinois (2012)

Myofilament length-dependent activation (LDA) is a universal property of striated muscle, yet the molecular mechanisms that underlie it are incompletely understood. LDA is characterized by an increase in both maximal Ca^{2+}-activated force (F_{max}) and calcium sensitivity upon an increase in sarcomere length (SL). My first aim was to determine the dynamic rate by which a change in SL is sensed and then transduced to the myofilaments. We employed the rapid solution-switch single myofibril technique which allows for the study of contraction activation/relaxation dynamics in the virtual absence of diffusion delays. We compared submaximal contraction kinetics at steady-state SL with contractions following rapid SL ramps to that same SL just prior to activation. Neither the activation/relaxation kinetics nor final submaximal force development was significantly different between the two contraction modes for SL ramps as fast as 5ms. We concluded that the transduction of the length signal by the cardiac sarcomere to modulate thin filament activation levels occurs virtually instantaneously.

The giant protein titin spans the entire sarcomere, transducing strain between the myofilaments. Additionally, the magnitude of LDA exhibited in striated muscle has been shown to vary with titin isoform length. Recently, a rat that harbors a homozygous mutation (HM) causing preferential expression of a longer titin isoform was discovered. Accordingly, my second aim was to investigate the role of titin isoform length on the magnitude of LDA exhibited in striated muscle. We measured myofilament force development and cross-bridge cycling kinetics as a function of SL in tibialis anterior and trabeculae isolated from wild-type (WT) and HM rats. SL-dependent changes in passive tension, F_{max}, calcium sensitivity, and ATP consumption were

attenuated in HM skeletal muscles. HM trabeculae exhibited a reduction in SL-dependent changes in F_{max} and calcium sensitivity compared to WT. Additionally, activation kinetics were reduced in skeletal HM myofibrils compared to WT, while relaxation kinetics were not affected. We established that the presence of a long titin isoform is associated with reduced myofilament force development and cross-bridge cycling kinetics, and a blunting of LDA. In conclusion, LDA develops virtually instantaneously, possibly from titin-strain mediated geometric rearrangement of thick and thin filament contractile proteins.

I. INTRODUCTION

A. Preface

In 1866 the first isolated perfused heart preparation was used at Carl Ludwig's Physiological Institute at Leipzig, a technique which was later used to investigate the relationship between ventricular pressure and pump function of the heart independently by Otto Frank and Ernst Starling (Zimmer 2002). Working independently, their experiments described the phenomenon which is collectively referred to as Frank-Starling's Law of the Heart. Although Frank and Starling experimented on cardiac muscle, they understood their results were similar to experiments investigating the variation of active force in skeletal muscle as a function of length (Blix 1892). These works describe a fundamental property of striated muscle, that upon an increase in sarcomere length a muscle will exhibit increased tension generating capacity. This property is termed length dependent activation and will be the major focus of my thesis.

I will begin this section with a brief background of striated muscle physiology, which will include descriptions of the basic structure and function of the smallest unit of contraction, the sarcomere. Next I describe a major topic of my thesis, the influence of sarcomere length on muscle contraction and the proposed molecular mechanisms behind this regulation. This is followed by a brief examination of the kinetics of contraction, with a special focus on the advantages of the rapid solution-switching single myofibril technique. Lastly, I present my major conclusions and how they provide a foundation for the specific aims of my thesis.

B. The Sarcomere

Originally, the term "striated muscle" was adopted for any muscle that was made up of parallel fibers and was mainly used to distinguish between skeletal and smooth muscle. Later,

the definition of striated muscle was expanded to include cardiac muscle. Although they are technically different types of tissue, structurally, cardiac and skeletal muscle are very similar. When striated muscle is viewed under a microscope, long chains of repeating sarcomeres appear as light and dark bands. The darker band was named the A-band (anisotropic) and contains the entire length of a single thick filament. The lighter band was named the I-band (isotropic) and is the part of the sarcomere that does not contain the darker thick filament, and therefore is mostly made up of thin filament proteins. The boundary separating two neighboring sarcomeres is called the Z-disk, and can be seen as a dark line in between adjacent I-bands. The two predominant proteins in a sarcomere are myosin and actin, which make up the majority of the thick and thin filament, respectively (Figure 1).

1. The Thick Filament

The thick filament is approximately 1.65 um long, and is mainly comprised of the motor protein myosin II (Gordon, Homsher et al. 2000). Each myosin molecule is made up of two heavy chains and four light chains. Each myosin heavy chain consists of a filamentous rod-like tail structure, a flexible hinge region (subfragment 2, or S2), and a globular head (subfragment 1, S1) that binds actin forming the cross-bridges required for force production. The arrangement of the two heavy chains of myosin is similar to that of a caduceus, with the myosin S1 globular head domains projecting outwards and held together by the tail structure, which forms a parallel coiled-coil. The polymerization of the rod domains of the myosin molecules makes up the backbone of the thick filament, which assembles in an antiparallel, bipolar fashion with the myosin heads projecting out from the center of the thick filament

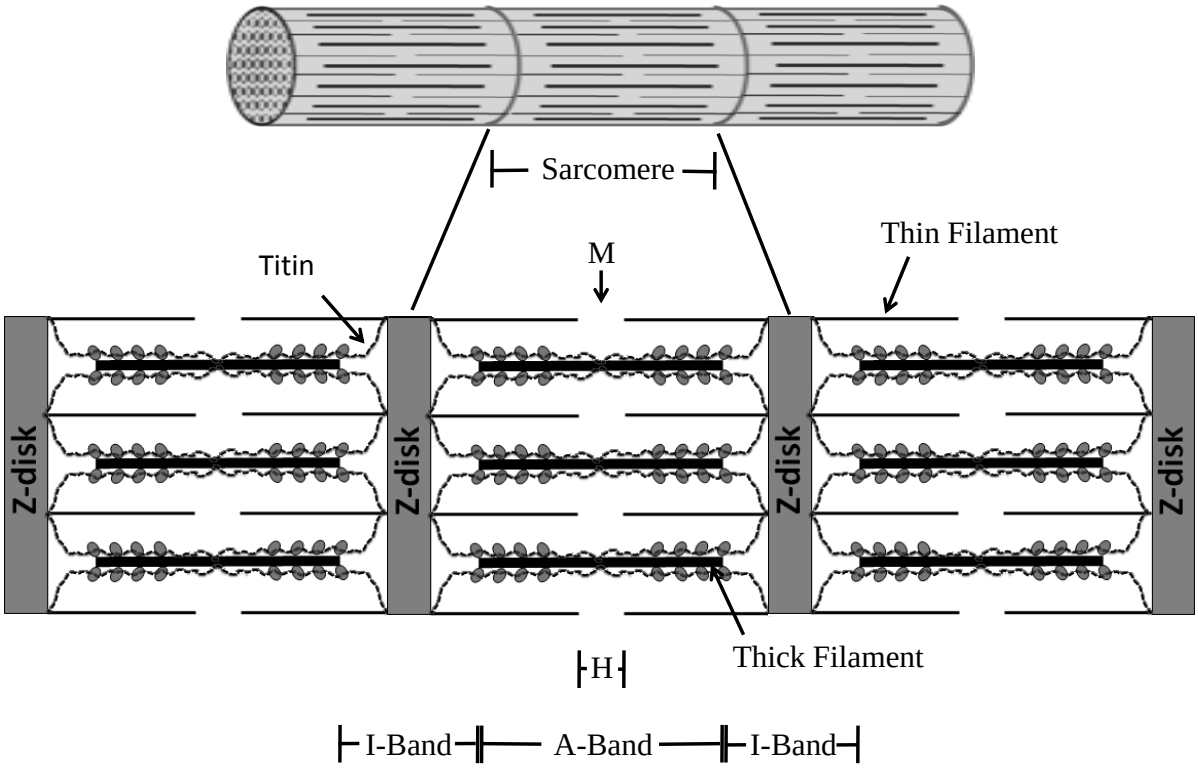

Figure 1. The Sarcomere. On top is a single myofibril, which is essentially sarcomeres in series. The bottom shows three sarcomeres. The A-band is the region of the sarcomere which is occupied by the thick filament. The I-band lacks the thick filament and is made up mostly of thin filament proteins. The M-line is the center of the thick filament, which does not contain any myosin heads. The H-zone is the region between the thin filaments, occupied only by the thick filament. Titin extends from the M-line to the Z-disk.

(Huxley 1963). This arrangement necessitates that the center of the filament to only be comprised of tail regions, and is termed the H-zone. The myosin S1 fragments, which contain the enzymatic and motor domains required for contraction, extend radially from the thick filament backbone. The heads are helically arranged around the thick filament with a 14.3 nm repeat between paired heads, and every third head projects outward in the same direction. Therefore, there are approximately 43 nm between heads that face the same direction, or that could potentially form crossbridges on the same actin filament (Gordon, Homsher et al. 2000).

Each myosin S1 contains a motor domain, which includes an actin binding site and an ATPase catalytic site that allows the energy released from ATP hydrolysis to power contraction. The motor domain of the S1 is connected to the tail region through a flexible "hinge" S2 region, which plays a vital role in allowing movement of the head during the power stroke to induce shortening of the sarcomere. Experiments using single myosin molecules have shown that the throw of a single head averages 11 nm and produce ~3 – 4 pN under conditions of low loads (Finer, Simmons et al. 1994). The neck region is stabilized by non-covalent association with two myosin light chains (Rayment 1996).

There are two myosin light chains (MLC) associated with the head region of each myosin dimer, a regulatory light chain (RLC, or MLC-2) and an essential light chain (ELC, or MLC-1) (Schaub, Hefti et al. 1998). The RLC is named "regulatory" because in smooth muscle phosphorylation of this light chain initiates contraction (Adelstein and Eisenberg 1980). The ELC is named from experiments that showed it was "essential" for myosin to be able to hydrolyze ATP, but further experimentation showed this original hypothesis to be incorrect (Wagner and Giniger 1981; Sivaramakrishnan and Burke 1982). While the ATPase activity of

isolated myosin is not affected by the presence or absence of either light chain, they play an important role in modulating contraction.

Myosin binding protein C (MyBP-C) is another thick filament protein that is involved in thick filament assembly and has roles in cross-bridge cycling (Stelzer, Patel et al. 2006) and length dependent activation (Muhle-Goll, Habeck et al. 2001). It is found in the A-band of the sarcomere, positioned 43 nm apart (Flashman, Redwood et al. 2004). Phosphorylation of MyBP-C by PKA increases the order of myosin heads and extends them away from the thick filament backbone, towards the thin filament (Levine, Weisberg et al. 2001). Increasing the level of phosphorylation increases the Ca^{2+} sensitivity of force and maximum Ca^{2+}-activated force (McClellan, Kulikovskaya et al. 2001). It is thought that this is due to the phosphorylation interrupting the interaction between MyBP-C and the hinge region of the myosin head, allowing them to more easily interact with actin, which is supported by the electron microscope data. Mutations in MyBP-C gene can cause familial hypertrophic cardiomyopathy, and to date there are over 150 mutations that have been published (Richard P 2006). Mice that have had their cardiac function compromised show a decrease in total MyBP-C phosphorylation. Furthermore, mice that have had the phosphorylatable serines replaced by alanines to mimic the dephosphorylated state of MyBP-C exhibited depressed cardiac contractility (Sadayappan, Gulick et al. 2005). Overall, MyBP-C is important in thick filament assembly and is essential for normal cardiac function, as exhibited by the large number of mutations that cause familiar hypertrophic cardiomyopathy.

2. The Thin Filament

The thin filament backbone is made up of actin, which spontaneously polymerizes under physiological conditions into a coiled-coil strand that extends from the Z-disk towards the center of the sarcomere. Each actin monomer is made up of four smaller subdomains, numbered 1 through 4 (Tobacman 1996). The myosin binding site is on subdomain 1, which along with subdomain 2 lies on the outer edge of the filament (Holmes, Tirion et al. 1993). The two larger subdomains (3 and 4) lie closer to the interior of the actin filament. When exposed, the myosin binding sites on actin allow the formation of cross-bridges, and therefore force production. Without any other proteins and in the presence of ATP, actin and myosin continually hydrolyze ATP and sustain cross-bridge cycling. Regulation of thin filament activation comes from two other proteins, tropomyosin and troponin. Tropomyosin and troponin are positioned along the thin filament at regular intervals of 7 actin, which together make up a "functional unit". A functional unit is the smallest size of the thin filament which maintains the appropriate stoichiometry of 7:1:1 (actin:tropomyosin:troponin).

Tropomyosin (Tm) is made up of two α-helical chains arranged in a coiled coil that spans approximately seven actin monomers along the thin filament. Adjacent Tm overlap in a head-to-tail configuration, which is thought to play a role in both the cooperativity of activation and assist in stabilizing Tm binding to actin (Mak and Smillie 1981). In resting muscle, Tm covers the myosin binding site, inhibiting the formation of myosin cross-bridges. Upon Ca^{2+}-dependent activation, Tm moves out of the major grove of actin and exposes myosin binding sites over several actins, relieving inhibition of cross-bridge formation. In vertebrates, there are three highly homologous major Tm isoforms that incorporate into the sarcomere: α,β and γ (Wolska and Wieczorek 2003). The isoforms do show muscle and developmental specificity, with α-Tm

being the predominant isoform expressed in both the heart and skeletal muscle (Pieples and Wieczorek 2000).

The troponin (Tn) complex is the main regulatory site of thin filament activation. The complex is made up of three subunits, each one named after its first discovered properties; the Ca^{2+}-binding TnC, inhibitory TnI, and tropomyosin-binding TnT (Tobacman 1996; Gordon, Homsher et al. 2000). Because troponin C (TnC) is the Ca^{2+} binding subunit, it is the main Ca^{2+} regulator of the thin filament. TnC is dumbbell shaped, made up of two globular domains which are connected by a long central helix (Gagne, Tsuda et al. 1995). Each globular domain has two metal-binding EF-hand motifs, making four total binding sites (named sites I through IV, according to their order in the primary structure) for either Mg^{2+} or Ca^{2+} (Tobacman 1996). Sites III and IV reside in the COOH-terminus and are considered structural rather than regulatory and have a high affinity for Ca^{2+} and Mg^{2+}. In these sites, the binding of divalent cations is important in the binding of TnC to the thin filament, most likely by enhancing TnC-TnI interaction (Zot and Potter 1982). Sites I and II are both low affinity sites, and are the regulatory sites responsible for Ca^{2+} activation in skeletal muscle. Evidence of this comes from studies using mutated TnC's that show inhibited actomyosin ATPase even in the presence of Ca^{2+} when sites I and II are disrupted (Sorenson, da Silva et al. 1995). Cardiac TnC (cTnC), found in both cardiac and slow skeletal muscle, is only regulated by Ca^{2+} binding to site II. Due to amino acid substitutions, site I lacks the amino acid sequence required for Ca^{2+} binding. As expected, elimination of Ca^{2+} binding to site II renders cardiac and slow skeletal fibers insensitive to Ca^{2+} activation. Only having a single binding site is also thought to contribute to the lower cooperativity exhibited in preparations containing cTnC compared to fsTnC (Piroddi, Tesi et al. 2003). Activation of the thin filament begins when Ca^{2+} released from the sarcoplasmic

reticulum binds to TnC, exposing a hydrophobic surface that interact with TnI (Herzberg, Moult et al. 1986).

Troponin I (TnI) is the subunit that is responsible for inhibiting actomyosin interaction in a Ca^{2+} dependent, reversible manner. There are three isoforms of TnI: fast skeletal (fsTnI), slow skeletal TnI (ssTnI), and cardiac TnI (cTnI). In the absence of the other Tn subunits and Tm, the introduction of TnI alone is enough to inhibit myosin binding to actin (Syska, Wilkinson et al. 1976). In fact, not even the entire TnI subunit is needed to inhibit cross-bridge formation, but only a specific fragment of TnI known as the inhibitory peptide. This inhibitory fragment was originally thought to consist of residues 96-116 (Syska, Wilkinson et al. 1976), but further experimentation showed that only residues 104-115 were necessary for inhibition (Van Eyk and Hodges 1988). There is only one difference in the inhibitory peptide between ssTnI and cTnI, cardiac muscle has a threonine (Thr144) whereas slow skeletal muscle has a proline (Pro110) in the corresponding position. Recent studies have shown that this particular amino acid difference alone might play a role in conferring the increased amount length dependent activation exhibited in cardiac muscle compared to fast skeletal (Tachampa, Wang et al. 2007; Tachampa, Kobayashi et al. 2008). Additionally, the threonine in cTnI can be phosphorylated by protein kinase C (PKC), but the functional consequences of this phosphorylation is not fully settled (Kobayashi, Jin et al. 2008). In relaxed muscle, TnI tightly binds to actin, and in concert with TnT maintains the position of tropomyosin, blocking actomyosin interaction. As mentioned earlier, Ca^{2+} binding to TnC exposes a hydrophobic patch on TnC. This causes the inhibitory region of TnI to lower its affinity for actin and bind to TnC.

Troponin T (TnT) is the subunit that is responsible for anchoring the Tn complex to actin through binding to Tm and actin (Tobacman 1996). It has an elongated-rod like structure which

is longer in cardiac muscle (20.5nm) than skeletal muscle (18.5nm) (Flicker, Phillips et al. 1982; Cabral-Lilly, Tobacman et al. 1997). TnT's COOH-terminal interacts with TnI and TnC, while the NH_2-terminal is long enough to interact with Tm where adjacent Tm overlap (Farah and Reinach 1995). Interestingly, the addition of TnT to reconstituted fibers increases actomyosin ATPase activity in the presence of Ca^{2+} and increases inhibition in the absence of Ca^{2+} (Greaser and Gergely 1971; Malnic and Reinach 1994). The fact that TnT interacts with the region of adjacent Tm overlap and spreads both activation and inhibition in a Ca^{2+} dependent manner suggests that it is involved in cooperative activation of the thin filament. The extended NH_2-terminal found in cTnT that is absent in skeletal TnT is important in determining the length of a functional unit, since in fibers lacking this region show increased TnT-Tm binding, decreased maximal force, and an increase in the rate of cross-bridge cycling and recruitment kinetics (Chandra, Montgomery et al. 1999; Chandra, Tschirgi et al. 2006). cTnT is targeted by various PKC isozymes, where phosphorylation results in reduced cross-bridge cycling dynamics, possibly by reducing thin filament activation (Sumandea, Pyle et al. 2003; Sumandea, Burkart et al. 2004).

3. **Titin**

Titin, originally called connectin, is the third most abundant protein in muscle and named because of its massive size (~2900 – 3700 kDa). It spans each half sarcomere from the Z-disk to the M-band, and due to overlapping of adjacent molecules, titin effectively forms a continuous filament along an entire myofibril (Obermann, Gautel et al. 1996; Tskhovrebova and Trinick 2003). The distinguishing characteristic of titin is its high degree of elasticity; the stretching and shortening of titin regulates sarcomere length (SL) and muscle function. Within

physiological SL's in both skeletal and cardiac muscle, titin bears nearly all of the passive tension exhibited (Horowits, Kempner et al. 1986; Greaser, Krzesinski et al. 2005).

Titin mainly consists of two types of domains, fibronectin type 3 (fn3) modules and immunoglobulin-like (Ig) domains. The A-band region of titin is inextensible and is made up of super-repeats of Ig and fn3 domains (Labeit and Kolmerer 1995). The elasticity of titin comes from the stretching of the extensible regions located in the I-band area. This area consists of tandemly arranged Ig-like domains, PEVK segments (rich in proline [P], glutamate [E], valine [V], and lysine [K]) and an N2 region (containing either N2B or N2A unique amino acid sequences) (Labeit and Kolmerer 1995). Alternative splicing of titin's mRNA results in isoforms with varying I-band lengths that have different stiffness. Since titin acts as a "molecular spring" that provides a restoring force when a muscle is stretched, longer titin isoforms produce lower passive tensions for a given change of SL.

Titin exists as multiple isoforms whose expression levels can be adjusted to finely tune the amount of titin-based passive stiffness during cardiac development and disease. Titin isoforms are largely differentiated by the components, and therefore the length, of their N2 sequence. Striated muscle contains two unique N2 sequences, a cardiac specific N2B sequence, and due to having more Ig domains and a longer PEVK region, a longer N2A sequence that can be found in both cardiac and skeletal muscle (Labeit and Kolmerer 1995). Even though skeletal muscle contains only the N2A region, it still expresses two titin isoforms; a longer isoform that is found in slow skeletal muscle, and a shorter isoform that is found in fast skeletal muscle. The longer titin isoforms found in slow skeletal muscles produce lower passive tension for a given change in SL than the shorter isoform expressed in fast skeletal muscle (Neagoe, Opitz et al. 2003). Cardiac muscle expresses a shorter N2B isoform and a longer N2BA isoform, which the

latter is comprised of both the N2B and N2A sequences. The additional N2A sequence in the N2BA isoform essentially adds another elastic element, allowing for lower passive tensions at all SL's in tissues that preferentially express the longer N2BA isoform.

C. **Contraction**

Luigi Galvani demonstrated that a jolt of static electricity to precisely the right spot, an exposed sciatic nerve of a frog, made the frog's legs jump as if they were alive. A quarter century prior to Galvani's experiments the basics of electricity were just beginning to unfold, which established that similar particles would repel each other while being attracted to different particles. Therefore, it was not a large jump in logic to assume that muscle contraction was due to an attraction between some kind of similar particles (Johnson 2008). These theories existed for over 50 years, until Theodor Schwann showed that if a muscle was shortened prior to being stimulated it produced less force than if stimulated at the same length that it was found in the body (Needham 1971). Because the attraction between two similar particles increases as they get closer together, this landmark experiment ruled out any theories of muscular contraction that depended on the attraction between particles. Schwann's experiments lead people to believe that muscle could be considered as obeying the law governing elastic bodies, meaning it followed Hookean physics and behaved like a stretched spring (Weber 1846).

If muscle acted like a spring, the amount of energy released during a contraction would be independent of its load. In an attempt to calculate the efficiency of work production in skeletal muscle, Wallace Fenn determined the relationship between the amount of heat liberated from a muscle to the amount of work performed. By changing the load on the muscle during contraction, he showed that the total amount of energy released by a muscle varies with the work

performed, which is now known as the “Fenn effect” (Fenn 1923). At this time, the most prominent theory of muscle contraction was that shortening was due to the folding of asymmetrical molecules (Katz and Lorell 2000).

It wouldn’t be until the 1950’s that the folding premise of contraction would be supplanted by the current sliding filament theory, which suggests that rather than fold, force and shortening occur when the myofilaments slide past each other (Huxley 2000). The sliding filament theory was developed independently by two groups. By using electron microscopy and x-ray diffraction, H.E. Huxley and Jean Hanson showed that the length of the different myofilaments did not change when muscle shortens (Huxley 1953; Huxley 1953; Huxley and Hanson 1954). Around the same time using interference microscopy, A.F. Huxley along with R. Niedergerke demonstrated that during contraction the length of the A-band remained constant, while the size of the I-band and H-zone decreased (Huxley and Niedergerke 1954). It was proposed that the filaments slide past each other due to small projections of myosin that would attach to actin, termed cross-bridges (Huxley 1957). Electron micrographs from longitudinal sections of skeletal muscle so thin that they only include myofilaments from a single layer clearly showed these cross-bridge projections (Huxley 1957). Support that cross-bridges contain an elastic element (initially proposed by (Huxley 1957)) and tension was generated by tilting of the myosin head came from measuring non-linearities in tension recordings following small rapid length changes (Huxley and Simmons 1971). Understanding of how the filaments slide past each other was further clarified by the notion that cross-bridges were uniformly distributed between the filaments and generated force independently of each other (Huxley 1988). It is now known that force production occurs when a myosin cross-bridge binds to actin, a tilting of the myosin head (stretching the elastic element) generates force, and then myosin detaches.

In the following sections I will describe the current understanding of muscle contraction. Muscle contraction can be broken down into three steps: an initial electrical stimulus which causes an increase in intracellular Ca^{2+}, Ca^{2+} activation of the thin filament, and finally cross-bridge attachment and cycling which ultimately leads to force generation.

1. Excitation-Contraction Coupling

Excitation-contraction coupling is a term coined in 1952 by Alexander Sandow to describe the events between a stimulus or excitation of the sarcolemma, and the subsequent contraction (Sandow 1952). The process of excitation-contraction coupling is similar in both cardiac and skeletal muscle, so only the major differences will be noted. In either tissue type, excitation-contraction coupling begins with an action potential that depolarizes the sarcolemma, originating from either pacemaker cells in the sinoatrial or atrioventricular nodes in cardiac muscle, or an alpha-motor neuron in the case of skeletal muscle. The depolarization travels along transverse tubules that contain voltage-dependent Ca^{2+} channels. The manner in which the voltage-dependent calcium channels cause Ca^{2+} release from the sarcoplasmic reticulum (SR) is the most prominent difference between cardiac and skeletal muscle excitation-contraction coupling. The cardiac sarcolemma contains dihydropyridine receptors that allow entry of a relatively small amount of Ca^{2+} into the cell. This causes the ryanodine receptors in the SR membrane to release Ca^{2+}, increasing the cytosolic $[Ca^{2+}]$ more than 100 fold. Because the Ca^{2+} release from the SR by the ryanodine receptors is triggered by Ca^{2+}, this process is called calcium-induced calcium release (Fabiato 1983). In skeletal muscle, the dihydropyridine receptors are mechanically linked to the ryanodine receptors. Depolarization of the sarcolemma causes a conformational change in the in the dihydropyridine receptors, which activates the

ryanodine receptors, allowing Ca^{2+} to flow from the SR into the cytosol. It is this increase in cytosolic Ca^{2+} that binds TnC starting the cascade of events which activates the thin filament and ultimately allows contraction.

In order for relaxation to occur, intracellular Ca^{2+} needs to decline, which allows Ca^{2+} to dissociate from TnC and Tm to move back into the groove of actin which inhibits cross-bridge formation. The majority of intracellular Ca^{2+} is removed by the SR Ca^{2+}-ATPase, which uses ATP to move calcium up its concentration gradient into the SR. Additionally, Ca^{2+} is transported out of the cell back into the extracellular fluid by the sarcolemmal Na^{+}/Ca^{2+}-exchanger (Blaustein and Lederer 1999).

2. **Thin Filament Activation**

When muscle is relaxed, or in diastole, intracellular calcium ($[Ca^{2+}]_i$) is approximately 0.1 µM, which is not a sufficient concentration to promote Ca^{2+} binding to TnC. In the absence of Ca^{2+} binding, cTnI strongly binds to actin and Tm is blocking the myosin binding site on actin, inhibiting strong cross-bridge formation. It was hypothesized early on that Tm might rest in a position on actin which inhibited cross-bridge formation (Gordon, Homsher et al. 2000). Then, with the theory that Ca^{2+} binding to TnC initiated the Tm transition, a two-state model for the "steric blocking" model of regulation was constructed (Hitchcock, Huxley et al. 1973). In general, the two state model states that in the absence of Ca^{2+} binding, Tm physically covers the myosin binding sites on actin, inhibiting cross-bridge formation. Upon Ca^{2+} binding, Tn allosterically regulates Tm uncovering the myosin binding sites allowing actomyosin interaction.

It was not very long until studies began to suggest that the simple two-state steric blocking model was not sufficient to explain regulation of contraction. Studies measuring high-frequency stiffness of muscles at low [Ca^{2+}] indicated that myosin binding to the thin filament might occur even in diastole (Brenner, Chalovich et al. 1986). Now, it is known that although Tm is sterically blocking myosin from strongly binding to actin, weak-binding cross-bridges exist, which very rapidly and transiently bind the thin filament in a non-force generating way (Holmes 1995). Additionally, discovery of the crystal structure of both actin (Kabsch, Mannherz et al. 1990) and myosin (Rayment, Holden et al. 1993) allowed more intense investigation of the interaction between actin and myosin on the level of individual amino acids. Currently, a more complex three-state model of thin filament regulation has supplanted previous models.

The three state-model states that Tm exists in one of three positions on actin; blocked, closed, and open (McKillop and Geeves 1993). In this model, in the absence of Ca^{2+}, Tm exists in the "blocked" state and does not allow myosin to strongly bind actin. Myosin can electrostatically interact with the thin filament though, forming the previously mentioned non-force generating weakly bound cross-bridges. Calcium binding to TnC allows Tm to move ~25° around actin into the "closed" position (Vibert, Craig et al. 1997; Xu, Craig et al. 1999). Tm moving from the blocked to closed position exposes additional sites for interaction between myosin and actin, without fully uncovering myosins binding site. Upon the binding of a myosin cross-bridge, Tm moves an additional 10° around actin, into the "open" state. Overall, Ca^{2+} only partially activates the thin filament, and myosin binding is required to fully activate the thin filament.

3. Cross-Cridge Cycle

In the presence of Ca^{2+} and ATP, myosin cross-bridges will continuously bind to actin, hydrolyze ATP and generate force by going through the steps of the cross-bridge cycle. Figure 2 shows a modern version of the cross-bridge cycle, consisting of 6 steps. As the individual steps are delineated, it is important to keep in mind that the "cross-bridge cycle" is simply the path of actomyosin interaction that is most kinetically favorable and that each step can be reversed or go through a less likely, slower transition between states.

Prior to Ca^{2+} binding, myosin is in the "cocked" position and retains the products of MgATP hydrolysis, ADP and inorganic phosphate (P_i). In this state, myosin only transiently forms weak binding cross-bridges with actin. The first step is regulated by Ca^{2+} and occurs when Ca^{2+} binding to TnC allows Tm to move into the closed state (step 1). With Tm in the closed state, myosin can transition from a weakly bound state to being strongly bound. This transition is closely coupled to an isomerization of the myosin head (Geeves and Lehrer 1994) and the release of P_i (Zhao and Kawai 1994) (step 2). The conformational change of the myosin head is commonly referred to as the "power stroke" and involves an extension of myosins "lever arm" that connects the motor domain to the rod portion. The extended lever arm of myosin pulls actin inwards towards the M-line, and is the force producing step in the cross-bridge cycle (step 3). Recent studies in single myofibrils have indicated that the force generating isomerization of myosin immediately precedes the release of Pi (Tesi, Colomo et al. 2002). Force generation is maintained until ADP is released (step 4). After the release of ADP, actin and myosin are in the strong binding "rigor" formation, until a new ATP binds to myosin, allowing it to detach from actin (step 5). When detached, myosin hydrolyzes the ATP, using the energy released to

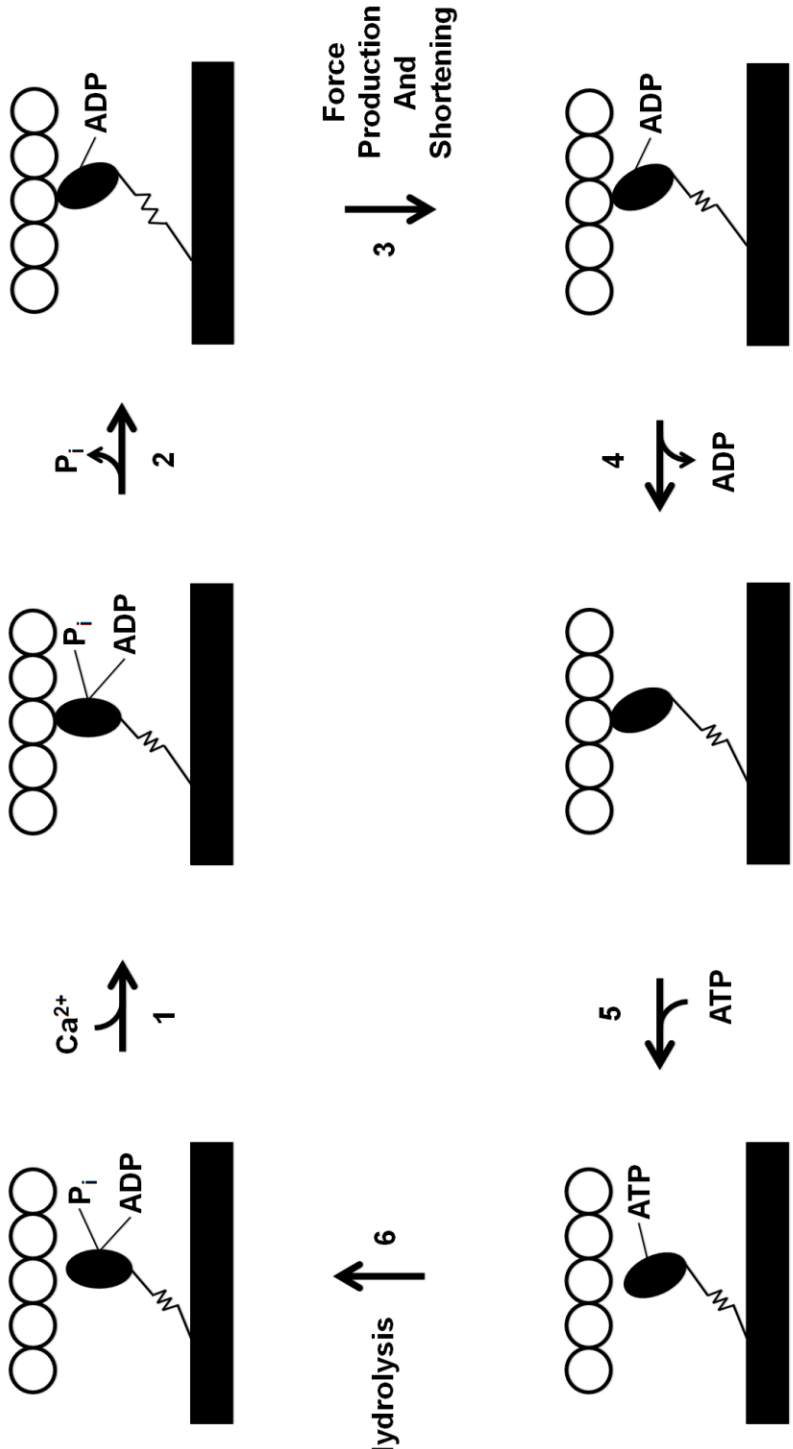

Figure 2. The steps of the cross-bridge cycle in striated muscle. Refer to the text for an explanation of the individual steps.

transition back into the "cocked" state (step 6). The probability that the myosin head will undergo another cycle is dependent on the activation level of the thin filament.

D. **Cooperativity**

Myofilament activation is a highly cooperative process, meaning that the increase in isometric force for a given amount of activating Ca^{2+} is much too steep to be due to Ca^{2+} binding alone (Hellam and Podolsky 1969; Julian 1969). This can be seen when the sigmoidal relationship between $[Ca^{2+}]$ and force can is fit with a modified Hill equation which states:

$$\frac{F}{F_{max}} = 1 + 10^{[n_H(pCa_{50} - pCa)]}$$

where F_{max} is the maximal force, F is the steady-state force, n_H is the hill coefficient, and pCa_{50} is the $-\log[Ca^{2+}]$ where F is 50% of F_{max}. Here, the hill coefficient is a measurement of the amount of cooperativity, and the pCa_{50} is an index of the Ca^{2+} sensitivity of the muscle. Figure 3 shows an example of a Hill fit (top) and Hill fits that show altered cooperativity or Ca^{2+} sensitivity (bottom). If there was no cooperativity, n_H would equal 1, meaning Ca^{2+} controls force in a one-to-one basis. Depending on the experimental conditions, n_H values as low as 2, and as high as 6 have been reported for skeletal and cardiac muscle (Brandt, Cox et al. 1980; Brandt, Diamond et al. 1987; Dobesh, Konhilas et al. 2002).

Cooperativity arises when the activation of one functional unit, either by Ca^{2+} or by strong binding cross-bridges, influences the probability that a neighboring functional unit will be activated. Cooperativity can exist in either a positive feed forward mechanism that increases thin filament activation, or in a negative feedback deactivating mechanism which inhibits thin filament activation. There are many possible sources of cooperative activation, such as Ca^{2+}

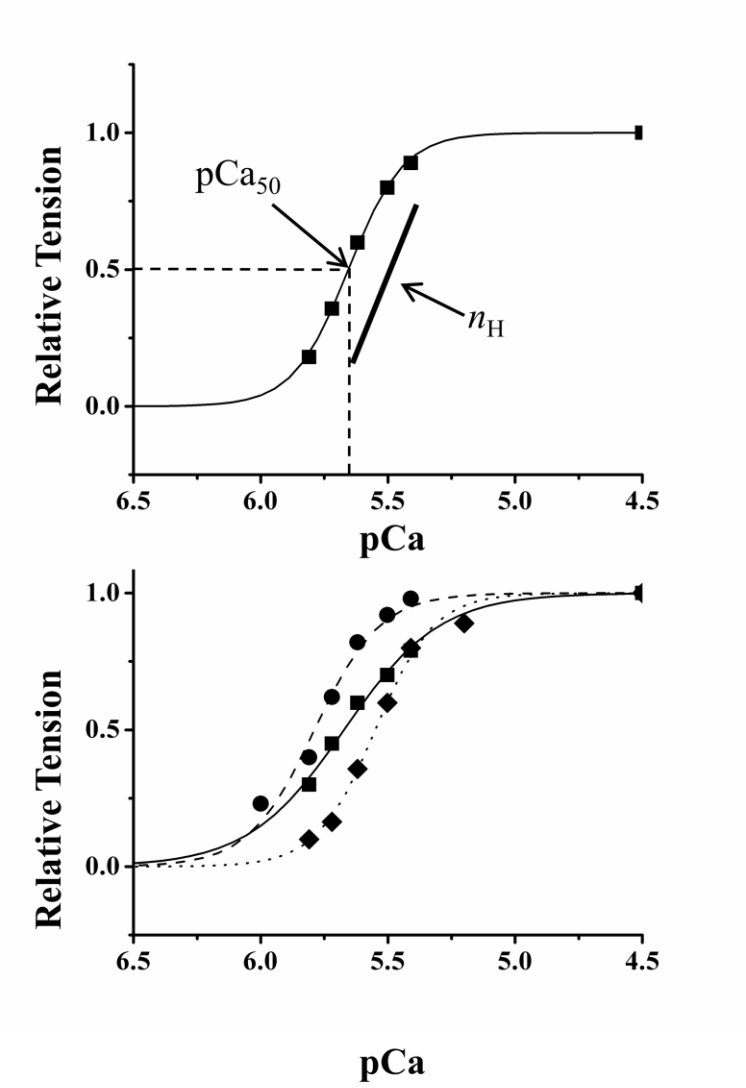

Figure 3. Examples of Hill fits to force-[Ca^{2+}] relationships. Top panel shows the Hill coefficient (n_H) and the pCa_{50}. n_H is the slope of force-[Ca^{2+}] relationship, and is used as a measurement of cooperativity. pCa_{50} is the amount of calcium required to produce 50% of F_{max}, and is an index of Ca^{2+} sensitivity. The bottom panel shows examples of reduced cooperativity (solid line, squares), increased Ca^{2+} sensitivity (dashed line, circles) and reduced Ca^{2+} sensitivity (dotted line, diamonds).

binding to one TnC influencing the probability that a neighboring TnC will bind Ca^{2+} (Butters, Tobacman et al. 1997). Studies using fluorescent probes have shown cooperativity of Ca^{2+} binding along the thing filament (Grabarek, Grabarek et al. 1983; Tobacman and Sawyer 1990). The previously mentioned overlap region between the head and tail regions of neighboring Tm's most likely plays a role in the spread of cooperativity between functional units (Pan, Gordon et al. 1989). Additionally, the two low affinity Ca^{2+} binding sites in skeletal TnC is another source of cooperativity, which is not present in cardiac muscle. When cardiac TnC is replaced by skeletal TnC in cardiac preparations, cooperativity increases (Babu, Scordilis et al. 1987). Although recent experiments have suggested this not to be true (Moss, Nwoye et al. 1991); the level of cooperativity provided by TnC remains controversial.

Another source of cooperativity occurs when a strong binding cross-bridge influencing the probability that another cross-bridge will bind in either its own functional unit, or a neighboring functional unit. In the three-state model of thin filament activation, the strong binding of a cross-bridge is required to move Tm into the open state and fully turn on a regulatory unit. In the absence of ATP, the cooperative spread of thin filament activation on either side of a rigor crossbridge extends from 3-12 of the flanking functional units (Vibert, Craig et al. 1997). Many of the studies on the effects of strong binding cross-bridges on thin filament activation use non-cycling strong binding myosin heads (NEM-S1), which greatly reduces the hill coefficient (Swartz and Moss 1992). It is important to note that the rigor state is short lived under physiological conditions, so the influence of NEM-S1 on thin filament activation compared to normally cycling cross-bridges is unknown. Additionally, strong binding cross-bridges might also increase cooperativity by influencing the probability of Ca^{2+} binding to TnC (Grabarek, Grabarek et al. 1983; Hofmann and Fuchs 1987). Because activation due to

Ca^{2+} binding is less complete in cardiac compared to skeletal muscle, the contribution of strong binding cross-bridges in cooperativity is thought to be more significant in cardiac muscle.

Recently though, the contribution of strong binding cross-bridges to myofilament cooperative activation has been challenged. Evidence that strong binding cross-bridges have minimal influence on cooperativity is provided by experiments that have used various fluorescent probes on TnC to measure structural changes in TnC accompanying calcium binding. Following incorporation of labeled TnC into skinned isolated ventricular trabeculae, preparations exhibit a normal fluorescence-calcium relationship. This suggests a simple relationship between TnC structure and force, whereby Ca^{2+} causes a structural change in TnC, and the amount of force developed is related to the percentage of TnC's that are Ca^{2+} bound. Inhibition of cross-bridges by either vanadate (Martyn, Regnier et al. 2001) or blebbistatin (Sun, Lou et al. 2009) decreased Ca^{2+} sensitivity without altering the steepness of the fluorescence-ca^{2+} relationship, suggesting a relationship between strong binding cross-bridges and pCa_{50}, but not cooperativity. In general, interventions which increase maximal force generally increase calcium sensitivity without changing the steepness of the force-calcium relationship (Sun and Irving 2010). Therefore, it is thought that strong binding cross-bridges might play a larger role in altering pCa_{50} while minimally influencing cooperativity.

E. **Impact of Sarcomere Length**

"Experiments carried out in this laboratory have shown that in an isolated heart, beating with a constant rhythm and well supplied with blood, the larger the diastolic volume of the heart (within physiological limits) the greater is the energy of its contraction."

- Starling EH and Visscher MB, 1926

1. **Frank-Starling Law of the Heart**

Studying the effect of muscle length on the regulation of contraction is one of the oldest and most pervasive techniques, and has contributed immensely to our current understanding of muscle physiology. One of the first studies on the effect of muscle length on contraction was done by Theodore Schwann in 1835, and was able to disprove a common theory of the time on exactly how muscle contracts (Needham 1971). Schwann demonstrated that the force produced by the gastrocnemius muscle of a frog was greatest when the muscle was kept at the same length that it was at in the body, and if the muscle was contracted at a shorter length the force it produced was smaller. A common ideology at the time was that muscle contracted due to an attraction between particles, and according to this ideology, the force of contraction should increase as a muscle is shortened. This simple experiment on the influence of muscle length on the force of contraction forced scientists to propose other theories of how muscle shortens.

Further experiments on the effects of muscle length on contraction were done independently by Otto Frank and Ernst Starling. Studying the force of contraction in frog hearts, Otto Frank showed that force production in the ventricle was greater if the aorta was clamped, than if the heart was allowed to eject blood (Frank 1895). These results are in agreement with Schwann's findings, since, in the heart isovolumetric force production is similar to keeping a muscle's length static, whereas allowing the heart to eject blood is analogous to allowing a

muscle to shorten. Later, Ernst Starling discovered that the largest factor in determining cardiac output is ventricular filling (Starling 1918). Regardless of ventricular pressure, an increase in the volume of the ventricle increased cardiac output. It is these two discoveries which were combined to form the Frank-Starling law of the heart. Whether the Frank-Starling law was a property of the whole heart, the individual muscle cells which made up the heart, or all a property of all striated muscle, would be debated for many years.

2. Length-Tension Relationship

To see if the Frank-Starling law of the heart was a property of individual cardiac muscle fibers, cardiac fibers were stretched and activated over various lengths. Similar to how increased ventricular filling stretches each muscle fiber and the heart produces more force, stretching, or increasing a cardiac fiber's length increase the force it produces. The length in which a cardiac fiber produces the most force was termed L_{max}, and smaller lengths were measured in percentages of L_{max}. This increased force upon lengthening was termed length-dependent activation (LDA) and was later discovered to be a property of all striated muscle. With further advancements in microscopy and x-ray diffraction it was possible to determine the relationship between muscle length, sarcomere length, and tension. These experiments demonstrated that it was sarcomere length, and not muscle length per se, which determined the amount of tension a muscle produces. Only now could detailed investigations of the amount of tension produced over a range of sarcomere lengths in different muscle types be mapped.

One of the early hypothesis of the mechanism behind the Frank-Starling law of the heart was that the higher forces seen at longer sarcomere lengths were due to changes in thick and thin filament overlap (Gordon, Huxley et al. 1966). Because cardiac and skeletal muscle filament

lengths are the same, if filament overlap was the major mechanism responsible for the Frank-Starling law they would be expected to have the same length-tension relationship. When the length-tension relationships between cardiac and skeletal muscle were compared (Sonnenblick and Skelton 1974), it was clear that cardiac muscle has a much steeper length tension relationship than skeletal muscle, suggesting there are other mechanisms besides filament overlap that are responsible for the length-tension relationship (Allen and Kurihara 1982). Mapping of the length-tension relationship also demonstrated how increasing sarcomere length not only increases maximal force, but it also increase the amount of force produced for a given level of activating calcium (Hibberd and Jewell 1982). Consequently, in addition to increasing maximal force, increases in SL also sensitizes the muscle to calcium (ter Keurs, Rijnsburger et al. 1980). Taken together, these phenomenon illustrate the two hallmarks of LDA; upon an increase in muscle length there is an increase in maximal force and an increase in calcium sensitivity.

A. **Two Phases of LDA**

It should be noted that there are two distinct phases of LDA, an initial phase that increases twitch force immediately, and then a slower increase which occurs over the course of several minutes (Parmley and Chuck 1973). By simultaneous measurement of intracellular calcium and twitch force, it was discovered that although tension immediately increased following an increase in SL, intracellular calcium remained unchanged. Intracellular calcium only increased along with twitch force during the slow phase of LDA (Allen and Kurihara 1982). Therefore, the initial phase of LDA appears to be mediated by the myofilaments, while the slower phase is mediated by alterations in calcium release from the SR.

Exactly how an increase in length causes an increase in intracellular calcium release is unknown, but is thought to include stretch-induced activation of the sarcolemmal Na^+/H^+ exchanger (Alvarez, Perez et al. 1999), possibly mediated by increased production of nitric oxide upon lengthening (Petroff, Kim et al. 2001). Since it is the initial phase that is responsible for the beat-to-beat modulation of the heart's response to stretch and is the predominant effect underlying the Frank-Starling mechanism, it will be the major focus of my thesis.

3. **Proposed Mechanisms**

Despite innumerable attempts to characterize and model LDA, the specific molecular mechanisms underlying it are still largely unknown. As previously mentioned, measurement of the length-tension relationship in both skeletal and cardiac muscle, along with alterations in intracellular calcium concentrations upon changes in length, have disregarded the hypothesis' that LDA is due to filament overlap or increased calcium release from the SR, respectively. I have grouped other remaining major mechanisms into three categories: lattice spacing, the giant protein titin, and cooperativity.

A. **Lattice Spacing**

One of the more popular mechanisms considered to play a role in LDA is lattice spacing (Millman 1998; Fuchs and Martyn 2005). In general, muscle tissue is considered to be isovolumetric, meaning that upon an increase in length its width narrows proportionally in order to maintain a constant volume (Rome 1968; Irving, Konhilas et al. 2000). Narrowing of a fibers width therefore brings the thick and thin filaments closer together. This potentially increases the odds of crossbridge attachment, providing a possible explanation for the increased

forces seen at longer SL's. Experimental evidence for the lattice spacing theory comes from experiments involving the use of large polymers, such as dextran T500, to change fiber width independently of changing SL. In order to have the same muscle width, and hopefully the same lattice spacing at both short and long SL, dextran is added (previous experiments used ~2-6%) to the fiber at a short SL. When dextran is used to match a fibers width at a short SL and long SL, calcium sensitivity at the short SL increases to a similar amount as seen at the long SL, suggesting that it is not length per se that alters LDA, but interfilament spacing (Godt and Maughan 1981; McDonald and Moss 1995; Fuchs and Smith 2001).

One caveat to many of these experiments is that due to the difficulty of measuring interfilament spacing, which requires the use of high powered x-rays, the actual interfilament spacing in these preparations is not known. Actual lattice spacing was only estimated by using a crude measurement of a fiber's width, so it is only assumed that lattice spacing is reduced the same degree. In order to address this concern, our lab has measured changes in fiber width, lattice spacing, and calcium sensitivity using varied amounts of dextran (Konhilas, Irving et al. 2002). When 3% and 6% dextran was applied to skinned rat trabeculae, like previously shown, calcium sensitivity increased similar amount compared to lengthening the fiber. When lattice spacing was measured directly though, it showed that the amount of dextran used compressed the lattice spacing to a much further degree than stretch alone. In order to maintain lattice spacing at both short and long SL, only 1% dextran was needed, which did not significantly alter calcium sensitivity, raising doubts that LDA is mediated by changes in lattice spacing and that dextran might increase calcium sensitivity in other ways.

To further test the hypothesis that LDA is mediated by changes in lattice spacing, the extent of changes in calcium sensitivity upon an increase in SL was compared to changes in

lattice spacing in three different tissue types from the rat (Konhilas, Irving et al. 2002). By using tissue from the same species, confounding variables such as different protein isoform expressions or other interspecies differences were minimized. If lattice spacing is the mechanism behind LDA, the extent of LDA should directly correlate to the change in lattice spacing. For instance, cardiac muscle exhibits a much larger degree of calcium sensitivity compared to skeletal muscle, so therefore it would be expected to have a larger decrease in lattice spacing. While the degree of lattice spacing change with a change in SL showed no significant changes between cardiac, fast skeletal and slow skeletal muscle of the rat, there were significant differences in the degree of length dependency exhibited by the three tissues suggesting again that something other than lattice spacing mediates LDA.

One concern regarding these experiments is that it is known that cross-bridge binding to actin has an effect on lattice spacing (Brenner and Yu 1985; Kawai, Wray et al. 1993) and measurement of lattice spacing in these experiments took place under relaxed conditions. To address this, lattice spacing was measured during under relaxing and activating conditions to determine consistency. Using feedback to maintain sarcomere length during the contraction, very brief (10ms) measurements of lattice spacing were taken during peak relaxation and peak contraction of rat trabeculae, and it was found that lattice spacing was maintained within 1% during the contraction (Farman, Allen et al. 2007).

If lattice spacing has less of a role in LDA than previously thought, then how does supraphysiological compression of the filament lattice by dextran alter calcium sensitivity? One hypothesis is that osmotic compression can affect the relative position of myosin heads with respect to the thick and thin filament, which is assessed by measuring the changes of the ratio of intensities of the 1,1 and 1,0 equatorial X-ray reflections ($I_{1,1}/I_{1,0}$) (Yu, Steven et al. 1985). By

examining how lattice spacing, the $I_{1,1}/I_{1,0}$ intensity ratio, and calcium sensitivity changes over a large range of osmotic compression, the linearity of the values seemed to change near 0.7%. Each variable had a population of values between 0.7-12% dextran that was markedly different than what was observed at below those amounts. Above 0.7% dextran, lattice spacing was continually compressed as osmotic pressure was increased. In contrast, both calcium sensitivity and the $I_{1,1}/I_{1,0}$ intensity ratio showed two distinct populations above and below 0.7% dextran, indicating a "switch-like" mechanism in how osmotic compression effects calcium sensitivity. Therefore, dextran might increase calcium sensitivity due to altering the position of myosin heads closer to the thin filament rather than through changes in lattice spacing.

The role of lattice spacing in LDA is difficult to analyze due to how the role it plays is obscured by the fact that many perturbations that alter LDA also alter lattice spacing. More recent experiments, even from different groups, directly attempting to directly correlate changes in LDA to changes in lattice spacing have shed doubt and suggested other mechanisms might play more definitive roles (Fukuda, J et al. 2001; Konhilas, Irving et al. 2002).

B. **Titin**

As previously mentioned, titin spans each sarcomere from the z-disk to the m-line. This makes it a perfect candidate not only for having a role in how muscle senses its length, but the sheer amount of interactions it has with the other proteins of the sarcomere, both mechanically and via signaling, also puts it in a position to play a role in altering calcium sensitivity and/or increasing the amount of actomyosin interaction (Cazorla, Wu et al. 2001; Granzier and Labeit 2004; Fukuda, Granzier et al. 2008; Linke 2008; Castro-Ferreira, Fontes-Carvalho et al. 2010; de Tombe, Mateja et al. 2010; Kruger and Linke 2010; LeWinter and

Granzier 2010). Since titin mechanically tethers the thick and thin filament together, any longitudinal passive tension provided will also impart a radial force pulling the thick and thin filaments closer together, decreasing lattice spacing. Indeed, decreasing titin-based passive force has been shown to expand lattice spacing (Cazorla, Wu et al. 2001). Since the role of lattice spacing was covered in the previous section, other mechanisms of how titin might alter LDA will be focused on here.

One very clever set of experiments has completely changed the way many people view the roles of passive tension and titin in LDA. Since 80% of the passive stiffness in the heart and 100% of the passive stiffness in skinned preparations is titin-based, the possibility that LDA is modulated through passive stiffness (rather than SL per se) was investigated by Cazorla et al. By altering the pre-history of stretch, they were able to change passive tension independently of SL and find which correlated better to changes in calcium sensitivity (Cazorla, Wu et al. 2001). They measured calcium sensitivity in skinned mouse cardiac myocytes at both 2.0 μm and 2.3 μm. They were able to achieve a ~10 fold difference in passive tension at the longer length depending on if they held the fiber at either 2.5 μm or 2.0 μm just prior to quickly releasing or stretching the fiber to 2.3 μm prior to activation, respectively. Interestingly, calcium sensitivity correlated better to passive tension than SL, with the higher passive tension group exhibiting a ~2.5 fold increase in LDA than the low passive tension group, as measured by ΔpCa_{50}. They also specifically degraded titin with a mild trypsin treatment, which reduced passive tension to a similar degree as a release from 2.5 μm. Regardless if the fiber was released from a longer SL or underwent a mild trypsin treatment, both groups exhibited very similar calcium sensitivities and maximal Ca^{2+} activated tension. This data suggests that titin might act as a molecular ruler of some sort, modulating LDA through changes in passive tension rather than SL per se.

More evidence for the modulation of LDA through titin-based passive stiffness comes from studies looking at the extent of LDA in preparations that have different titin isoforms. There are numerous experiments comparing different titin-based passive stiffness and in each case the amount of LDA varies with the amount of passive tension and not SL per se (Cazorla, Vassort et al. 1999; Cazorla, Wu et al. 2001; Fukuda, Sasaki et al. 2001; Fukuda, Wu et al. 2003; Fukuda, Wu et al. 2005; Terui, Sodnomtseren et al. 2008). Regardless if the altered passive stiffness is due to naturally occurring different titin isoforms (Piroddi, Belus et al. 2007), a transgenic KO mouse missing the N2B region of titin (Lee, Peng et al. 2010), or even myocytes obtained from different regions of the ventricular wall that had altered passive stiffness due to varied regulatory protein phosphorylation (not titin isoform) (Ait Mou, le Guennec et al. 2008), the extent of LDA correlated to the amount of passive stiffness exhibited.

While it is clear that passive stiffness correlates to LDA, and titin is the major contributor to passive stiffness, mechanisms suggesting how titin modulates LDA are less abundant. One intriguing mechanism revolves around the discovery that the A-band region of titin consists of super-repeats that contain fibronectin-type III (fn3)-like domains that were found to have myosin S1 binding sites. When skinned cardiomyocytes were incubated with fragments of the fn3 domain that showed myosin S1 binding, they showed reduced length dependency (Muhle-Goll, Habeck et al. 2001). The reduced LDA was due to increased submaximal Ca^{2+} activated tension and calcium sensitivity, which was more pronounced at short SL. Therefore, the fn3 domains found in the A-region of titin might inhibit actin-myosin interaction by binding the S1 region, which is relieved from competitive binding of exogenous fn3 fragments. Additionally, this inhibitory effect of the endogenous titin fn3 domains might be more pronounced at short SL's,

explaining the greater relief of inhibition from the exogenous fragments at short SL. Therefore, titin might inhibit actomyosin interaction at short SL's, which is relieved upon lengthening.

Due to the constantly increasing information regarding the multiple roles titin has in striated muscle, additional experiments need to be done do delineate a specific involvement in LDA. Experiments involving degradation of titin suggest that it is necessary for LDA, but it is very possible that titin is simply just a player in a much larger network of protein-protein interactions that all need to be present in order to increase calcium sensitivity and maximal Ca^{2+} activated force.

C. **Cooperativity**

As mentioned previously, cardiac muscle activation, and to a lesser extent skeletal muscle activation, is a highly cooperative process. A role for cooperativity in LDA comes from studies that show the amount of cooperativity tends to correlate to the extent of LDA in a given preparation. For instance, not only does cardiac muscle have a higher degree of cooperativity than skeletal muscle, it also has a higher degree of LDA (Metzger 1995; Konhilas, Irving et al. 2002) . Although cardiac muscle and slow skeletal muscle initially have the same TnI isoform, in cardiac muscle it changes to a specific cardiac isoform shortly after birth in most species (Kruger, Kohl et al. 2006). When slow skeletal TnI (ssTnI) was transgenically re-introduced into cardiac muscle, the SL-dependent change in calcium sensitivity was reduced compared to controls, meaning LDA was reduced (Konhilas, Irving et al. 2003). In addition to the lack of SL-dependent changes in calcium sensitivity, fibers containing ssTnI also exhibited reduced SL-dependent changes in cooperativity, as indexed by the n_H. This suggests that TnI, and therefore

the thin filament, plays an important role in the transduction of cooperativity and LDA across the cardiac sarcomere.

There are a few differences between cTnI and ssTnI, but one interesting difference is within the highly conserved inhibitory domain, the presence of either threonine or proline in equivalent positions in cTnI or ssTnI respectively. Similar to the transgenic model previously described, exchange with recombinant Tn complex with ssTnI instead of cTnI caused a large reduction in LDA (Tachampa, Wang et al. 2007). To determine if the differences in LDA were due to the single amino acid difference in the inhibitory regions of each isoform, substitution of proline with threoninie in ssTnI increased LDA nearly back to the level seen with cTnI. Furthermore, substitution of threonine with proline in cTnI virtually eliminated LDA and reduced cooperativity. The authors conclude that LDA may involve the cooperative spread of thin filament activation, which may require the presence of threonine 144 in TnI. Clearly, Tn, and more specifically the inhibitory region of TnI, are important in the transduction of LDA in the cardiac sarcomere.

Considering that cooperativity allows an increase in the amount of force for a given level of activating calcium (e.g. one strong binding cross-bridge acting through the thin filament increases the odds of binding of a neighboring strong binding cross-bridge), LDA could be due to increased cooperativity at a longer SL. Whereby one strong binding cross-bridge promotes even more strong binding cross-bridges to form, explaining the increase in force upon an increase in length. Indeed, it was shown early on that the hill coefficient does increase upon an increase in SL in skinned preparations (Kentish, ter Keurs et al. 1986). Unfortunately, the study had two components, which in retrospect were not optimal. First, the concentration of Mg^{2+} in the study was ~300% above the now known physiological concentration in myocardium (Godt

and Maughan 1988; Jelicks and Gupta 1991) . Second, in order to obtain an accurate assessment of cooperativity, there needs to be a sufficient amount of data points around the steepest part of the force-ca^{2+} curve to result in a better estimated hill coefficient, which was lacking. Therefore, in order to address if cooperativity increases as SL increases, skinned cardiac trabeculae underwent multiple maximal and submaximal Ca^{2+} activated contractions at 5 different SL's in solutions containing the appropriate amount of Mg^{2+}. The calcium concentrations and SL's were randomized, and any fiber that did not maintain 90% of its original force/CSA was not included in the study. These very meticulous experiments suggest that the hill coefficient at each SL was the same, and therefore, cooperativity does not change with changes in SL (Dobesh, Konhilas et al. 2002).

Whether or not cooperativity is SL-dependent is not completely resolved though. More recent experiments have suggested that the spread of cooperative activation along the thin filament is important in LDA, especially at short sarcomere lengths. This was tested by examining the SL-dependence of force and Ca^{2+} sensitivity in trabeculae following inhibition of either cross-bridges or Ca^{2+} binding to TnC (Farman, Allen et al. 2010). When cross-bridges were inhibited with blebbistatin, there was no effect on the SL-dependence of force production or Ca^{2+} sensitivity. When native TnC was replaced with a mutant TnC which does not bind Ca^{2+}, there was a larger decrease in Ca^{2+} sensitivity and cooperativity at short SL than exhibited at long SL. Therefore, inhibition of thin filament activation by reducing Ca^{2+}-TnC binding at short sarcomere lengths strongly influences Ca^{2+} sensitivity more so than inhibition of thick filament cross-bridge binding. The authors suggest that at a long SL the cooperative spread of Ca^{2+}-TnC binding via the thin filament is greater than at a short SL, possibly due to stiffening of tropomyosin, so that activation of one Tn unit is capable of activating more Tn units for a given

level of Ca^{2+}. Clearly there is a correlation between how much cooperativity and LDA a muscle exhibits, but exactly how cooperativity and LDA are related and if cooperativity is SL-dependent remains unknown (de Tombe, Mateja et al. 2010).

F. **Kinetics of Myofilament Activation and Relaxation**

I previously delineated the individual steps of the cross-bridge cycle, which were elucidated by measuring the rates of the individual steps under certain conditions. For example, it was originally thought that ATP hydrolysis by myosin was mostly completed when myosin was attached to actin (Eisenberg and Moos 1968; Eisenberg, Zobel et al. 1968; Eisenberg and Moos 1970). These reactions were examined in mixing baths, which did not have a sufficiently high enough time resolution to measure the very fast kinetics of these reactions. Measurement of the very fast ATP hydrolysis kinetics required the stopped-flow technique, which allowed a reaction to be initiated and halted within milliseconds. By comparing the rate of ATP hydrolysis between myosin and actomyosin, it was found that ATP was hydrolyzed faster in the myosin state, meaning myosin must hydrolyze ATP after dissociating from actin (Lymn and Taylor 1971). So by measuring the rates of individual reactions, the most likely path a cross-bridge will take during a single cycle can be determined.

Traditionally, kinetics of Ca^{2+} binding to TnC and thin filament regulation is investigated with isolated proteins, and force kinetics are studied in muscle fibers. One major reason for this is that a muscle fiber has a very large diffusion barrier that is difficult to overcome, which makes it very difficult to measure activation and relaxation kinetics. For instance, if a skinned trabeculae is submerged into a high Ca^{2+} solution, force rises until it reaches steady state. The rate of the rise of force is not dependent on the kinetic rates of the thin filament or cross-bridges,

but it is dependent on the diffusion of Ca2+ into the filament lattice. In order to circumvent diffusion in order to measure individual kinetic steps of activation and relaxation, scientists have had to develop different techniques. For instance, caged compounds work by putting a photolabile cage over a molecule, such as ATP, which makes it inert when put into solution. Then, after it has completely diffused into the muscle, the cage can be split by an intense pulse of light freeing the ATP and causing contraction, circumventing the diffusion barrier (McCray, Herbette et al. 1980).

Another method that is used to investigate kinetics in striated muscle involves subjecting a muscle to length perturbations while under steady-state activation, and measuring changes in force production. Brenner and Eisenberg utilized this technique to investigate the rate constant of cross-bridge attachment in skeletal muscle (Brenner and Eisenberg 1986). These experiments were done by allowing a "skinned" muscle to reach steady-state isometric force at a particular $[Ca^{2+}]$. At steady-state activation, Ca^{2+} has completely diffused into the muscle, the thin filament is activated and cross-bridges are cycling. Next, the fiber is allowed to rapidly shorten ~20% of its original length and then it is restretched to its original SL (eliminating any changes in force due to changes in SL). Upon shortening force decreases, and then following the rapid stretch, force initially increases (due to distortion of currently attached cross-bridges) and then drops to nearly zero before force redevelops back to steady-state levels (Figure 7, top panel). By measuring the rate of the redevelopment of force, the rate of cross-bridge attachment and force production can be estimated. This release-restretch technique is termed a k_{TR} and is ubiquitously used in muscle mechanics.

Unfortunately, despite how helpful these and other unmentioned techniques are, they have their limitations. The stopped-flow technique can only be used with muscle that is

unloaded, and it is known that the kinetic steps of the cross-bridge cycle are highly strain dependent. Caged compounds partially overcome this limitation, but only one compound can be released at a time. This means that a fiber cannot be initially activated and subsequently relaxed, nor can a muscle undergo step-wise increases of a compound or be introduced to different compounds successively. Many of these limitations are eliminated by utilizing the rapid solution-switching single myofibril technique described next.

1. **Single Myofibril Kinetic Studies**

While single myofibrils have been used for years to study structure, it wasn't until relatively recently that it was possible to pick them up individually, activate and relax them and measure the incredibly small nN amounts of force they produce. This technique involves picking up a single myofibril between two glass tools. One tool is calibrated glass cantilever, which acts as a force probe, while the other glass tool is attached to a piezo-motor allowing subjecting the muscle to rapid length changes. The small diameter of the muscle allows it to equilibrate in the bathing solution in around a millisecond (Tesi, Colomo et al. 2000), circumventing the diffusion barrier which was troublesome for so long. By using a motorized double barreled pipette the bathing solution can be changed within a few miliseconds, allowing multiple reactions in succession with different solutions to be measured. Additionally, constant perfusion of bathing solution along with the small diameter of the preparation protects against the buildup of products within the myofilament lattice that might introduce artifacts into the results. Although the single myofibril technique has contributed to understanding the kinetics of activation and relaxation immensely over a short period of time, I have chosen two findings I will describe.

A. Cross-bridges are Rate Limiting in Myofilament Activation

Are activation kinetics following a stepwise increase in [Ca^{2+}] (k_{ACT}) different than the activation kinetics following a large mechanical (k_{TR}) perturbation? The former not only involves the rate of cross-bridge cycling, but also Ca^{2+} binding to TnC and the subsequent thin filament activation. In contrast, the rise in force following a k_{TR} simply involves the rate of cross-bridge cycling. In an attempt to answer this using caged compounds in skinned trabeculae, it was reported that k_{ACT} is significantly slower than k_{TR} (Regnier, Martin et al. 2004). Since it is known that that inorganic phosphate speeds up cross-bridge kinetics, there is a concern that the faster activation rates following a k_{TR} might have been influenced by a buildup of inorganic phosphate within the muscle lattice (Stehle, Solzin et al. 2009). Experiments with striated myofibrils obtained from different species have revealed that the rate of activation is not different between k_{ACT} and k_{TR} (Stehle, Kruger et al. 2002; Stehle, Kruger et al. 2002; Tesi, Colomo et al. 2002; Tesi, Piroddi et al. 2002; Piroddi, Belus et al. 2007). Therefore, Ca^{2+} binding and subsequent thin filament activation in both skeletal and cardiac muscle is too fast to exert any rate limiting effects on force development.

B. Sarcomeric Inhomogeneity Contributes to Relaxation

What are the determinants of myofilament relaxation following rapid removal of Ca^{2+}? It has been shown that upon Ca^{2+} removal that isometric force decays as fast or faster than it develops during Ca^{2+}-activation (Palmer and Kentish 1998). This is in contrast with models of cross-bridge kinetics, which predict that cross-bridge kinetics are faster during Ca^{2+} activation than they are relaxation (Huxley 1957; Brenner 1988). In order to address this,

force was measured following rapid Ca^{2+} removal in guinea-pig cardiac single myofibrils (Stehle, Kruger et al. 2002). One very important aspect of these experiments was that instead of measuring force using a photodiode, it was measured with atomic force cantilevers. By having force measurement separate from microscope optics, they were able to measure force and view the single myofibrils using phase contrast video miscroscopy.

In single myofibrils, relaxation occurs in two phases; an initial slow linear phase (k_{LIN}) which lasts for the duration t_{LIN}, followed by a ~20 times faster exponential phase (k_{EXP}). When the myofibril was viewed during relaxation, it was discovered that the transition from the linear phase to the exponential phase of relaxation was initiated by a single sarcomere relaxing, which propagated relaxation outwards until the entire fiber was relaxed (Stehle, Kruger et al. 2002). Further clarification of sarcomere dynamics during relaxation was obtained by labeling the Z-disks and M-lines of cardiac myofibrils (Telley, Denoth et al. 2006). This demonstrated two important facts. First, each half sarcomere operated independently of the other half, if two halves were connected through the Z-disk or M-line they behaved the same, implicating the half sarcomere as the smallest functional unit of contraction. Second, half sarcomeres relaxed individually, and relaxation propagated 46 ms faster when the half sarcomeres were connected by the M-line than a Z-disk.

The initial linear phase of relaxation is thought to be governed by the apparent rate of cross-bridge detachment (g_{app}), since interventions that alter g_{app} alter the slope of the linear phase similarly (Tesi, Piroddi et al. 2002). The rapid exponential phase occurs sooner when the myofibril is subjected to increased $[P_i]$ or strain, which favor the reversal of the power stroke. Therefore, the exponential phase of relaxation occurs more rapidly due to sarcomeric

inhomogeneity, causing an increase in the reversal of the power stroke in lengthening sarcomeres and an increase in g_{app} in shortening sarcomeres.

G. **Conclusions and Specific Aims**

Length dependent activation (LDA) is as fundamental a process of muscle physiology as the fact that contraction is initiated by a rise in intracellular [Ca^{2+}], shortening involves myosin cross-bridges binding to actin, and this process requires the energy released by the hydrolysis of ATP. Yet, while the molecular processes underlying these phenomenon were slowly elucidated over years of research, how a muscle senses a change in sarcomere length and alters myofilament activation remains unknown. The importance of LDA can easily be underestimated. In the heart, LDA ensures that equal amounts of blood are pumped into the systemic and pulmonary circulation. If there was a mismatch where your left ventricle pumped out only 1 ml more than your right ventricle during each heartbeat, your pulmonary circulation would be drained in less than 10 minutes (Campbell 2011). LDA also matches cardiac output to the metabolic demands of the body and to vascular peripheral resistance on a beat to beat basis.

In skeletal muscle, LDA allows each individual sarcomere in a myofibril, which being biological tissue have varying force producing capabilities, to produce the same force as a neighboring sarcomere by adjusting its length (Telley and Denoth 2007). This is even true on the descending limb of the length-tension relationship; experiments have shown that isometric steady-state contracting skeletal muscles that are stretched further down the descending limb exhibit enhanced force production (Rassier, Herzog et al. 2003). If this didn't exist, a few naturally occurring stronger sarcomeres could pull on weaker neighboring ones, causing the stronger ones to get progressively stronger while the weaker to get progressively weaker. If a

myofibril is thought of as a chain made out of individual links, the chain would only be as strong as the weakest link. By being able to alter its force production by changing its length, a stronger sarcomere will reduce its sarcomere length by pulling on a weaker one, equalizing the force each sarcomere bears and maintaining the integrity of the myofibril.

Therefore, gaining further understanding of how sarcomere length modulates myofilament activation was the major goal of my thesis. The experiments described herein were constructed to answer two specific aims.

1. **Specific Aim #1:**

What is the temporal aspect of LDA? Upon an increase in SL, a muscle must first sense the length change, and then transduce that signal to the myofilaments in order to allow them to have an increase in maximal force and Ca^{2+} sensitivity. Clearly this process must take some amount of time, but exactly how long it takes is unknown.

Determining the temporal aspect of LDA involved activating a muscle at a steady-state SL and comparing its force production to a muscle that is rapidly stretched to that same SL immediately prior to activation. In order to accomplish this, we utilized the fast solution switching single-myofibril technique, which has advantages compared to other techniques. As mentioned previously, the small fiber size (1-3 μm) virtually eliminates any diffusion barriers. This is not only required to assess activation and relaxation kinetics, but it also allows for much shorter ramp stretch times compared to other preparations. Experiments were done in absence or presence of P_i, which allowed for more accurate assessment of kinetics or increased myofibrillar integrity, respectively. In addition to rapid stretches, the effect of rapidly releasing a myofibril from a longer SL was completed. Finally, any alterations in kinetics or LDA following rapid

length changes could be correlated to changes in passive tension, since it is also recorded, and has been shown to influence LDA (Cazorla, Wu et al. 2001).

2. **Specific Aim 2:**

What is the role of titin isoform length in LDA? The amount of LDA in a muscle has been shown to correlate to the titin isoform present (Piroddi, Belus et al. 2007). Furthermore, studies have demonstrated that the amount of LDA exhibited in a muscle more closely correlates to the amount of titin-based passive tension than SL per se (Cazorla, Wu et al. 2001). To examine this, we utilized a recently discovered rat that harbors a homozygous autosomal mutation causing it to preferentially express a longer form of titin (Greaser, Krzesinski et al. 2005).

To investigate the influence of titin isoform length on LDA, force-Ca^{2+} relationships and ATP consumption were determined at two SL's in both wild-type (WT) and HM tibialis anterior muscle. In this way, the influence of titin isoform on the extent of LDA can be determined. Assessment of activation and relaxation kinetics in both WT and HM tissue was completed by utilizing the rapid solution-switching single myofibril technique. Finally, since LDA is most prominent in the heart, force-Ca^{2+} relationships were determined in WT and HM right ventricular trabeculae.

A general methods section for all studies is described in the following chapter. This is followed by chapters 3 and 4 which are the major findings of this thesis. Chapter 5 is a general discussion of the results along with speculation of the mechanisms involved in LDA.

II. METHODS

A. Tissue Procurement

All experiments were performed according to institutional guidelines concerning the care and use of experimental animals. All solutions which came in contact with tissue contained a custom protease inhibitor cocktail (see solutions). Guinea-pigs (Dunkin-Harley, 4-6 months old) were anaesthetized with an intraperitoneal injection of pentobarbital (50mg/kg) plus heparin (1.5 mL) before rapid excision of the heart. Hearts were perfused retrograde with Krebs-Henseleit solution (see solutions), which contained BDM and KCl to inhibit spontaneous beating of the heart. The left ventricle was isolated, cut into ~100 mg segments that were flash frozen, and subsequently stored in liquid nitrogen for further use.

The wildtype (WT) and homozygous mutant (HM) rats used to investigate the role of titin isoform size in length dependent activation experiments were generated as described in chapter III section B, METHODS. Skeletal muscle was obtained by anesthetizing either WT or HM rats with pentobarbital (50mg/kg) before removal of the left and right tibialis anterior (TA). The TA can be differentially identified from the extensor digitorum longus by pulling on the tendons at their insertion points and observing the movement of the ankle. Pulling on the extensor digitorum longus tendon will not only cause dorsiflexion of the ankle but will also extend and splays the toes; whereas pulling on the TA tendon will only cause dorsiflexion of the ankle. After removal, the TA was placed into overnight solution (see SOLUTIONS) and cut longitudinally into three or four smaller pieces (~3mm wide by ~20 mm strips) on ice. The strips were tied to small wooden sticks at near physiological muscle length and placed in a 50% (v/v) glycerol/rigor solution (see SOLUTIONS) at ¯20°C. After 24 hours the rigor-glycerol solution

was replaced with fresh solution in order to achieve a greater degree of permeabilization. The tissue then was stored at ¯20°C for up to 6 months.

Skinned trabeculae were obtained in a similar way as the TA muscle previously described above. WT or HM rats were anaesthetized with pentobarbital (50mg/kg) plus heparin (1.5mL) before removal of the heart. The heart then underwent retrograde perfusion with Krebs-Henseleit solution while the right ventricle was reflected outward under a binocular microscope (10-40x magnification, Olympus) to reveal the trabeculae. Long, thin, and unbranched trabeculae were dissected out and then skinned overnight in relaxing solution (see solutions) containing 1% Triton X-100. The tissue underwent a brief wash in ice cold relaxing solution to remove any triton before being stored in relaxing solution at 4°C and used within 24 hours.

B. **Single Myofibril**

1. **Preparation of Myofibrils**

To prepare myofibrils, guinea-pig frozen myocardium was thawed in high potassium, calcium free overnight solution at 4°C, then cut into small strips (1mm wide by 10mm long) and held at near physiological muscle length with minutia pins before being chemically permeabilized in relaxing solution containing 1% Triton X-100 for 3 hours at 4°C. Resulting fibers were stored in relaxing solution for up to 4 days. Single myofibrils (or small bundles of two to three myofibrils), 1-5 μm thick and ~35-50 μm long, were obtained from mechanical homogenization (18k rpm for 2 seconds) of the permeabilized left ventricular muscle strips in ~1mL of relaxing solution on ice. Large bundles of myofibrils and debris was removed by filtration through a 30 μm nylon filter. Myofibril preparations were stored at 4°C and used for up to 4 days after preparation.

Skeletal myofibrils from rat tibialis anterior were obtained in a similar fashion as was previously described for the frozen guinea-pig tissue. Small strips of muscle (1mm wide by 10mm long) were dissected from the larger bundles which were previously tied to sticks and stored in the rigor-glycerol solution. Then, the strips were homogenized (9k rpm, 6 seconds) in ~1mL of relaxing solution on ice, before being filtered (30 μm nylon filter) to remove large aggregates and debris. The HM tissue required slightly slower, but longer homogenization speeds (6k rpm, 12 seconds) to obtain good quality myofibrils, possibly due to the tissue having less mechanical stiffness related to the longer titin isoform. Myofibril preparations were then stored at 4°C and used for up to 4 days after preparation.

2. **Microfabrication and Calibration of Force Probes**

In order to measure the minute forces that single myofibrils produce, it was necessary to use custom glass microneedles. Such needles were made through a process in which borosilicate glass rods were microfabricated into an appropriate geometry to act as a force probe and then calibrated to obtain their stiffness. More specifically, these glass rods (World Precision Instruments Inc., Item Number: G4100-4) were pulled using a Flaming/Brown type pipette puller (Sutter Instrument Co. Model P-87) to obtain a steady taper down to a very fine (< 1μm) thickness. Then, the needles were transferred to a microforge (Narishigi MF-9, 10 μm platinum wire) and depending on the desired stiffness they were cut at a specific diameter (~8-20 μm) and fire polished. To insure the glass microneedles had a high frequency response, they were bent ~90 degree's using the microforge's heating element. High heat and low duration is important in obtaining the 90 degree bend since extended heating causes accumulation of glass at the bend which grossly increases the needles stiffness. Needles that did not have the appropriate

geometry (90 ± 5 degrees, 800-1200 μm length), or required more than ~4 pulses of heat to bend were discarded. Otherwise, the needles were individually calibrated in order to obtain their stiffness using one of the two methods described below.

The first method involved cross-calibration with nanofabricated reference cantilevers (Figure 4A) that have known stiffness, which were obtained from other very generous groups (initially Dr. Pollock, and then Dr. Leonard). The reference cantilevers were made using optical lithography of silicon-nitride wafers and contained three sets of two cantilevers each with different stiffness. Cross calibration was completed under 40x magnification and utilizing IonOptix edge detection software to measure the needle's displacement. The basic process involved using one of the cantilever pairs to push against the microneedle being calibrated, while the other cantilever was used as a reference to obtain the first cantilevers displacement (Figure 4 Panels B and C). By taking the displacement of the microneedle and dividing it by the displacement of the reference needle a ratio of the needles' relative stiffness was obtained. Then by using the reference cantilever's known stiffness, the microneedle's stiffness could be extrapolated.

The second method involved utilizing software developed Dr. Peter N. Ayittey. The software estimates the microneedle's stiffness from its geometry with a similar level of error as the previously mentioned cross-calibration method. The software was created using a finite-element analysis model to simulate how different needle geometries affect their overall stiffness as a function of applied force (Ayittey, Walker et al. 2009). The analysis concluded that the length of the microneedle after the 90° bend and the diameter of the microneedle immediately after the bend had the largest impact on overall stiffness. Additionally, it was determined that the diameter immediately prior to the bend and the tip diameter play a small role in the

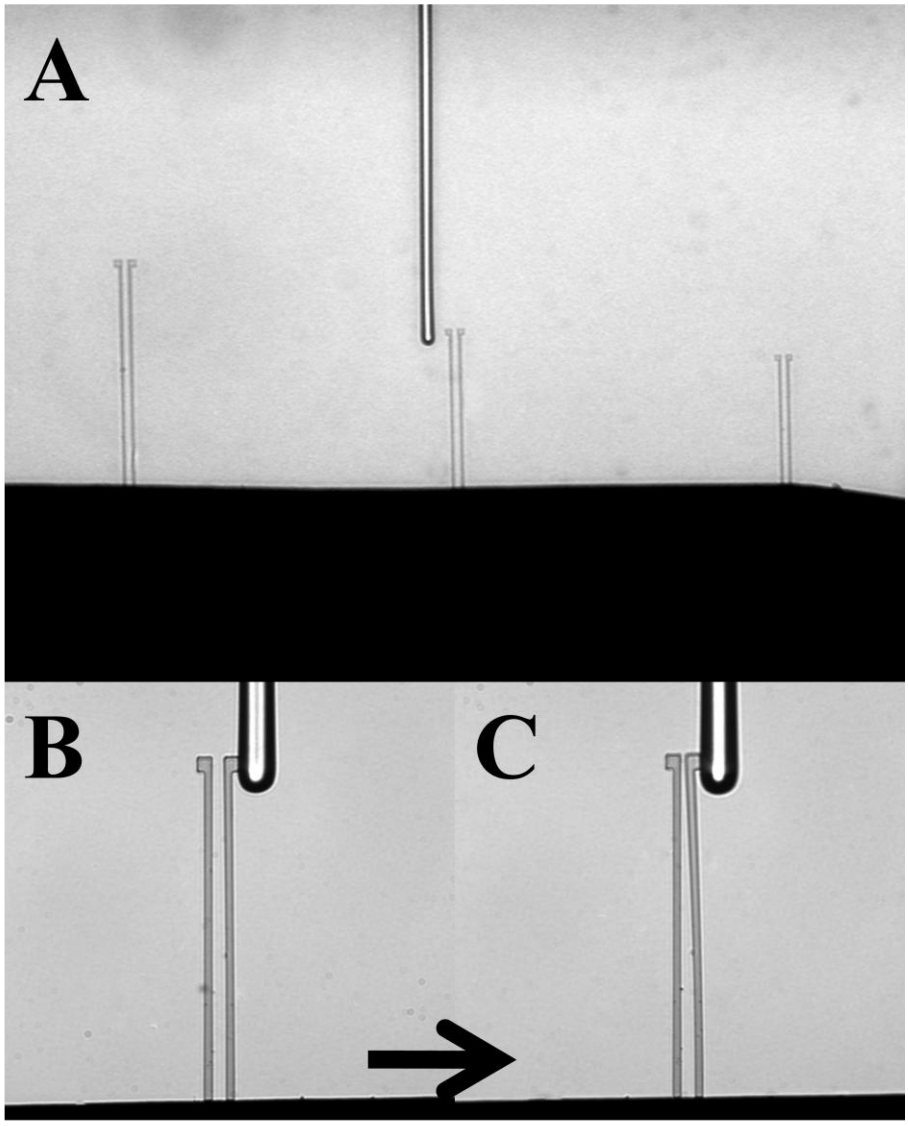

Figure 4. Calibration of force probes. Panel A shows the glass microneedle that acts as a force probe along with 3 sets of calibration cantilevers with known stiffness, the longest and most compliant pair is on the left. Calibration occurs when the calibration cantilevers are used to deflect the force probe, and then extrapolating to obtain the microneedles stiffness. Panel B is before any deflection, and panel C shows their relative positions after movement. The cantilevers are in pairs so that the deflection of the cantilever in use can be determined by measuring its relative position to its neighboring cantilever.

microneedle's overall stiffness. Therefore, by measuring these geometries of a microneedle and then putting the appropriate measurements into the software it is possible to quickly estimate its stiffness.

3. Calibration of the Perfusion Pipette's Solution Flow

In order to insure proper solution flow and minimize artifacts from having unequal flow rates from each barrel the gravity driven double barrel perfusion pipette needs to be calibrated frequently. This is done by measuring the time it takes a drop of solution to form on the end of the pipette, get too large to support itself, and then fall. Therefore, the size of an average drop needs to be ascertained for each perfusion pipette made. While there are several ways to accomplish this, one simple method involves using a weigh boat or any other dish to collect multiple drops from the perfusion pipette and then weighing the amount of water. Then, by dividing the total weight of the water by the number of drops, the weight of an individual drop can be estimated. Once the weight is determined, by knowing that one gram of water is approximately one milliliter, its volume can be calculated. Due to the small volumes of water, evaporation can be an issue so this process should be completed as quickly as possible. Once the average drop size is ascertained, it is possible to determine the amount of time that should elapse between drops using the total flow rate desired and the following two equations:

(1) [total flow rate] / (2 * [the volume of each drop]) = number of drops per minute

(2) 60 / [number of drops per minute] = time elapsed between drips

For example, with an average drop size of 45 uL and a total desired flow rate of 200 uL per minute, there should be ~27 seconds between drops. It should be noted that these equations assume you are calibrating the flow of the two barrels one at a time. Because gravity is the

driving force of the solution flow, the flow rate can be changed by moving the syringe solution reservoirs either higher or lower for faster or slower flow, respectively. In general, to reduce flow-related artifacts, it is more important to minimize flow differences between solutions than it is to make sure the flow rate is exactly the same between experiments.

4. **Apparatus**

The experimental apparatus and protocol have been previously described (Colomo, Piroddi et al. 1997; de Tombe, Belus et al. 2007). Briefly, to start an experiment, an aliquot of myofibril suspension (~50 µl) in relaxing solution was pipetted onto the glass cover slip of a water cooled bath mounted on the stage of an inverted microscope (Olympus IX-70) and left for 5 minutes to allow settling. Then, ~2.5 mL of bath solution (see solutions) was gently pipetted into the bath and allowed to sit for another 2-5 minutes for additional settling. Searching for myofibrils to select for experiments in the bath was done under 10x magnification and using phase contrast. Once a myofibril is selected, it is attached horizontally between two glass tools (see Mounting Myofibrils); one is a stiff straight glass "reference" pipette which is used to hold one end of the myofibril in place, while the other tool is a calibrated microneedle acting as a force probe (Figure 5A). Since the myofibrils attach to the glass tools without the use of glue, a few steps need to be taken to insure there is proper attachment and avoid having the myofibril tear off during a contraction. Prior to each experiment the reference pipette should be fire polished using the heating element on the microforge to prevent any build up of tissue or debris. To maximize attachment on the force probe, it is first dipped in acetone (to remove any previously added black ink) and then under a dissection scope the tip of a pen (water insoluble

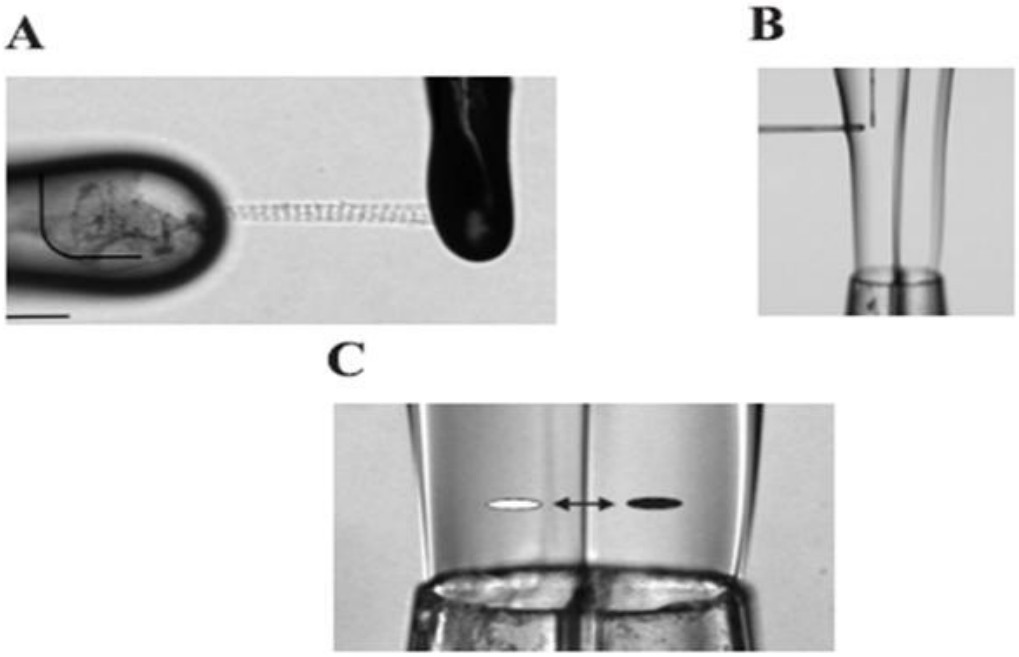

Figure 5. A mounted myofibril and the fast solution switching double barreled pipette. Panel A shows a myofibril attached between a glass reference pipette (left) and a black ink coated calibrated microneedle acting as a force probe. The myofibril is put into the one of the laminar streams emanating from a double barreled perfusion pipette (Panel B). Panel C shows an enlargement of the double barreled pipette to show the two solution streams.

ink) is depressed multiple times to create a small puddle of black ink, which the cantilever is dipped in to provide an even coating of ink for the myofibril to attach to.

The reference pipette is attached to a piezo motor (Nano-driveOP30) which is capable of very fast horizontal displacement (30 μm range of motion, 0.06 nm resolution, <5ms) providing the ability to rapidly change the length of a myofibril during an experiment. Force is determined by measuring the displacement of the force probe via edge detection (IonOptix), which the black ink coating also assists in by providing contrast. Sarcomere length is measured using FFT analysis of the myofibril striation pattern (IonOptix). Experiments were performed at 15°C.

5. **Mounting Myofibrils**

There are two methods used to mount single myofibrils between the glass microneedles, the "flat" method and the "scoop" method. The methods are illustrated in Figure 6, with the flat method on top and the scoop method on the bottom. The instructions set forth here are based on the assumption that the straight reference pipette is located on the left side, and the force probe is located on the right side. The flat method has two advantages over the scoop method. First, due to both the fiber (for SL measurement) and the force probe (for force measurement) being parfocal, it allows for simultaneous measurement of both SL and force. Second, since the fiber is not wrapped around the force probe (as it is using the scoop method) it allows shorter myofibrils to be picked up than would otherwise be possible. After a myofibril is selected to be picked up, the left stiff reference pipette is lowered onto the glass cover slip directly over the myofibril pressing down on it. Contact with the myofibril and/or cover slip is realized by either movement of the myofibril or, more commonly, lateral movement of the pipette. The reference pipette is then lifted up a small amount and attachment is confirmed by

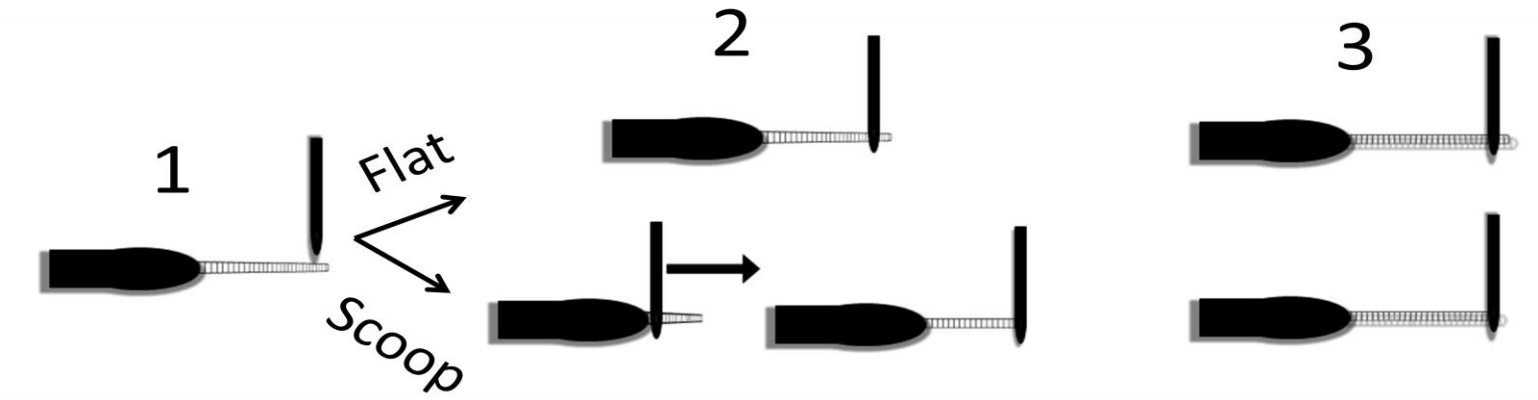

Figure 6. Mounting a myofibril. The larger left object is the reference pipette, and the vertical thinner black object on the right is the force probe. Step one shows the myofibril attached on the left side to the force probe, and the glass cover slip on the right, with the force probe in place. To pick up the myofibril with the flat method, the force probe is used to pick up the right hand side (step 2). For the scoop method, the reference pipette is picked up vertically as much as it can (which is limited by the length of the myofibril), while the force probe is placed underneath the myofibril. Then, by moving the force probe to the right, it scoops up the myofibril (step 2). The final step shows the myofibril mounted, the flat method is on top (notice the myofibril extending past the force probe) and the scoop method on bottom. Refer to the text for a more detailed explanation.

observing that the muscle moves in accordance with the pipette (Step 1). Next, the force probe is lowered onto the muscle in the same fashion, with the fiber length dependent on where the force probe is attached. Once again, the probe is picked up and attachment is confirmed visually (Step 2, top).

The scoop method is superior when myofibrils are either longer, or, due to the myofibril being wrapped around the force probe, when there is an increased incidence of the myofibril slipping or tearing off the force probe. To perform this method, the fiber is picked up on the left side using the reference pipette, using the same process as the flat method. Then, the reference pipette is raised vertically as high as possible directly overhead of the muscle's attachment to the glass cover slip (Step 2, bottom). The force probe is then lowered down until it touches the glass under the reference pipette, to the left of the muscle's attachment on the cover slip. Using micromanipulators, the force probe is drawn to the right, "scooping" up the myofibril as it passes under it.

6. **Experimental Protocol**

After mounting the myofibril, it is raised up ~1mm with the aid of motors (Newport newton), this minimizes artifacts generated when solution from the double barreled pipette bounces off the bottom of the cover slip and causes turbulence. Next, the double barrel perfusion pipette needs to be placed so that the myofibril is in the laminar flow of one of the two continuous solution streams emanating from the perfusion pipette (Figure 5B). This way, upon rapid translation of the perfusion pipette the myofibril can be maximally activated (pCa 4.0) or relaxed (pCa 10). A typical force tracing of an activation and relaxation cycle of a guinea pig left ventricular myofibril is shown in figure 7. Initially, since the myofibril is being perfused

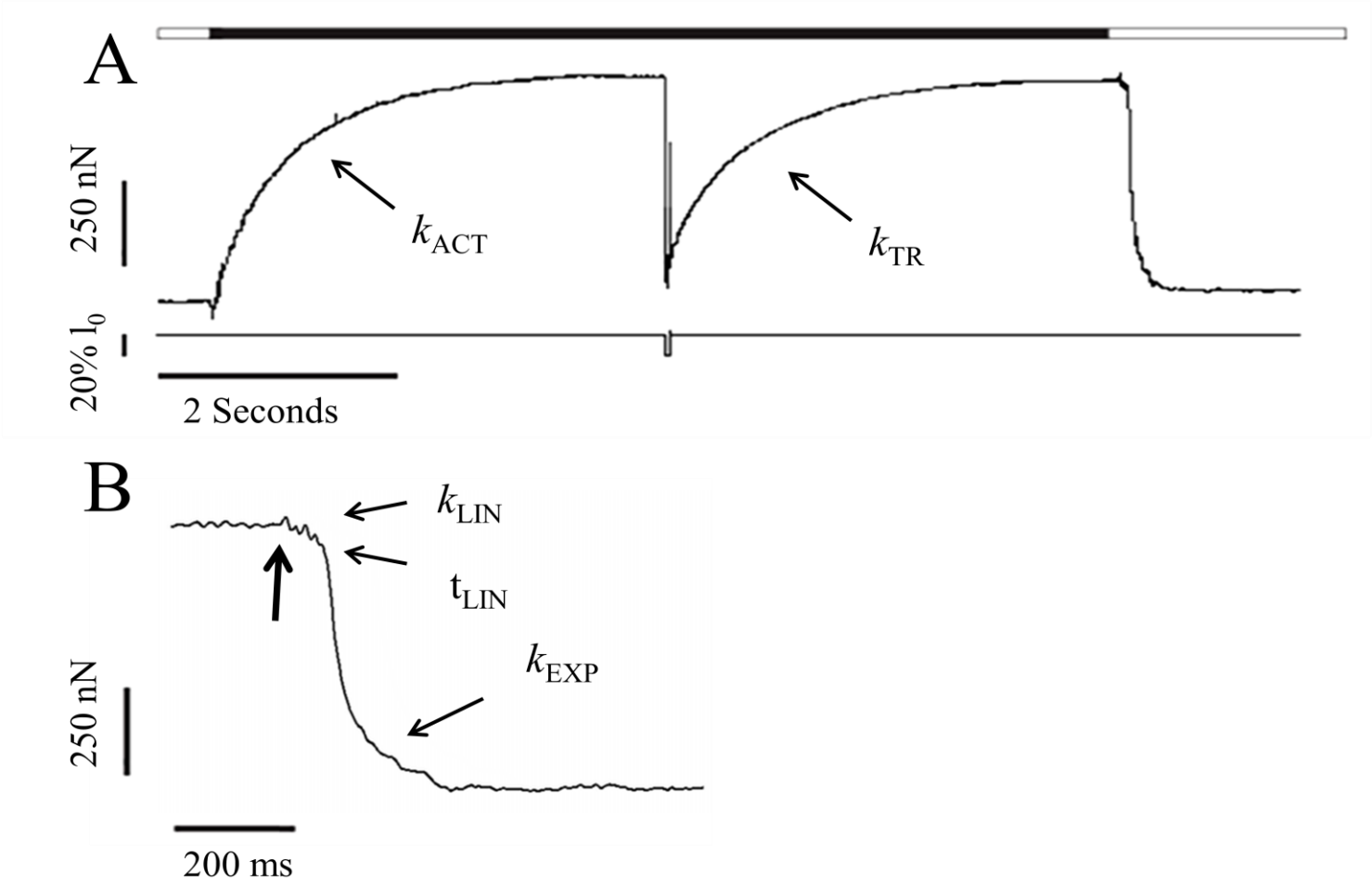

Figure 7. Typical activation and relaxation force tracing of a cardiac single myofibril. The black bar on top shows when the muscle is being perfused with maximal activating solution (pCa = 4.0). Panel A shows a typical activation-relaxation cycle, with a release restretch maneuver performed under steady-state activation conditions. Note the muscle length tracing under the force tracing. Panel B shows biphasic relaxation upon removal of Ca^{2+} (indicated by the arrow). Each activation-relaxation cycle allows determination of activation kinetics (k_{ACT}, k_{TR}) and relaxation kinetics (k_{LIN}, t_{LIN}, k_{EXP}).

with relaxing solution, force is low. Upon translation of the perfusion pipette, the myofibril is exposed to maximal activating solution (black bar) and force rises monoexponetially until it reaches a new steady-state. Then, while the myofibril is under stead-state conditions, it was subjected to a release-restretch maneuver (k_{TR}) which allows the rate of cross-bridge cycling to be estimated. This is done by releasing the fiber and then very rapidly stretching it back to its original SL, which mechanically breaks all of the currently attached cross-bridges (which is seen by the force dropping to zero), and since the thin filament is still activated force is allowed to redevelop back to steady-state levels. Then, the perfusion pipette goes back to its original position, and the fiber is exposed to relaxing solution. Myofibrils relax in two phases, an initial slow linear phase (k_{LIN}) that lasts for the duration t_{LIN}, during which the sarcomeres stay isometric. Followed by a rapid exponential relaxation phase (k_{EXP}) initiated by a single sarcomere "giving" which allows adjacent sarcomeres to elongate which rapidly speeds up relaxation (Stehle, Kruger et al. 2002; Tesi, Piroddi et al. 2002).

Due to the very fast translation of the perfusion pipette (~10ms) and the minimal diffusion delay (~1ms) resulting from the small diameter of the preparation(Tesi, Colomo et al. 2000), it is possible to rapidly and homogenously expose myofibrils to solutions of variable compositions. This ability allows myofibrils to undergo unique experiments which are impossible using other preparations and techniques. For example, our lab wanted to investigate the effect of blebbistatin, a novel myosin-II ATPase inhibitor, on force inhibition in skeletal muscle (Farman, Tachampa et al. 2008). The use of thicker preparations would allow rapid exposure and then removal of blebbistatin, but it would be impossible to measure the rate of force inhibition due to large diffusion barriers. To circumvent diffusion barriers caged compounds could be used, but then it would be impossible to remove blebbistatin once it was

released from its cage to see if the inhibition was reversible. It is only by using single myofibrils that a muscle preparation could be maximally activated, and when force reaches steady-state levels, rapidly switch to activating solution containing blebbistatin. As can be seen in Figure 8, immediately following the solution switch from activating alone to activating with blebbistatin, force decreases linearly. Only after the solution switches back to activating without blebbistatin force inhibition ceases and goes back to being steady-state, showing that force inhibition by blebbistatin is not reversible. Additionally, only in single myofibrils could any lingering effects of blebbistatin on relaxation kinetics be studied.

7. Data Processing and Statistical Analysis

The rate of the rise of tension following activation (k_{ACT}) and the rate of the fast exponential phase of relaxation (k_{EXP}) were estimated using a single exponential fit. The rate of the slow phase of relaxation (k_{LIN}) was estimated using linear regression. The length of time it took to develop half maximal steady state force (T_{50}) was obtained one of two ways. Either by measuring the time it took the muscle to produce 50% of the steady-state submaximal force, or by estimation of a single exponential fit of the rise of tension following activation (k_{ACT}) and then using the following equation to calculate the T_{50}; T_{50}=-(ln(0.5)/ k_{ACT}). Differences between means were analyzed by either a one-way analysis of variance (ANOVA) or a two-way repeated measures ANOVA, when appropriate. Significance was determined at $P < 0.05$, data are presented as mean (± S.E.M.).

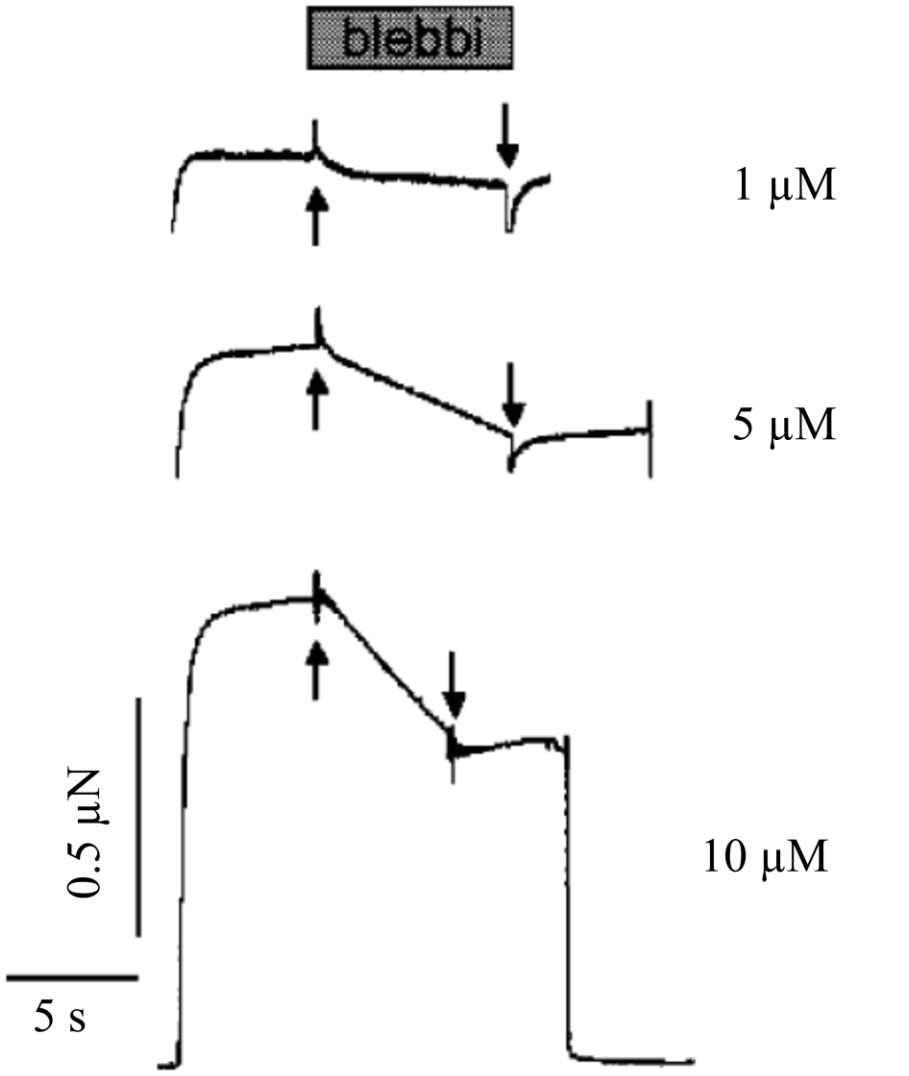

Figure 8. Inhibition of force by blebbistatin. Force traces of rabbit skeletal muscle, illustrating the effects of force inhibition by blebbistatin. The rapid solution switching technique allowed switching between Ca^{2+}-activating solution and Ca^{2+}-activating solution containing the myosin-II ATPase inhibitor blebbistatin (indicated by arrows). The amount of force inhibition increased with increased blebbistatin concentration, and was not reversible. Adapted from (Farman, Tachampa et al. 2008).

B. ATPase Methods

1. Preparation of Permeabilized Tibialis Anterior and Trabeculae for Measurement of ATPase Activity

Small bundles (~5 mm wide by ~10 mm long) of TA were dissected from the larger tissue aliquots in ice cold relaxing solution. Compared to cardiac muscle, skeletal muscle has very long and ordered groups of fiber bundles that can be visually identified from each other. Under a dissection microscope and using very fine forceps, smaller bundles were dissected away from the original larger tissue sample. Depending on the desired size, single larger bundles can continue to be separated into two smaller bundles until the appropriate size is obtained (0.1-0.25 mm wide by 1-2.5 mm long). Dissected bundles were stored up to 3 days in relaxing solution at 4°C. Immediately prior to an experiment, bundles were crimped in aluminum T-clips in order to attach to hooks mounted on the force transducer and motor arm. Trabeculae were prepared by crimping them in aluminum T-clips immediately prior to an experiment.

2. Experimental Apparatus

The ATPase apparatus has been described previously (de Tombe and Stienen 1995; Rundell, Manaves et al. 2005). The skinned skeletal or cardiac fibers were attached via the aluminum T-clips between an optical force transducer (World Precision Instruments model KG4A; 0-20mN range 4μN resolution) and a high-speed length controller (Aurora Scientific Inc. model 315C; 200 microsecond step response time, 2.4 kHZ frequency response). The force transducer and length controller were mounted on a horizontal sliding arm which allowed for rapid translocation of the fiber between the different chambers on the apparatus. The apparatus contained a mounting chamber; a windowed SL measurement chamber; two temperature

controlled incubation baths; and a temperature controlled experimental chamber for force, stiffness, and ATP consumption measurement.

3. **Measurement of ATPase Activity**

Since NADH absorbs ultraviolet (UV) light (340 nm) and NAD^+ does not, the consumption of ATP was stoichiometrically coupled to NADH consumption and NADH levels were monitored. Pyruvate kinase and lactate dehydrogenase (LDH) were used to set up the following ATP regeneration system:

(1) $ATP \leftrightarrow ADP + P_i$

(2) $ADP + PEP \leftrightarrow Pyruvate + ATP$

(3) $Pyruvate + NADH \leftrightarrow Lactate + NAD^+$

During Ca^{2+} activation, the muscle consumes ATP and subsequently releases ADP and inorganic phosphate (P_i). Pyruvate Kinase quickly phosphorylates the newly formed ADP back into ATP using phosphoenol pyruvate (PEP) as a substrate, leaving behind pyruvate as a reaction product. Next, LDH converts the pyruvate into lactate consuming NADH as a substrate, converting it into NAD^+. The method is illustrated in Figure 9; upon activation of the muscle by increasing the $[Ca^{2+}]$ in the bathing solution, UV light absorbance (proportional to [NADH]) decreases concomitant with the development of muscle tension, reaching a steady state NADH consumption rate when muscle tension development stabilizes. Following removal of the muscle from the measurement chamber into a chamber containing relaxing solution, tension development relaxes and NADH consumption ceases. UV absorption is calibrated following each contraction by repeated injections of 500 pmol ADP into the measurement chamber (25 nl; 10 mM).

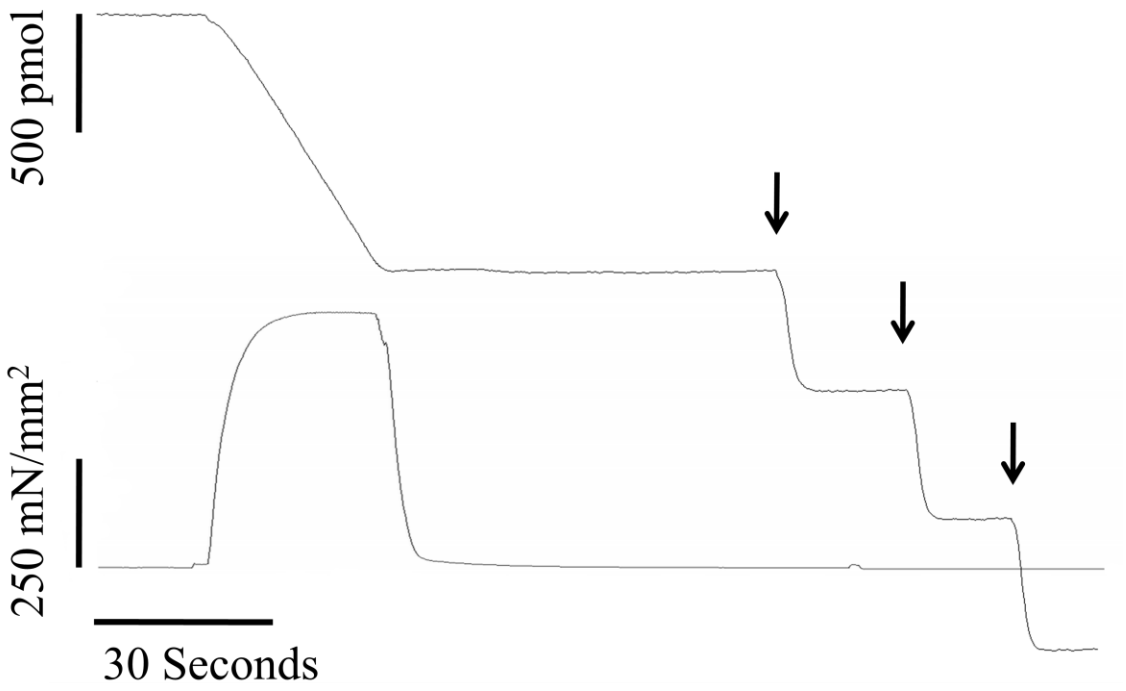

Figure 9. Typical tracing of ATP consumption and force development of rat skeletal muscle. The top tracing is UV absorbance, and though an enzyme coupled reaction allows determination of ATP consumption. Force development is on the bottom. Notice how UV absorbance decreases while the muscle is producing force, and then levels off after the muscle is removed from the measurement chamber. Calibration of the UV signal is achieved by correlating the signal change following injections of ADP (500 pmol, indicated by downward arrows) to the signal change during steady-state force production.

4. **Measurement of Fiber Dimensions**

This was done with the preparation in the SL measurement chamber in relaxing solution. A binocular microscope (10-40x magnification, Olympus) containing an optical reticle allowed the accurate measurement of the fiber's length and width. A 45° angled mirror was placed next to the chamber to measure the fibers height. Accurate measurement of fiber dimensions allowed calculation of the fibers volume, cross sectional area, and length in order to report the fibers ATPase/vol, tension/CSA and to do 1% length oscillations to measure fiber stiffness, respectively.

5. **Measurement of Sarcomere Length**

SL was measured using laser diffraction (Research Electro-Optics, Helium-Neon Laser, 633 nm wavelength, 5.0 mW output power). Due to the fact that striated muscle is a highly ordered tissue, the muscles sarcomeres causes diffraction of a laser beam that passes through it. By measuring the first order diffraction on a calibrated screen the SL can be calculated using the following equation: $\sin\theta=(w/d)$. Micromanipulators on the force transducer and the motor allowed stretching or releasing of the preparation to achieve the desired SL.

6. **Experimental Protocol**

The general protocol is as follows. After getting fiber measurements and setting the SL, the fiber is moved into the first temperature controlled bath, which is filled with ATPase relax solution containing enzymes, and is allowed to incubate for ~5 minutes to allow diffusion of the enzymes into the lattice. If the fiber is being relaxed after an activation, it only needs to be in the relaxing bath long enough for force to drop to pre-activation levels. Next, the fiber is

placed into the pre-activating bath for 2 minutes before being moved into the experimental chamber for force and ATPase consumption. The experimental chamber can be filled with activating solution containing different Ca^{2+} concentrations and is constantly being stirred by an electric motor. The fiber initially undergoes a maximal activation (pCa 4.5) in order to take up any slack in the attachments of the muscle to the transducer and motor, and then SL and fiber length are adjusted if necessary. Next the fiber undergoes another maximal activation (to obtain maximal ATPase and force/CSA), followed by 4-8 submaximal Ca^{2+} activations; intermediate Ca^{2+} concentrations were obtained by mixing activating and relaxing solutions. Finally, a last maximal activation is completed to assess fiber rundown. Additionally, high frequency muscle length perturbation (1%; 500 Hz) was applied continuously to measure high frequency stiffness, an index used to assess the relative number of attached actively cycling cross-bridges during tension development.

7. Data Processing and Statistical Analysis

Both the mechanical measurements and ATP consumption values were fit for each fiber individually and then pooled to report the mean values. Force development was normalized to cross-sectional area and fit to a modified hill equation: $F/F_{max}= 1 + 10\text{^}[n_H(pCa_{50}-pCa)]$ where F_{max} is the maximal force, F is the steady-state force, n_H is the hill coefficient, and pCa_{50} is the $-\log[Ca^{2+}]$ where F is 50% of F_{max}. ATP consumption was normalized to muscle volume and plotted as a function of normalized force obtained at the various $[Ca^{2+}]$ and fit by linear regression to obtain tension cost, the amount of ATP consumed to maintain a certain level of tension development. Data was analyzed by a one or two way ANOVA, with or without

repeated measures as required. Significance was determined at $P < 0.05$, data are presented as mean (± S.E.M.).

D. **Solutions**

The compositions of the solutions and were calculated according to the procedures developed by Fabiato as described previously (de Tombe and Stienen 1995). All solutions which came in contact with permeabilized tissue contained a custom protease inhibitor cocktail added to the solutions fresh daily, made up of: leupeptin (10 µM), pepstatin (5 µM), phenylmethyl sulphonyl fluoride (200 µM), sodium azide (500 µM) and dithiothreitol (10 mM). Krebs-Henseleit contained (in mmol/L) NaCl (118.5), KCl (5.0), NaH_2P_{O4} (H20) (2.0), MgS_{O4} (1.2), glucose (10), $NaHCO_3$ (25), $CaCl_2$ (0.7), KCl (10) and was continuously bubbled with 95% 02/5%CO_2. Overnight solution contained (in mmol/L): Tris (50), NaCl (100), KCl (2), $MgCl_2$(2), EGTA (1); pH was adjusted to 7.00 using HCl. Rigor solution contained (in mmol/L): Tris (50), KCl (100), $MgCl_2$ (2), ethylene glycol tetraacetic acid (EGTA) (1); pH was adjusted to 7.00 using HCl. Relaxing solution used in prepping myofibrils contained (in mmol/L): EGTA (1), MgATP (5), free Mg^{2+}(1), MOPS (10), phosphocreatine (10). pH was adjusted to 7.0 using KOH. Potassium proprionate was added to adjust the final ionic strength to 180 mM. Relaxing solution for prepping and mounting ATPase solutions contained (in mmol/L): Na_2ATP (6.3), $MgCl_2$ (6.48), EGTA (10), creatine phosphate (10), Kprop (49.76), BES (100), and Creatine phosphokinase (10 units per mL). pH was adjusted to 7.0 using KOH.

1. **Myofibril Solutions**

Activating and relaxing solutions both contained (in mmol/L): EGTA (1), MgATP (5), free Mg^{2+}(1), MOPS (10), phosphocreatine (10). The pH was adjusted to 7.0 using KOH. Potassium proprionate (Kprop) was added to adjust the final ionic strength to 180 mM. A range of free [Ca^{2+}] was obtained by mixing activating solution (free [Ca^{2+}] = 0.1 mM) and relaxing solution (free [Ca^{2+}] ~ 1 nM). Bath solution was identical to relaxing solution except for inclusion of 10 mM EGTA. When indicated, inorganic phosphate was added to the activating, relaxing, and bath solutions in the form of 2.0 mM KH_2PO_4 to preserve myofibril integrity throughout the experimental protocol. For the experiments performed under "zero phosphate" conditions, contaminant P_i was reduced by adding the enzyme purine nucleoside phosphorylase with the substrate 7-methyl guanosine which acts as an P_i scavenging system (Tesi, Colomo et al. 2000).

2. **ATPase Solutions**

The three main solutions used were made including protease inhibitors, so the previously mentioned protease inhibitor cocktail was not added. Activating solution contained (in mmol/L): $CaCl_2$ (10), EGTA (10), $MgCl_2$ (6.63), Kprop (14.28), ATP (6.29). Preactivating solution contained (in mmol/L): EGTA (0.2), HDTA (9.8), $MgCl_2$ (6.69), Kprop (34.35), ATP (6.2). Relaxing solution contained (in mmol/L): EGTA (10), $MgCl_2$ (6.92), Kprop (33.99), ATP (6.2). In addition, all three solutions contained (in mmol/L): BES (100), NaN_3 (5), PEP (10), dithiothreitol (1) , NADH (0.9), Pepstatin (1); and (in umol/L): Leupeptin (10), PMSF (100), Oligomycin (10), A2P5 (20), and the enzymes pyruvate kinase (4 mg/mL-500 U/mg) and lactate dehydrogenase (0.24mg/mL-870 U/mg). All three solutions were adjusted to pH 7.0 using KOH.

III. The Temporal Aspect of Length Dependent Activation

A. Abstract

Myofilament length-dependent activation is a universal property of striated muscle, yet the molecular mechanisms that underlie this phenomenon are incompletely understood. Additionally, the dynamic rate by which sarcomere length (SL) is sensed and then transduced to form length-dependent activation is unknown. Here, using isolated guinea-pig myocardium, we employed the rapid solution-switch single myofibril technique that allows for the study of contractile action/relaxation dynamics in the virtual absence of diffusion delays. We compared contraction kinetics at submaximal activation at steady-state SL with contractions following rapid SL ramps to that same SL just prior to activation. Neither the activation and relaxation kinetics nor final submaximal force development was significantly different between the two contraction modes for SL ramps as fast as 5 ms. We conclude that the transduction of the length signal by the cardiac sarcomere to modulate thin filament activation levels occurs virtually instantaneously, possibly resulting from geometric rearrangement of the contractile proteins.

B. Introduction

The Frank-Starling law of the heart describes an important regulatory system whereby the heart has the ability to alter cardiac output to meet changes in the energy demands of the body. The cellular basis for this property resides in the cardiac sarcomere; that is, a change in sarcomere length (SL) alters the responsiveness of the myofilament to Ca^{2+}. This phenomenon has been termed myofilament length-dependent activation (LDA). Despite intense investigation, the molecular mechanisms that underlie LDA remain largely unknown (de Tombe, Mateja et al. 2010). It has been determined that modulation of steady-state contraction force by sarcomere

length is due to a proportional variation of strongly attached, force generating cross-bridges. Sinusoidal sarcomere length perturbation studies in activated permeabilized isolated myocardium have revealed two distinct force responses to dynamic SL changes (Ford, Chandra et al. 2010). Initially there is a quasi-elastic force response (distortion) which is thought to be due to the stretching of the elastic regions of attached cross-bridges, followed by a slower developing delayed-force response (recruitment) which is thought to reflect the attachment of new cross-bridges to produce force. It has been assumed that cross-bridge recruitment does not occur instantaneously following a change in length, previous groups modeling the response of cardiac muscle to sinusoidal length changes estimated the delay to be ~100ms in rabbit myocardium at 25°C. These data suggests that LDA develops relatively slowly, that is, within the time frame of the first ~25% of the heartbeat (Campbell, Taheri et al. 1993; Campbell, Razumova et al. 2001). However, the term "LDA" principally refers to the impact of a SL change that occurs before myofilament activation. In contrast, the delayed-force response dynamics include both LDA and subsequent downstream processes, including attachment and detachment of cross-bridges (Ford, Chandra et al. 2010). Hence, the rate at which LDA develops, that is, the rate by which a SL perturbation induces a change in calcium responsiveness of a relaxed myofilament, is not known.

To ascertain the rate that LDA appears after a rapid length change, we compared the force responses of activated cardiac myofibrils at a long SL (2.3 μm) to the force responses of cardiac myofibrils that were rapidly stretched or released to the same SL just prior to activation. The single myofibril technique was utilized since it allows for the measurement of activation and relaxation kinetics following a step-wise rapid change in the concentration of activating calcium ions due to the virtual absence of a diffusion delay in these small preparations (Tesi, Colomo et al. 2000). Therefore, rapid-solution switching results in a rapid (~1 ms) and homogenous

alteration of the ionic milieu surrounding the myofilaments throughout the preparation. Here, we rapidly activated single, isolated guinea-pig myofibrils under submaximal (~50%) activation conditions at either steady-state SL, or after rapid ramp changes to that SL just prior to activation. I reasoned that a delay in the development of LDA would manifest as delayed force development dynamics. Guinea-pig myocardium, which is a generally slow and predominantly beta-myosin containing species (Stehle, Kruger et al. 2002), as well as low temperature (de Tombe, Belus et al. 2007), were used to maximize my ability to assess the dynamic rate of LDA development. Both rapid ramp SL stretches (n = 29) and ramp SL releases (n = 5) perturbations were examined.

C. **Methods**

1. **Determining the Timing of the Solution Switch using a Photomultiplier Tube**

During an activation/relaxation cycle in an experiment, there is an inherent uncertainly regarding the exact timing of the solution switch takes place at the level of the muscle. This is due to the inevitable delay between the displacement of the perfusion pipette and the arrival of the new solution at the level of the attached myofibril. To ascertain the proper sequence of the rapid muscle length change and subsequent Ca^{2+} activation, we added a small amount of red dye (ponceau) to the relaxing solution [3% of a 1% solution] and used a photomultipler tube (Spex Industries Inc) to detect the presence or absence of the dye. By using an aperture that only permitted light to pass through from an area immediately proximal to the location of the preparation, I was able to detect the timing of the solution switch at the level of the myofibril. Since this delay is not consistent between experiments, it needed to measure it each time. Before doing a rapid stretch, the fiber was sub-maximally activated and the delay

between the command of the solution switch and the actual solution switch (at the level of the myofibril) was measured. As illustrated in figure 10C, this approach allowed for a protocol in which the muscle length change was completed immediately before the actual solution switch. Preliminary experiments revealed no impact on force or kinetics in the presence of the small concentration of the red dye.

D. **Results**

To investigate the temporal aspect of LDA in guinea pig myocardium, we compared the force responses of myofibrils activated at steady-state SL, to myofibrils that underwent a rapid length change to the same SL just prior to activation. Traces from a typical experiment are shown in Figure 10A. Initially, myofibrils were maximally activated (pCa = 4) at SL = 2.3 μm to measure Ca^{2+} saturated force development. This contraction also served as a reference to assess force rundown. Then, two submaximal contractions (pCa = 5.7) were initiated at the long and short steady-state SL (2.3 μm and 2.0 μm, respectively). Steady-state SL was attained by holding SL constant for five minutes. Next, the myofibrils were rapidly stretched from SL = 2.0 to SL = 2.3 μm and immediately activated with the pCa = 5.7 solution. A final contraction at maximum activation at SL = 2.3 μm allowed us to assess force rundown. Myofibrils that displayed more than 20% rundown were not included in the study. The order of activation at either steady-state SL or after a rapid SL change at pCa 5.7 was randomized.

1. **5ms Stretches**

Average Ca^{2+} activated maximum force at SL = 2.3 μm was 31.5 ± 3 mN/ mm^2. As illustrated in this Figure 10B, guinea-pig myocardium displays robust LDA; that is,

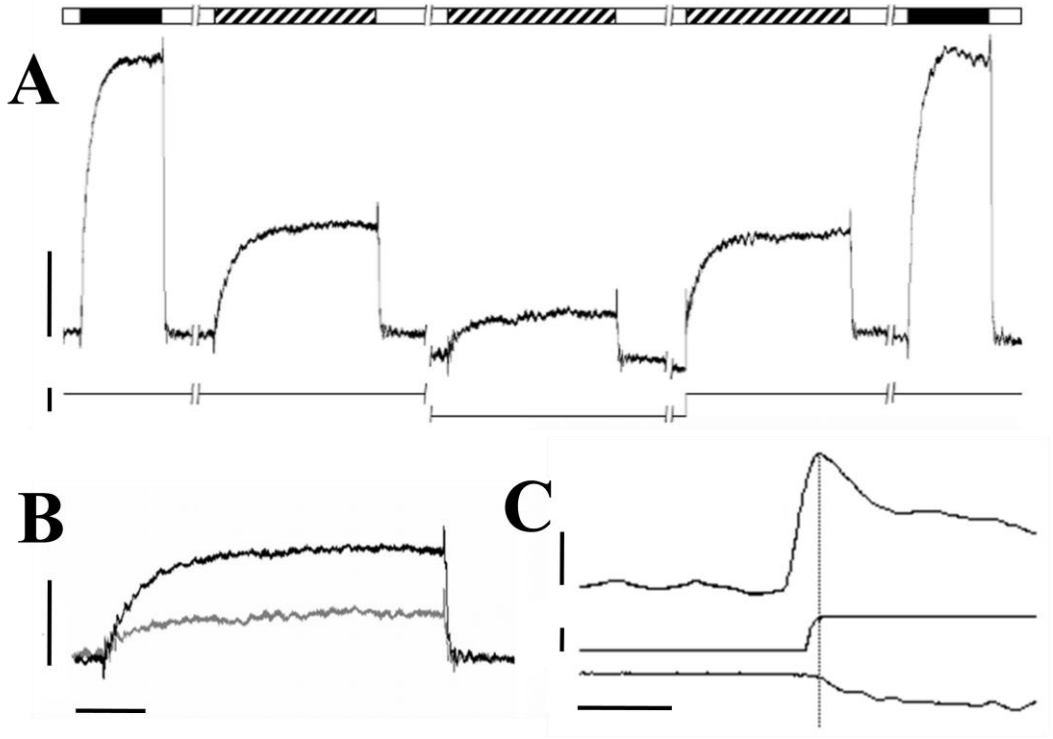

Figure 10. Temporal aspect of LDA methods. Panel A shows the five consecutive myofibril activation-relaxation cycles of a typical experiment. (open bar, pCa = 9;closed bar, pCa = 4.0; hatched bar, pCa = 5.7). Note the length signal on the bottom. Panel B is steady-state contractions at both short (SL = 2.0 μm) and long (SL = 2.3 μm) SL showing the robust length dependency of guinea pig myocardium. Panel C shows force (top), myofibril length (middle), and PMT output (bottom). By using the PMT we were able to time the rapid length change so that it would be completed at the same time as solution switch. Calibration bars: 40 nN for force, 0.15 L_0 for length, 2 seconds (B), and 200 ms (C).

submaximal force development strongly depends on SL. Normalized to the maximum force at SL = 2.3 μm, submaximal activation at steady-state short SL was, on average, 23 ± 2%, while submaximal activation at steady-state long SL resulted in 51 ± 6% force development. Final submaximal force development following a ~5 ms rapid stretch from short to long SL was not different compared to steady state (50 ± 5% and 51 ± 6% for rapid stretch and steady state respectively). As mentioned previously, the addition of inorganic phosphate increased activation and relaxation kinetics making them unresolveable. Therefore, to compare activation kinetics the time it took the fibers to reach 50% of submaximal steady state force (T_{50}) was measured. The rate of sub maximal force development was likewise not affected by the mode of contraction (T_{50}: 0.85 ± 0.04 and 0.84 ± 0.03 seconds for steady-state and rapid stretch, respectively).

Rapid stretch in the absence of Ca^{2+} activation resulted in a rapid increase in passive force during the stretch that subsequently decayed to the steady-state passive force seen at SL = 2.3 μm (Figure 11A, PF trace). Subtraction of the passive force response resulted in the traces shown in Figure 11B, where the SS trace represents the steady-state SL contraction and the AF trace represents only the active force following rapid SL stretch. The similarity between the traces illustrates that the processes that allows increased force and calcium sensitivity upon an increase in SL are complete within 5 ms.

2. **Stretches and Releases in the Absence of Phosphate**

In order to improve the stability of the preparation, the previous 5ms stretches were done in the presence of 2 mM inorganic phosphate. The increased stability presumably results from an overall lowering force development, which decreases rundown. When less than 2 mM inorganic phosphate was added, myofibrils exhibited a linear decrease in steady-state force,

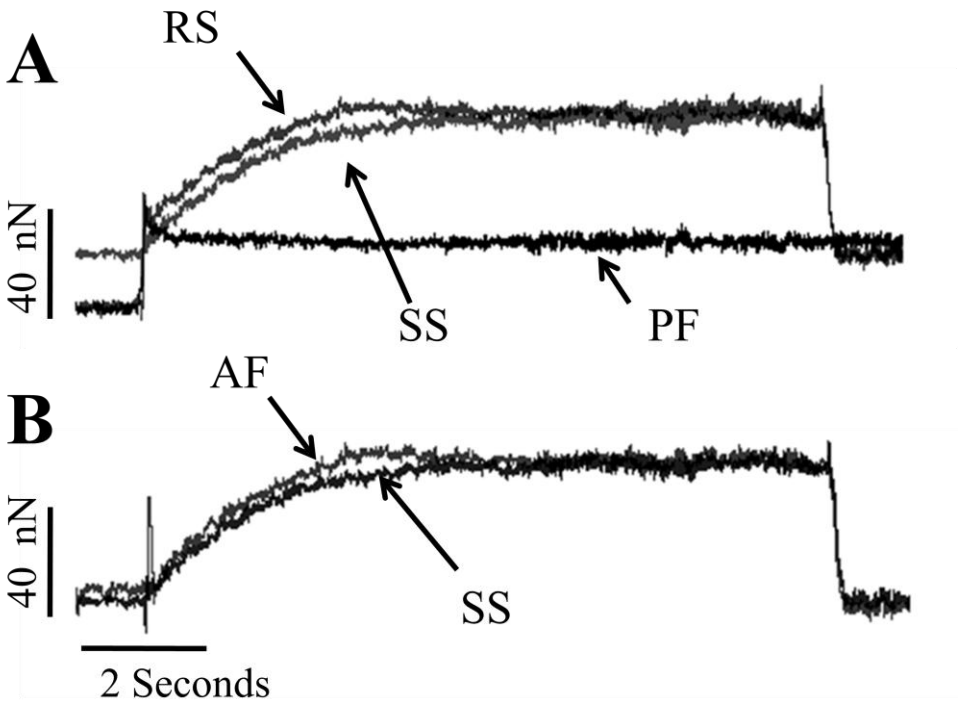

Figure 11. 5ms rapid stretches. Panel A shows submaximal force at steady state SL = 2.3 µm (SS) or after a rapid stretch from steady-state SL = 2.0 µm (RS). Rapid stretching in the absence of Ca^{2+} activation resulted in a sharp increase in passive force (PF) which slowly decayed to the steady-state passive force exhibited at SL = 2.3 µm. Panel B shows the similarity between active force (AF, total force – passive tension) of a rapidly stretched fiber compared to steady-state force (SS).

whereas more than 2 mM simply depressed force further without any increase in myofibrillar integrity (Figure 11). Unfortunately, the inclusion of phosphate also increased contractile dynamics (Tesi, Colomo et al. 2000), thereby precluding an accurate assessment of relaxation kinetics. Therefore, to insure that the addition of inorganic phosphate did not qualitatively alter the results, additional experiments were done in the absence of inorganic phosphate by employing an enzymatic "phosphate mop" (Tesi, Colomo et al. 2000).

Removal of inorganic phosphate resulted in ~3 times slower contractile dynamics, which is consistent with previous reports (Tesi, Colomo et al. 2000) and also allowed slower SL ramp speeds, ~50 ms. The removal of phosphate also allowed for assessment of relaxation kinetics. In addition to rapid stretches, releases from SL = 2.5 μm to SL = 2.3 μm were also completed in the absence of phosphate.

The average dynamic parameters are summarized in Table I for fibers that were rapidly stretched or released in the absence of inorganic phosphate. On average, neither Ca^{2+} activation kinetics, final steady-state force, nor the biphasic relaxation kinetics were affected by contraction mode, be it rapid stretches or rapid releases. Representative traces of either rapidly stretched and rapidly released fibers are shown in Figure 12.

E. **Discussion**

Length dependent activation can be seen as the increase in force for a given level of activating calcium upon an increase in sarcomere length. The purpose of this study was to investigate the effect of very rapidly stretching a muscle to a long SL compared to a muscle that has been held at the same long SL for five minutes. We found that rapidly stretching (or releasing) a cardiac myofibril has no effect on submaximal force, activation kinetics, calcium

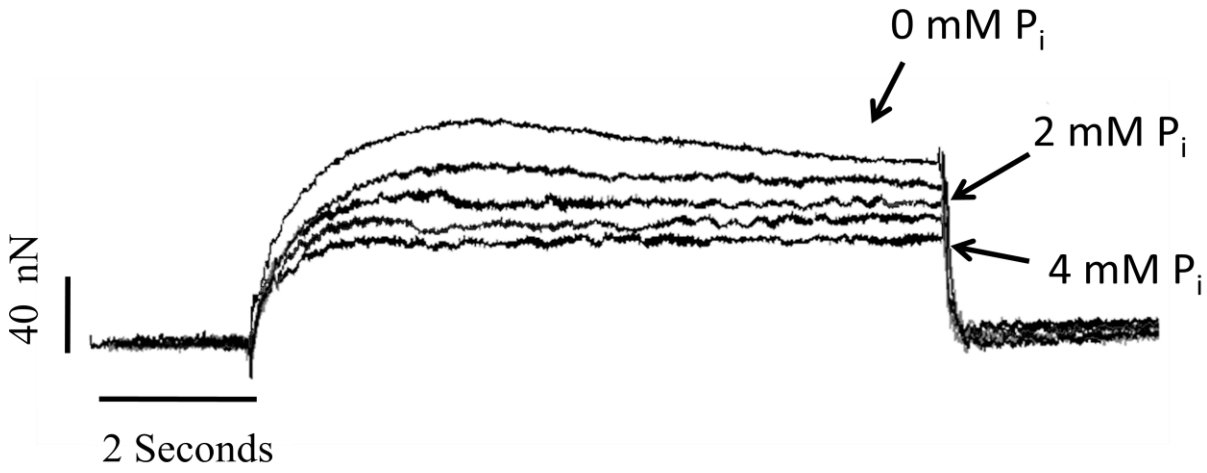

Figure 12. Effect of inorganic phosphate concentration on force rundown. Zero and 1 mM inorganic phosphate (P_i) show rundown, whereas 2, 3, and 4 mM do not exhibit any rundown.

		SL (μm)	$T_{sub\text{-}max}$ (% T_{max})	T_{50} (s)	k_{LIN} (s^{-1})	t_{LIN} (ms)	k_{EXP} (s^{-1})
Stretch	**Steady State**	2.30 ± 0.01	42 ± 3.0	2.9 ± 0.4	2.2 ± 0.4	0.10 ± 0.01	11 ± 1.1
	Rapid Stretch	2.33 ± 0.01	44 ± 4.1	3.0 ± 0.7	2.2 ± 0.4	0.11 ± 0.01	11 ± 0.9
Release	**Steady State**	2.30 ± 0.01	30 ± 3.8	3.4 ± 0.4	2.4 ± 0.2	0.12 ± 0.01	12 ± 1.2
	Rapid Release	2.28 ± 0.01	29 ± 4.4	3.2 ± 0.5	2.2 ± 0.3	0.12 ± 0.02	12 ± 1.3

Table I. Submaximal activation and relaxation kinetics for rapidly stretched and released myofibrils. Activation and relaxation dynamic parameters for steady-state (SL=2.3 μm) and rapidly stretched (from SL=2.0 μm) or released (from SL=2.5 μm) contractions in the absence of inorganic phosphate. Values shown are the means (± S.E.M.) of sub-maximal tension (measured at pCa 5.8, $T_{sub\text{-}max}$), activation kinetics (T_{50}), and relaxation kinetics (k_{LIN} , t_{LIN} , k_{EXP}).

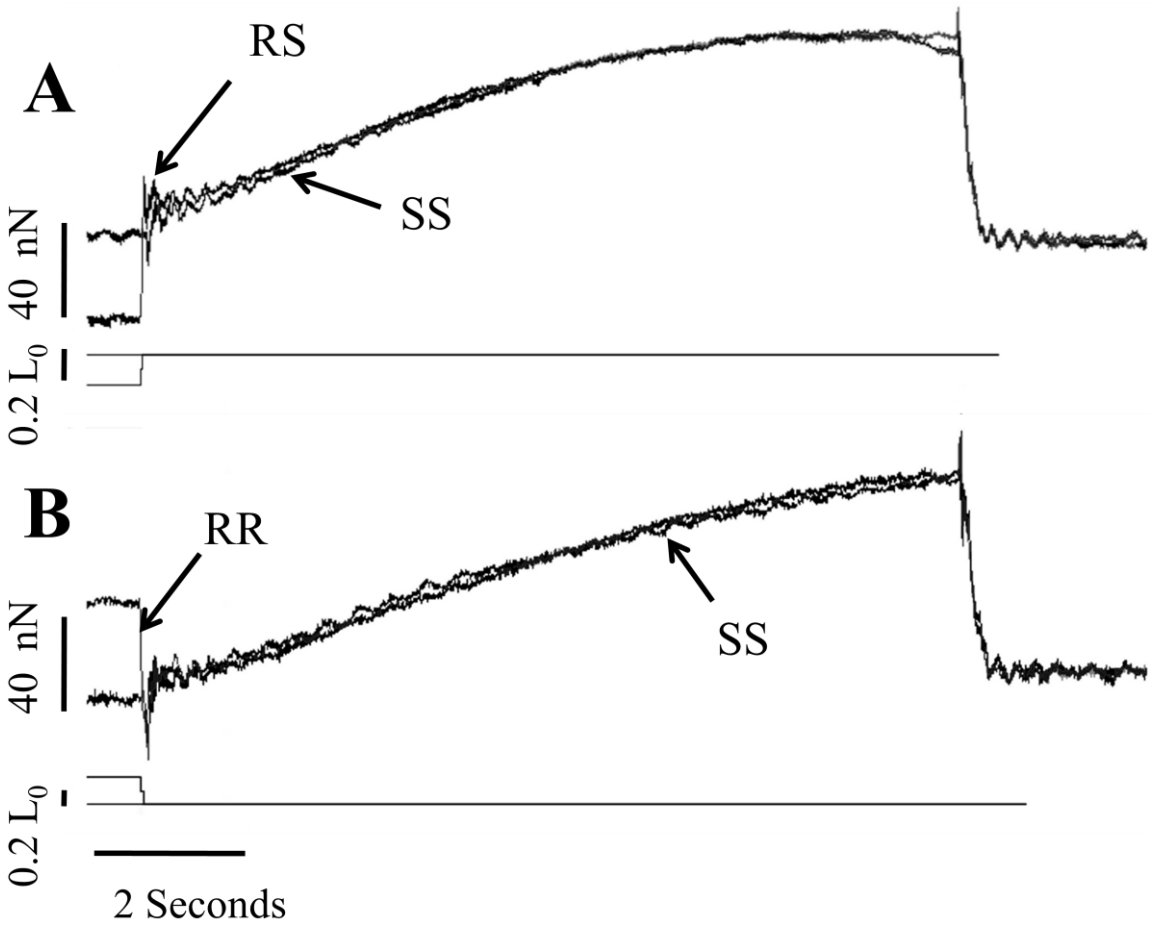

Figure 13. Representative force traces of rapidly stretched or released myofibrils in the absence of inorganic phosphate. Panel A shows submaximal force at steady-state SL = 2.3 μm (SS) or after a rapid stretch (RS) from steady-state-state SL = 2.0 μm. Panel B shows submaximal force at steady-state SL = 2.3 μm (SS) or after a rapid release from steady-state SL = 2.5 μm (RR).

sensitivity and therefore the extent of LDA exhibited. This was true in both the presence and absence of inorganic phosphate. The results from the current study indicate that the molecular processes that lead to myofilament LDA are complete within ~5 ms. That is, transduction of the SL signal to alter the Ca^{2+} responsiveness of the contractile apparatus in the heart is virtually instantaneous.

The force response of small-amplitude stepwise changes in length in active muscle is composed of two dynamic variables, distortion and recruitment (Ford, Chandra et al. 2010). The large force spike following a quick stretch is thought to be dominated by distortion dynamics. Distortion is mainly be due to the stretching of extensible regions in currently attached crossbridges, and is seen as the sharp increase in force. Then, as those attached crossbridges begin to detach force starts decaying back to pre-stretch levels, recruitment dynamics begin to dominate over distortion dynamics. Recruitment dynamics are thought to be due to the recruitment of new cross-bridges that were not attached during the stretch, which increases force until a new steady-state is reached at the new length. Altered cross-bridge recruitment following a change in length is not thought to be instantaneous; other groups have estimated that in rabbit myocardium at 25°C there is a ~100ms delay between the change in length and the subsequent change in cross-bridge recruitment (Campbell, Taheri et al. 1993; Ford, Chandra et al. 2010). I hypothesized that a delay in LDA would result in delayed cross-bridge recruitment following a rapid stretch compared to steady-state, which was not evident. Here, we used guinea-pig myocardium which contains almost exclusively the slower beta isoform of myosin, which is similar to what is found in the rabbit myocardium used previously. Additionally, these experiments were done at significantly lower temperatures than the previous study. Therefore, it is unlikely that we were unable to detect such a significant delay in LDA.

Are the force responses here governed by the same distortion and recruitment variables? Most likely, the distortion variable contains not only Ca^{2+} activated processes such stretching of attached cross-bridges, but also passive processes, such as the smaller forces that are provided by the stretching of titin. Since these muscles were stretched *prior* to activation, only passive forces would contribute to distortion dynamics, which is evident by the blunted spike in force immediately following the stretch compared to previous experiments where fibers were stretched while activated. Furthermore, force traces of the steady-state fibers would not contain a distortion component at all, and only recruitment of new crossbridges would contribute to force. Therefore, if passive tension (distortion component) is subtracted from the rapidly stretched fibers it would be expected to appear the same as the steady state (recruitment only), which it very closely does (Figure 11B). Taken together, it seems like the length sensing mechanism and subsequent alterations that allow an increase in force and calcium sensitivity occur nearly instantaneously, and the rate limiting factor in LDA is crossbridge cycling.

The virtually instantaneous (within ~5 ms) LDA suggests that the mechanism might result from a length induced geometric rearrangement of either thick and/or thin filament regulatory proteins. In order for this to occur, there must be some mechanism to rapidly transmit alterations in strain along both the thick and thin filament. Naturally, titin might play a role in the transmission of strain on account that it starts at the Z-line, goes along the I-band region of the thin filament before crossing over to the thick filament, finally ending near the M-band. This allows strain to travel between the thick and thin filament in the absence of cross-bridge attachment. There are most likely many mechanisms along both the thick and thin filaments that allow LDA to occur since recently our lab showed that upon an increase of SL (2.3 μm) there were structural changes in both the thick and thin filaments compared to slack length (~1.9 μm)

as assessed by x-ray diffraction (Hsu, Mou et al. 2012). Titin has been shown to alter the thick filament upon increases in SL through such mechanisms as relieving crossbridge strain (Muhle-Goll, Habeck et al. 2001) or by moving myosin heads radially inward towards the thin filament (Farman, Gore et al. 2011). Titin has also been shown to bind the thin filament near the I-band, and might alter thin filament structure. Lastly, the role of titin stiffness and extent of LDA has been reported extensively, with increased stiffness causing increased LDA, implicating a role of titin strain on transmitting LDA (Cazorla, Wu et al. 2001; Piroddi, Belus et al. 2007; Ait Mou, le Guennec et al. 2008; Patel, Pleitner et al. 2011). Overall, our results suggest that LDA results from instantaneous length induced geometric rearrangement of either thin filament regulatory proteins, thick filament proteins, or a combination of these structures.

IV. Impact of Titin Isoform on Length Dependent Activation and Cross-Bridge Cycling Kinetics

A. Abstract

The magnitude of length dependent activation (LDA) exhibited in striated muscle has been shown to vary with titin isoform (Piroddi, Belus et al. 2007; Patel, Pleitner et al. 2011). Recently, a rat that harbors a homozygous autosomal mutation (HM) causing preferential expression of a longer, giant titin isoform was discovered (Greaser, Krzesinski et al. 2005). Here, we investigated the impact of titin isoform on myofilament force development and cross-bridge cycling kinetics as function of sarcomere length (SL) in tibialis anterior skeletal muscle isolated from wild type (WT) and HM rats. Skeletal muscle bundles from HM rats exhibited reductions in passive tension, maximal force development, myofilament calcium sensitivity, maximal ATP consumption, and tension cost at both short and long sarcomere length (SL=2.8 μm and SL=3.2 μm, respectively). Moreover, the SL-dependent changes in these parameters were attenuated in HM muscles. Additionally, myofilament Ca^{2+} activation-relaxation properties were assessed in single isolated myofibrils. Both the rate of tension generation upon Ca^{2+} activation (k_{ACT}) as well as the rate of tension redevelopment following a length perturbation (k_{TR}) were reduced in HM myofibrils compared to WT, while relaxation kinetics were not affected. Furthermore, since LDA is most prominent in cardiac tissue, we examined the SL dependence of Ca^{2+} force production in trabeculae from WT and HM rats at two SL's. Increasing SL from 2.1 μm to 2.2 μm caused an increase in maximal force development and calcium sensitivity in WT trabeculae, which was blunted in the HM tissue. We conclude the presence of a long isoform of titin in the striated muscle sarcomere is associated with reduced

myofilament force development and cross-bridge cycling kinetics, and a blunting of myofilament length dependent activation.

B. **Introduction**

Spanning each half sarcomere from the Z disk to the M band, titin is the largest and third most abundant protein in mammalian striated muscle (Tskhovrebova and Trinick 2003). Additionally, because adjacent titin filaments overlap in both the Z disk and the M band, titin effectively forms a continuous filament along an entire myofibril (Obermann, Gautel et al. 1996). The A-band region of titin is inextensible and contains super-repeats of immunoglobulin (Ig) and fibronectin type 3 (fn3) modules (Labeit and Kolmerer 1995). The stretching of titin upon increases in sarcomere length (SL) occurs in the I-band region that includes extensible regions consisting of tandemly arranged Ig-like domains, PEVK segments (rich in proline [P], glutamate [E], valine [V], and lysine [K]) and an N2 region (containing either N2B or N2A unique amino acid sequences) (Labeit and Kolmerer 1995). While it is expressed from a single gene, alternative splicing of titin mRNA in the I-band region allows for expression of different titin isoforms of varying size. Therefore, it is by altering the length of the extensible I-band regions that titin isoforms of varying stiffness are obtained.

The components, and therefore the length, of the N2 sequence largely differentiate titin isoforms. There are two unique N2 sequences in striated muscle, a cardiac specific N2B sequence, and due to having more Ig domains and a longer PEVK region, a longer N2A sequence that can be found in both cardiac and skeletal muscle (Labeit and Kolmerer 1995). Even though skeletal muscle contains only the N2A region, it still expresses two titin isoforms; a longer isoform that is found in slow skeletal muscle, and a shorter isoform that is found in fast

skeletal muscle. Since titin acts as a "molecular spring" which provides a restoring force when a muscle is stretched, the longer titin isoforms found in slow skeletal muscles causes it to produce lower passive tension for a given change in SL than the shorter ones found in fast skeletal muscle (Neagoe, Opitz et al. 2003). Cardiac muscle not only contains the N2B isoform, but also a longer N2BA isoform which is comprised of both the N2B and N2A sequences. The addition of the N2A segment essentially adds another elastic element along with the N2B segment. This allows for lower passive tension at all SL's in muscles preferentially expressing the N2BA isoform in contrast to muscles that more highly express the N2B isoform. When compared to skeletal muscle, cardiac muscles I-band region of titin is shorter, causing it to produce much higher passive tension.

Due to the spanning the entire half sarcomere and having interactions with both the thick and thin filaments, titin is thought to play a role in myofilament length dependent activation. Length dependent activation (LDA) is characterized by an increase in maximal Ca^{2+} activated force and calcium sensitivity upon an increase in SL, which is particularly important in the heart where the mechanism underlies the Frank-Starling Law of the heart (de Tombe, Mateja et al. 2010). While the precise mechanism underlying LDA is unknown, many studies have shown that the amount of passive stiffness in a specific muscle type or preparation correlates to the amount of LDA exhibited (Cazorla, Wu et al. 2001; Fukuda, Wu et al. 2003; Piroddi, Belus et al. 2007; Ait Mou, le Guennec et al. 2008). This implicates titin as playing a pivotal role in myofilament length dependent activation since in skeletal muscle and permeabilized cardiac preparations, titin bears nearly all of the passive tension within physiological SL's (Horowits, Kempner et al. 1986; Greaser, Krzesinski et al. 2005). Furthermore, reducing the amount of passive tension carried by titin, either by specific degradation using trypsin or by modifying the

muscles history dependence of stretch, has shown to greatly reduce or eliminate LDA (Helmes, Trombitas et al. 1996; Cazorla, Wu et al. 2001).

To investigate the contribution of titin based passive stiffness in LDA, we utilized a rat that harbors a homozygous autosomal mutation (HM) causing preferential expression of a giant N2BA-G titin isoform. In the rat, titin undergoes developmental isoform changes; the longest isoforms are expressed during the embryonic stages and progressively get replaced by shorter isoforms (Greaser, Krzesinski et al. 2005). A recent investigation on the length of the titin isoforms in various muscles during development in both wild-type (WT) and HM rats showed that among all of the skeletal muscle examined in WT rats, the tibialis anterior (TA) undergoes the greatest extent of developmental shortening (Li, Guo et al. 2011). The TA titin isoform starts out at 3.7 MDa after birth, and by 180 days there are two shorter isoforms present, a 3.42 MDa isoform and a more abundant 3.29 MDa isoform. Only further developmental shortening is seen in rat cardiac titin, which shortens from 3.7 MDa to 2.9 MDa during development. Due to the lack of normal developmental isoform shortening, HM rats maintain the much longer N2BA-G titin isoform in both the TA (3.7 MDa) and in the heart (3.8 MDa) (Warren, Krzesinski et al. 2004; Li, Guo et al. 2011). Accordingly, we investigated the SL dependence of Ca^{2+} activated force production and ATP consumption in both WT and HM TA skeletal muscle bundles. Then, to examine the effect of titin isoform on cross-bridge cycling kinetics, we measured the rates of maximal activation and relaxation in WT and HM tibialis anterior myofibrils. Furthermore, since LDA is most prominent in the heart, we explored the SL dependence of Ca^{2+} force production in WT and HM right ventricular trabeculae.

C. Methods

1. Generation of Homozygous Mutant Rats

The rats used here were fortuitously discovered by Dr. Greaser while studying alternative splicing during development in rat cardiac titin (Greaser, Krzesinski et al. 2005). They noticed a litter of Sprague-Dawley rats that did not exhibit the normal developmental shortening of titin observed with samples from other rats. Originally they assumed that the atypical samples were due to regional diversity in the heart, but resampling provided the same results. Since the longer titin samples all came from the same litter, they suspected the aberration might originate genetically. After accidental breeding of littermates resulted in a few pups who all expressed the longer titin, the group successfully bred rats from the original litter into a homozygous strain where all progeny expressed this longer form of titin. This was accomplished by breeding the original Sprague-Dawley rats with Fisher 344 inbreeds, and then with Brown-Norway rats. Therefore, the current rats were 25% Sprague Dawley, 25% Fisher 344 and 50% Brown Norway, who all contained a homozygous autosomal mutation which caused altered alternative splicing resulting in expression of much longer titin isoforms than found in WT rats.

2. Titin Isoform and Myofilament Protein Expression

To determine titin isoform expression in both WT and HM TA muscle, TA homogenate samples were suspended in SDS sample buffer and underwent electrophoresis using vertical SDS agarose gels designed for high molecular weight protein separation as described previously (Warren, Krzesinski et al. 2003). Additionally, to assess the lower molecular weight

myofilament proteins, homogenates samples were separated using standard SDS-PAGE (12%); gels were stained with Coomassie blue.

D. Results

1. Titin Isoform and Myofibrillar Protein Expression Profile

Figure 14A shows a typical agarose SDS gel analysis of rat tibialis anterior muscle (TA). As has been reported previously, wild-type (WT) TA expresses two titin isoforms at ~3.44 MDa and ~3.30 MDa, while homozygous (HM) muscles express the much larger titin isoform at ~3.75 MDa (Li, Guo et al. 2011). As is illustrated by the SDS-PAGE analysis in Figure 14B, overall myofilament protein expression was comparable between WT and HM TA muscles.

2. Passive Tension Development

Fiber bundles and single myofibrils of both WT and HM muscles were stretched over a range of SL's (~2.5 μm to ~4 μm) and passive tension was recorded several seconds following each SL change, that is, at a time when a large component of immediate stress relaxation had dissipated. Passive tension was recorded in both fiber bundles and single myofibrils; Figure 15A illustrates a WT (top) and HM (bottom) single myofibril at short (SL = 2.8 μm) sarcomere length. Additionally, passive tension was measured in trabeculae from both WT and HM rats similarly, albeit over a shorter range of SL's (~2.0 μm to ~2.5 μm). As illustrated in Figure 15, passive tension was markedly reduced at all sarcomere lengths in TA bundles (Panel B), single myofibrils (Panel C), and trabeculae (Panel D) in HM compared to WT

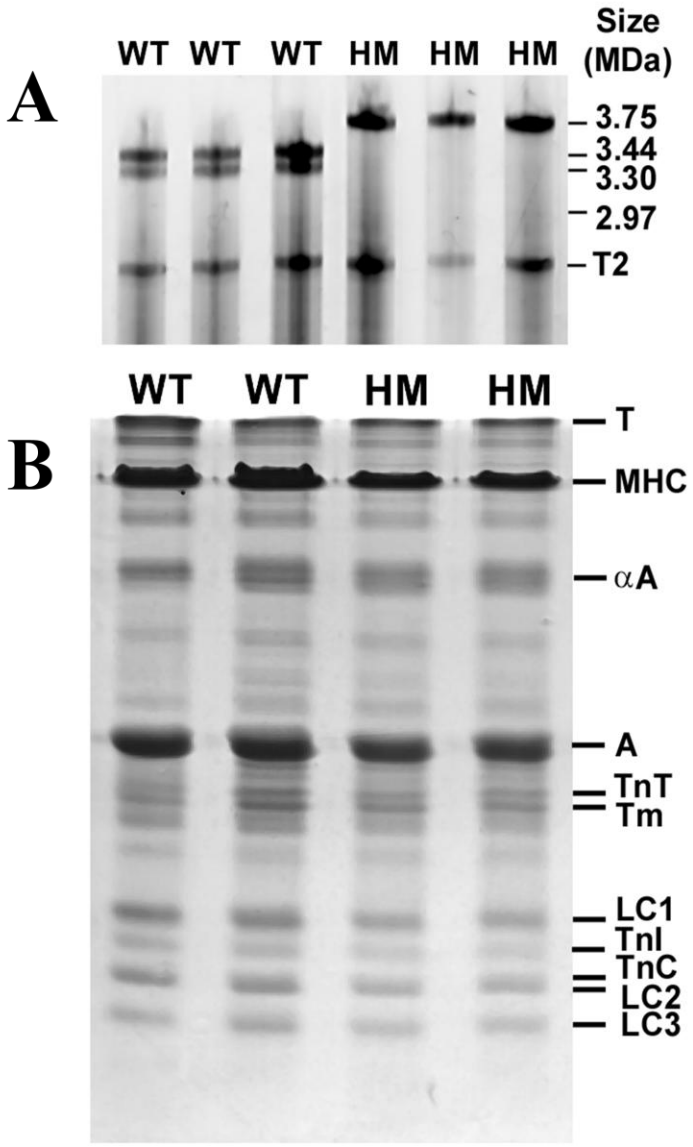

Figure 14. Protein composition SDS-PAGE analysis of Tibialis Anterior . Panel A shows how homozygous mutant (HM) TA muscle expresses a single titin isoform that is significantly larger than the two major isoforms expressed in wild-type (WT) Tibialis Anterior (TA) muscle. T2 is a titin breakdown product which was similar in size between the WT and HM muscles. Panel B shows there were no differences in myofilament contractile proteins between WT and HM muscle. T, titin; MHC, myosin heavy chain; αA, alpha actin; TnT, troponin T; Tm, tropomyosin; LC1, myosin light chain 1; TnI, troponin I; TnC, troponin C; LC-2, myosin light chain 2; LC-3, myosin light chain 3.

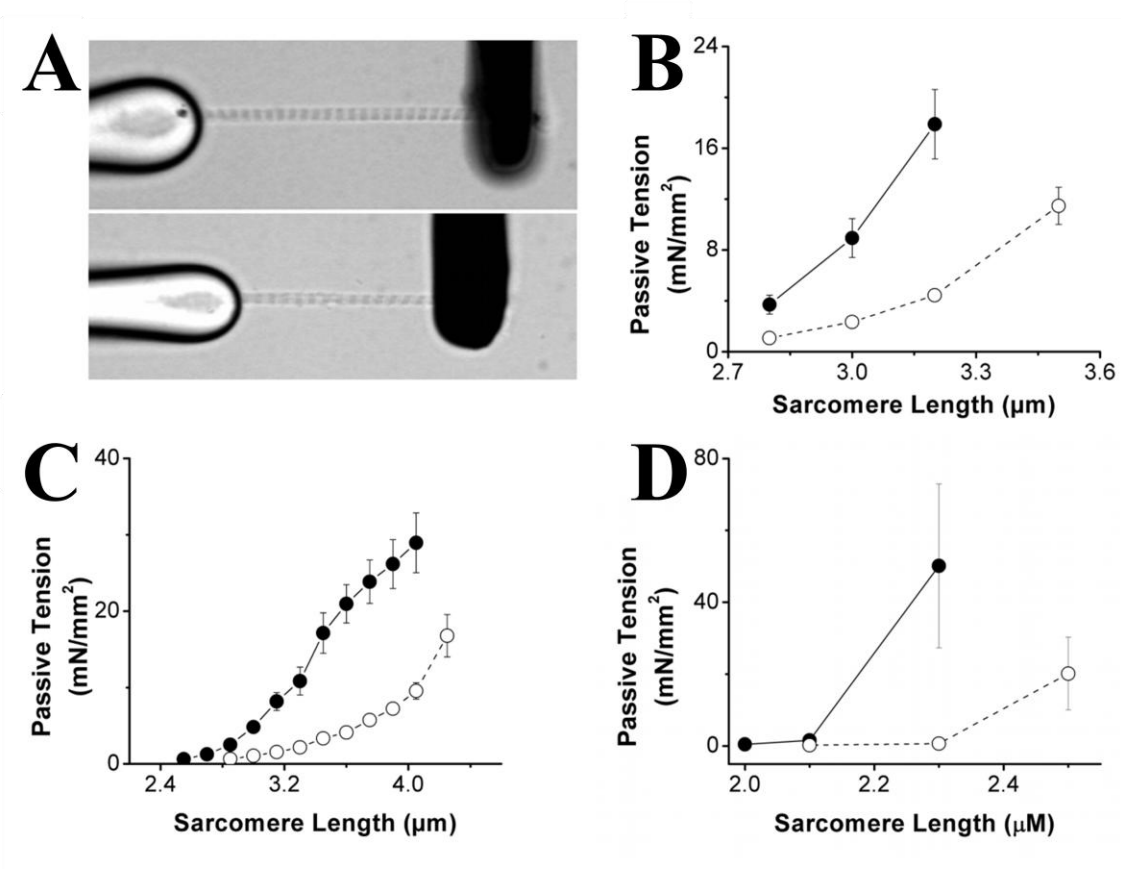

Figure 15. Passive Tension in WT and HM muscles. Panel A shows a WT (top) and HM (bottom) single myofibril at short SL (SL = 2.8 μm). Passive tension as a function of SL is shown for TA single myofibrils (Panel B), TA fiber bundles (Panel C) and trabeculae (Panel D). Passive tension was significantly reduced in HM (dashed lines, open symbols) compared to WT (solid lines, closed symbols) preparations.

preparations. This significant depression in the passive force-SL relationship in the HM group is consistent with the longer titin isoform (N2BA-G) expressed in HM muscles compared to the shorter isoforms found in the TA (N2A skeletal specific) or trabeculae (predominantly N2B) WT preparations.

3. **Tension and ATPase Activity in TA Fiber Bundles**

Tension development and ATPase activity were measured in fiber bundles of WT and HM TA muscles as illustrated in Figure 16A for a contraction at maximum saturated [Ca^{2+}] and SL = 2.8 μm. Upon activation, tension development (top panel) increases towards steady state concomitant with a reduction in [NADH] (bottom panel) in the measurement chamber, indicative of ATP consumption by active cycling cross-bridges. As this typical example illustrates, both steady state tension and ATP consumption rate were significantly reduced in the HM fiber bundle compared to the WT fiber bundle. That this was the case at all [Ca^{2+}] studied is shown by the force-Ca^{2+} relationships shown in Figure 16B indicating, on average, maximum tension development was ~25% lower in the HM fiber group. Moreover, the entire force-Ca^{2+} relationship was displaced to lower [Ca^{2+}] (~0.06 pCa units) indicating decreased myofilament calcium sensitivity in the HM fiber group. There were no differences in the level of cooperativity, as indexed by the Hill coefficient, between the WT and HM fiber groups.

Maximum ATPase activity was, on average, ~40% lower in the HM fiber group (not shown). Tension-cost, the amount of ATP consumed as function of tension development over a range of [Ca^{2+}], was on average ~25% lower in the HM group as shown in Figure 16C. This result is consistent with the larger reduction in ATPase activity than tension development

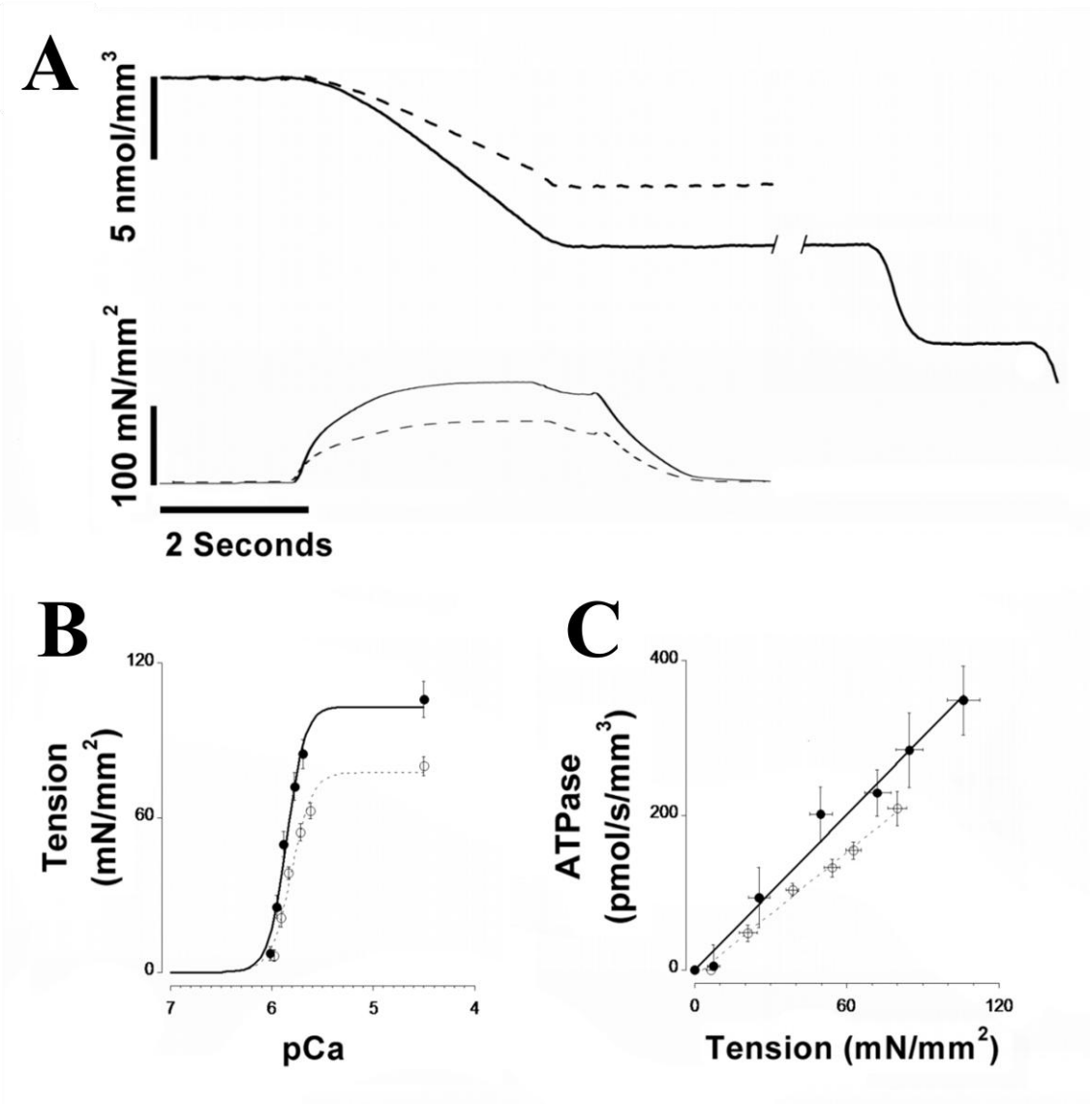

Figure 16. Tension development, ATPase activity, and tension cost in fiber bundles. Multi-cellular skinned fiber bundles were prepared from WT (solid line and closed symbols) and HM (dashed line and open symbols). Panel A shows typical recordings of [NADH] (top trace) and tension development (bottom trace). Upon activation of the fiber bundle, tension develops concomitant with reduction of [NADH], indicative of increased ATPase activity by the muscle. Following removal of the fiber bundle from the measurement chamber, [NADH] is calibrated by repeated injections of 500 pmol ADP (shown for the WT trace only). Panel B shows average tension-Ca^{2+} relationships, while panel C shows average tension-ATPase relationships obtained in the WT and HM fiber bundles. HM fiber bundles exhibited reduced tension development, myofilament Ca^{2+} sensitivity, and tension-cost. Temperature, 20 °C; SL=2.8 μm.

indicating a reduction in cross-bridge cycle kinetics (Brenner 1988; Wannenburg, Janssen et al. 1997; Rundell, Manaves et al. 2005) in myofilaments containing the larger titin mutant. There were no differences in stiffness relative to tension development between WT and HM fiber groups. Accordingly, it can be assumed that any differences ATPase consumption rate were not due to changes in force generation per cycling cross-bridge (Rundell, Manaves et al. 2005).

4. **Impact of Sarcomere Length in Fiber Bundles**

Increasing SL from 2.8 μm to 3.2 μm resulted in increased (~10%) maximum tension development (Figure 17A) and significantly increased myofilament Ca^{2+} sensitivity (+0.05 pCa units; Figure 17B) in the WT fiber bundles, consistent with robust myofilament length dependency properties in WT muscles. In contrast, increased SL in HM fiber bundles was associated with a reduced increase in maximum tension (~7.5%) and lack of a significant change in myofilament Ca^{2+} sensitivity (+0.2 pCa units). SL did not affect maximum ATPase activity (Figure 17C) in either muscle group, while tension cost (Figure 17D) was significantly reduced upon an increase in SL only in the WT muscle group to approach values recorded for the HM muscle at either SL. Thus, myofilament length dependent activation properties were recorded in WT fiber bundles, and these properties were significantly blunted in the HM fiber bundles.

5. **Activation and Relaxation Kinetics in Myofibrils**

Activation-relaxation force kinetics were studied in single myofibrils to further assess cross-bridge cycle kinetics. The method is illustrated in Figure 18A. Upon rapid solution switch to the activating solution, myofibril tension increases exponentially to reach steady at which time a rapid release-restretch maneuver is used to measure tension redevelopment rate,

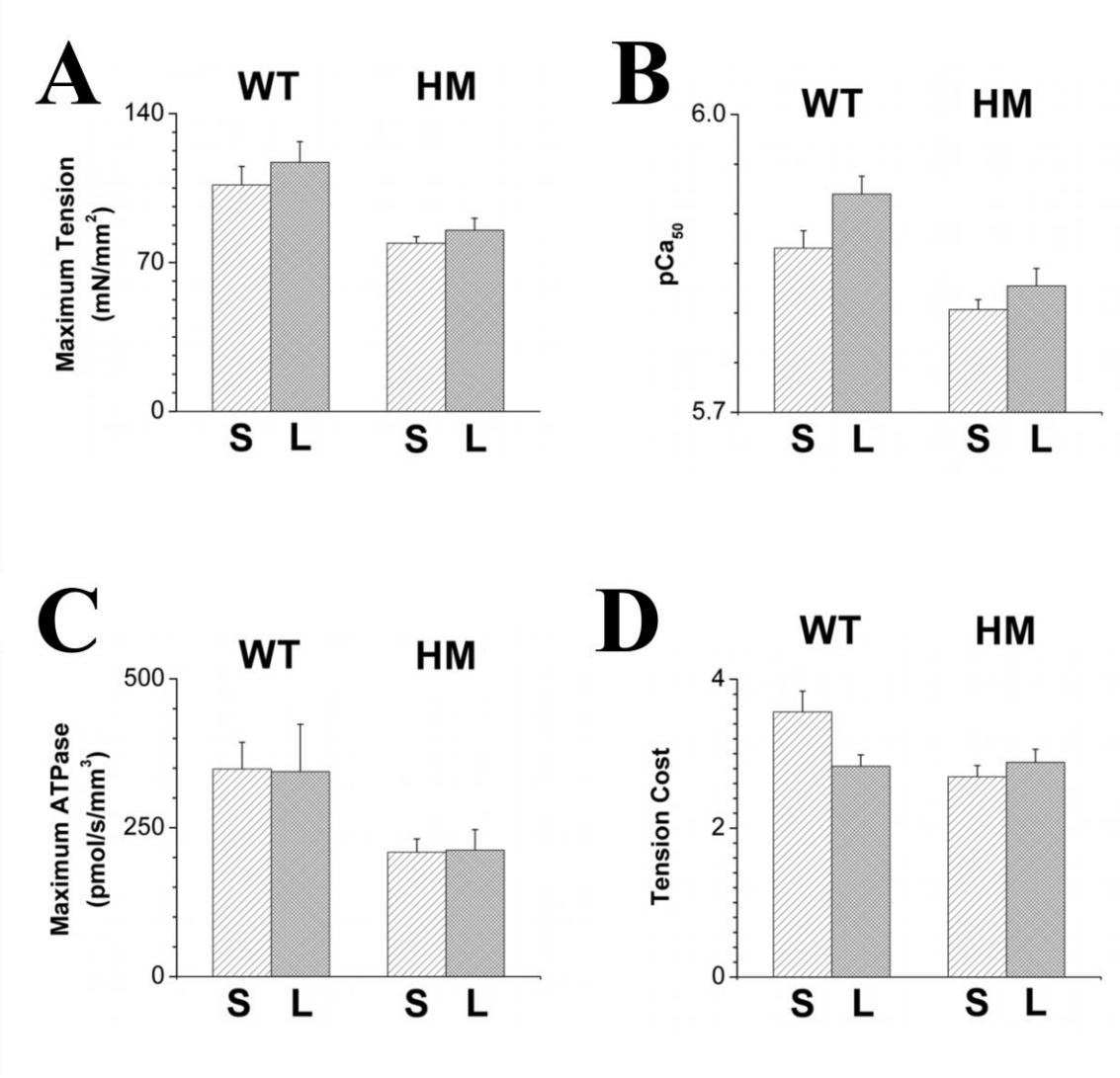

Figure 17. Impact of sarcomere length in fiber bundles. Tension-Ca^{2+} and tension-ATPase relationship were measured in WT (light bars) and HM (dark grey bars) fiber bundles at short (S, SL = 2.8 μm) and long (L, SL = 3.2 μm) sarcomere length. Maximum tension (panel A), calcium sensitivity (panel B), maximum ATPase (panel C) and tension-cost (panel D) were reduced in HM compared to WT fiber bundles at short and long SL. Presence of the shorter isoform in the WT fiber bundles was associated with robust myofilament length dependent activation of maximum tension, calcium sensitivity, and tension-cost that was blunted in the HM fiber bundles.

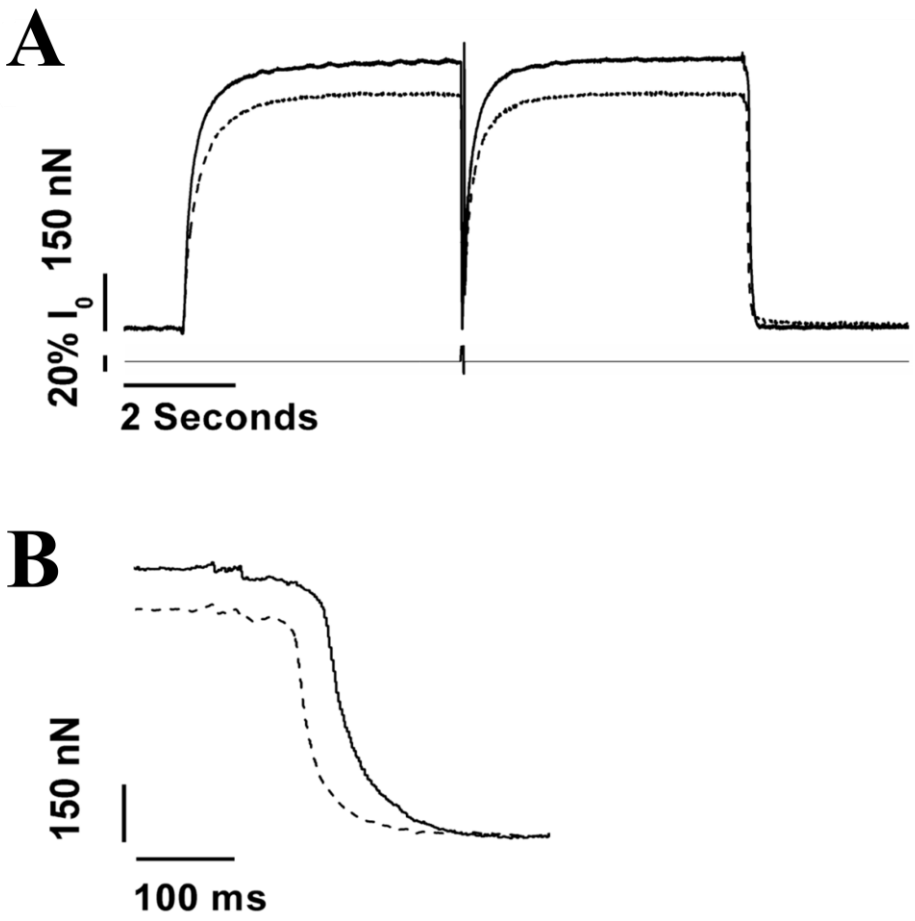

Figure 18. Activation-relaxation kinetics by fast solution switching in single myofibrils. Panel A shows typical tension recordings from an activation/relaxation cycle in wild type (solid line) or homozygote mutant (dashed line) TA single myofibrils. Upon Ca^{2+} activation, tension increased exponentially towards steady state, at which time a quick release-restretch protocol (20% muscle length) was employed to assess exponential tension redevelopment rate. Upon rapid removal of activating Ca^{2+}, tension relaxation follows a biphasic pattern as illustrated by the expanded traces in panel B. HM myofibrils displayed reduced maximum tension and reduced activation kinetics. Temperature 15 ^{o}C; SL = 2.8 μm.

k_{TR}. Upon rapid solution switch back to the relaxation solution, tension relaxes in a biphasic fashion, as has been reported previously (Stehle, Kruger et al. 2002; Tesi, Piroddi et al. 2002), first following a close to linear trajectory at a relatively slow rate, followed by a faster exponential phase. This portion of the activation-relaxation cycle is shown more clearly by the expanded traces shown in Figure 18B. Activation (k_{ACT}), k_{TR}, and the rapid relaxation phase (k_{EXP}) kinetics were estimated by exponential fits to the tension data, while the slow linear relaxation kinetics were estimated by linear regression fit of the tension data. The average fit parameters are summarized in Table II. As was the case in the multicellular fiber bundles (cf. Figure 17A), maximum tension development was significantly reduced (~25%) in HM compared to WT myofibrils. Moreover, tension development kinetics, for both Ca^{2+} activation (k_{ACT}) and tension redevelopment (k_{TR}), were reduced by ~20% in the HM myofibrils, consistent with the 25% reduction in tension-cost measured in multicellular fiber bundles (cf. Figure 17D). On the other hand, there were no differences in rate parameters between the WT and HM myofibrils for both the slow linear phase and the faster exponential phase of relaxation. There was a small (~8%), albeit non-significant, decrease in the duration of the linear relaxation phase in the HM myofibrils.

	Maximum Force (mN/mm^2)	**k_{ACT} (s^{-1})**	**k_{TR} (s^{-1})**	**k_{LIN} (s^{-1})**	**t_{LIN} (ms)**	**k_{EXP} (s^{-1})**
WT Short	110 ± 10	3.26 ± 0.16	4.07 ± 0.16	2.44 ± 0.18	130 ± 10	31 ± 2.0
HM Short	80 ± 10 †	2.64 ± 0.24 †	3.30 ± 0.27 †	2.40 ± 0.14	120 ± 10	34 ± 4.7

† HM values are significantly different from WT

Table II. Mean measurements of wild-type and homozygous mutant tibialis anterior myofibrils at SL = 2.8 μm. Values shown are means (± S.E.M.) of maximal Ca^{2+} activation (pCa 4.0), activation kinetics (k_{ACT}, k_{TR}), and relaxation kinetics (k_{LIN}, t_{LIN}, k_{EXP}). Significance was determined at $P<0.05$

6. **Impact of Sarcomere Length in Trabeculae**

Tension development was measured in WT and HM trabeculae at two SL's, mean values are reported in Table III. Increasing SL from 2.1 μm to 2.3 μm resulted in a ~15% increase in maximum tension development, and increased myofilament Ca^{2+} sensitivity by 0.08 pCa units in the WT trabeculae. The increased length dependency in WT trabeculae compared to WT TA bundles is consistent with cardiac muscle having an increased sensitivity to changes in length than skeletal muscle (Allen and Kentish 1985). In contrast, HM tissue exhibited reduced increases in maximum tension (~9%) and Ca^{2+} sensitivity (0.02 pCa units) following an increase in SL. There were no differences in stiffness relative to tension development between WT and HM trabeculae, so it can be assumed that any differences tension development were not due to changes in force generation per cycling cross-bridge (Rundell, Manaves et al. 2005). Overall, HM trabeculae expressing a longer titin isoform exhibited blunted length dependent activation compared to WT trabeculae.

		T_{max} (mN/mm^2)	pCa_{50}	n_H	Stiffness
WT	Short	39 ± 3.5	5.58 ± 0.02 *	6.50 ± 0.98	1.01 ± 0.25
	Long	46 ± 3.7	5.66 ± 0.02	4.15 ± 0.50	0.86 ± 0.16
HM	Short	32 ± 2.7 †	5.56 ± 0.03 †	6.74 ± 0.54	1.11 ± 0.30
	Long	35 ± 2.0 †	5.58 ± 0.03 †	5.46 ± 0.62	0.81 ± 0.21

† HM values are significantly different from WT
* long is significantly different than short

Table III. Mean force-Ca^{2+} -relationship parameters obtained from WT and HM trabeculae at short (SL = 2.1 μm) and long (SL = 2.3 μm) lengths. Values are expressed as means (± S.E.M.) of maximal Ca^{2+} activation (pCa 4.0, T_{max}), calcium sensitivity (pCa_{50}), the hill coefficient (n_H) and stiffness. Significance was determined at $P<0.05$

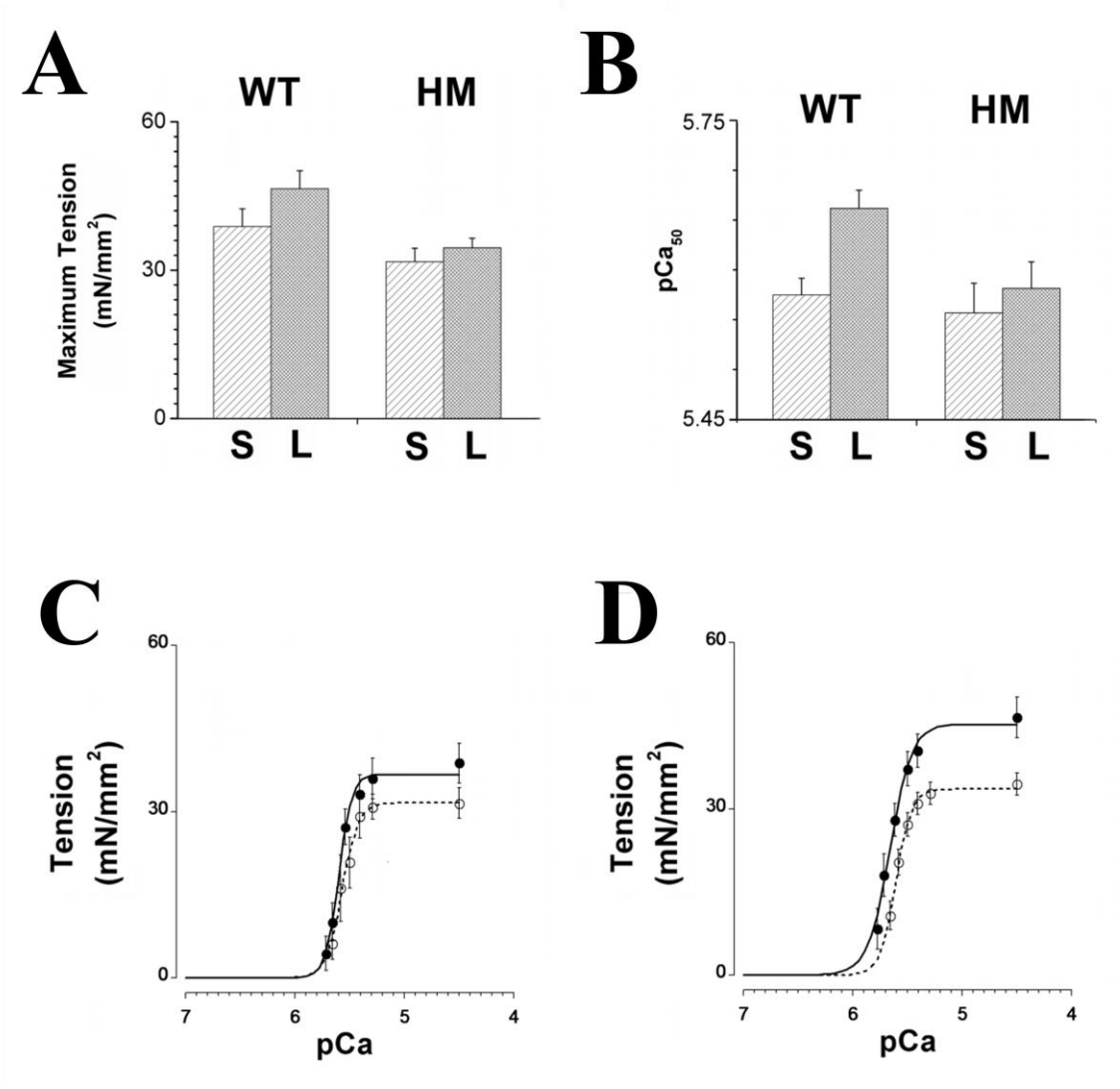

Figure 19. Cardiac maximum tension and calcium sensitivity. Tension-Ca^{2+} relationship was determined in WT (light bars top, solid line and closed symbols bottom) and HM (grey bars top, dashed line and open symbols bottom) trabeculae at short (S, SL = 2.1 μm) and long (L, SL = 2.3 μm). Panel A shows maximum tension, which was reduced in HM compared to WT at both short and long SL. Panel B shows the reduced SL-dependence of calcium sensitivity in HM tissue compared to WT. Bottom panels show average tension-Ca^{2+} relationships at both short (panel C) and long (panel D) SL's. HM fiber bundles exhibited reduced Ca2+ sensitivity at both lengths.

E. **Discussion**

The purpose of this study was to investigate the consequences of expressing a longer titin isoform on the SL dependence of force production and ATP consumption in rat tibialis anterior (TA) muscle and trabeculae. Previously, to study the effect of titin isoform on striated muscle mechanics it was necessary to use different tissues expressing different titin isoforms. One caveat to this approach, however, is that tissues that naturally express alternative native titin isoforms also contain differences in other major contractile proteins. For instance, in both skeletal and cardiac muscle there is a positive correlation between the MHC isoform expression, the rate of ATP hydrolysis and the length of the titin molecule. This introduces ambiguity in assigning the impact of each individual contractile component on biophysical parameters such as myofilament length dependent activation (Cazorla, Freiburg et al. 2000; Prado, Makarenko et al. 2005). Here, we were able to circumvent such confounding factors by using a rat that has an autosomal mutation causing it to differentially express the giant N2BA-G titin isoform. Moreover, the lack of major differences in other contractile proteins between WT and HM in the TA muscle (figure 14B) raises confidence that chemo-mechanical differences between WT and HM muscle preparations was indeed due to the presence of the longer titin isoform. Nearly all of the passive tension in permeabilized striated muscle is carried by titin. Indeed, the inclusion of the longer titin isoform in HM preparations resulted in much lower passive forces as compared to WT preparations, and is consistent with previously published results (Figure 15, Panels B, C, D) (Greaser, Warren et al. 2008; Patel, Pleitner et al. 2011).

Considering that many studies have found correlations between titin isoform length and length dependent activation, a major purpose here was to determine whether muscles harboring a longer titin maintain a similar level of regulation by sarcomere length as muscles from WT rats

(Cazorla, Wu et al. 2001; Fukuda, Wu et al. 2003; Piroddi, Belus et al. 2007; Ait Mou, le Guennec et al. 2008). WT TA tissue and trabeculae displayed length dependency in terms of maximum tension development and Ca^{2+} sensitivity, which was blunted in HM tissue (cf. Figures 17 and 19). This result indicates that expression of a longer titin isoform does not eliminate, but rather attenuates LDA. Moreover, HM skeletal and cardiac tissue also exhibited a blunted length dependency of tension cost compared to WT tissue. However, presence of a longer titin isoform did not appear to alter either cooperativity or the force per cross-bridge as indexed by the hill coefficient and high-frequency muscle stiffness, respectively. Therefore, titin must alter contraction through mechanisms other than cooperativity or the force per cross-bridge.

In addition to blunting the influence of length on the regulation of contraction, there was a reduction in overall maximal force, maximal ATP consumption, and tension cost in TA fiber bundles from the HM rats compared to WT. The greater reduction in maximum ATPase (~40%) compared to the decrease in maximal force production (~25%) is in agreement with the overall lower tension cost in the HM tissue. Tension cost is related to *g*, or the rate by which cross-bridges detach and leave the strong binding state. Based on the Huxley two state cross-bridge model, a reduction in the rate of detachment shifts the equilibrium of cross-bridges from weakly bound state to the strongly bound state. Because the amount of force a muscle can produce is directly related to the percentage of cross-bridges in the strongly bound, force producing state, a decrease in *g* is expected to increase maximal force, opposite from what we observed in the present study. Therefore, the effects of a longer titin on cross-bridge kinetics cannot be explained by a simple reduction in the rate of cross-bridge detachment.

To gain further insight into the effect of the titin mutant on force production and cross-bridge kinetics, we additionally examined activation and relaxation kinetics in the single

myofibril preparation. Maximum tension developed by a multi-cellular muscle preparation is directly proportional to both cross-sectional area and the density of myofibrils per unit of cross-sectional area (Colomo, Piroddi et al. 1997). Single myofibrils from HM tissue exhibited a similar decrease in maximal tension production compared to WT myofibrils (Table 2) as we observed in the multi-cellular fiber bundles. Therefore, the reduction in tension development in the HM muscles could not have been the result of a loss of overall contractile machinery, but rather must have been the result of altered contractile protein functional properties. Similar to tension cost, the slope of the initial phase of relaxation in myofibrils (k_{LIN}) and the duration of this phase (t_{LIN}) are thought to reflect the rate of cross-bridge detachment. While there was a trend for a reduction of k_{LIN} in HM myofibrils, this was not statistically significant. Thus, presence of the mutant titin in the HM myofibrils minimally impacted relaxation kinetics. The rate of force development following either a step-wise increase in $[Ca^{2+}]$ or following a release-restretch maneuver is related to the combined rates of cross-bridge attachment (f) and detachment (g). Single myofibrils from HM tissue showed a reduction in force development compared to WT myofibrils, suggesting an overall slowing of cross-bridge cycling kinetics. The combination of a decrease in maximal force, a reduction in g (measured through tension cost and suggested in single myofibrils) and a reduction in $f + g$ (suggested from activation kinetics in single myofibrils) suggests that presence of a longer titin isoform in the sarcomere more strongly influences the apparent rate of cross-bridge attachment (f) than it does the apparent rate of detachment (g).

One mechanism that might explain why tissue expressing a longer titin isoform would display reduced maximum tension development, calcium sensitivity, and cross-bridge cycling kinetics is related to lattice spacing (reviewed in (Millman 1998; Fuchs and Martyn 2005)). The

muscle sarcomere maintains nearly a constant volume. Therefore, upon an increase in sarcomere length there is a reduction in muscle width as well as the spacing between the thick and thin filaments (Irving, Konhilas et al. 2000). This reduction in sarcomere lattice spacing may increase the probability of a myosin head attaching to actin. Titin is thought to play a role in the reduction of lattice spacing upon an increase in SL since it provides a radial force on the thick and thin filament upon stretch, bringing them closer together. Therefore, a longer titin isoform would be expected to provide less of a radial force, thereby reducing lattice spacing less and subsequently reducing the probability of actin and myosin interaction. This is supported by the observation that specific degradation of titin with trypsin causes a reduction in length dependency concomitant with an increase in lattice spacing (Cazorla, Wu et al. 2001). Previous data published from our laboratory, however, have shed doubt on the influence of lattice spacing in LDA, suggesting other mechanisms might be responsible. For instance, rather than only pulling the thick and thin filaments together, the strain produced by titin with an increase in SL is also transmitted lengthwise along the thick and thin filaments, and has been shown to induce geometric rearrangements that favor actin-myosin interaction (Farman, Gore et al. 2011), and that possibly also affects cross-bridge cycle kinetics. Presumably, a longer titin transmits less strain along the thick and thin filaments for a given change in SL and therefore would be expected to have an attenuated response to changes in length, as seen here. Our data showing a reduction in cross-bridge kinetics and length dependency are in agreement with the hypothesis that the presence of a longer titin isoform reduces maximal force, calcium sensitivity and cross-bridge cycling kinetics by reducing the amount of longitudinal strain transmitted along the thick and thin filaments. We propose that strain transmitted by titin to the contractile apparatus affects

cross-bridge cycle kinetics and that this mechanism may underlie length dependent properties of striated muscle.

V. General Discussion

A. Conclusions

The overall goal of these experiments was to gain a better understanding of how sarcomere length modulates myofilament contraction. Length dependent activation (LDA) is the underlying mechanism behind the Frank-Starling law of the heart, which describes the relationship between end diastolic volume and end systolic pressure. This regulation is on a beat to beat basis, and is able to modulate cardiac output to both acute (exercise) and chronic (heart disease) changes of the body. The amount of LDA exhibited in the heart is related to titin isoform expression, and changes with age and disease. In fact, the heart can finely tune its titin-based passive stiffness by incorporating different amounts of the two major isoforms. Reducing titin-based passive stiffness has also shown to attenuate or eliminate LDA. Accordingly, to gain a better understanding of LDA we first attempted to determine how long it takes a muscle to recognize a change in length and alter the myofilaments to form LDA, and second we investigated the role of titin-based passive stiffness on LDA.

While there are many studies attempting to figure out exactly what protein complexes or amino acids are involved in a muscle forming LDA, there have not been many studies investigating how long it takes a muscle to form LDA. Just like it is important to measure the kinetics of activation as it is the final steady-state force, understanding the kinetics of LDA is equally important in elucidating the molecular mechanisms responsible for it. One of the few measurements of how long it might take a muscle to form LDA estimated a delay of ~100 ms between a length change and the subsequent change in cross-bridge cycling kinetics in rabbit myocardium (Campbell, Taheri et al. 1993). This was an estimate from a fitting a model rather than a direct attempt to measure how long LDA takes. Additionally, this was done by measuring

force transients following small length perturbations in active muscle, rather than a muscle being stretched in the diastolic state, such as what happens during ventricular filling. Therefore, there are not any strong estimates of the kinetics of LDA.

Accordingly, we decided to try and measure how long it takes muscle to form LDA (Chapter III). To do this, we utilized the fast solution-switching technique in single myofibrils harvested from guinea-pig myocardium. This technique allowed us to very rapidly lengthen a myofibril and then homogenously activate it, circumventing any diffusion barriers which would severely limit the rate at which we could perform these experiments. The duration of LDA was investigated by comparing the force responses of a muscle that was activated at a steady-state sarcomere length (SL) to one that was rapidly stretched to that same SL prior to activation. The fastest we were able to lengthen a myofibril and then activate it with Ca^{2+} was 5 ms, and by using a photo-multiplier tube we could time the solution switch to occur immediately following the stretch. We found no differences in activation kinetics or steady-state force between muscles activated following a rapid stretch compared to stead-state. In fact, the traces are so similar that when superimposed on each other there are very few differences between them. The largest deviation between the traces occurs at the very beginning, when passive tension is highest in the rapidly stretched myofibrils. When passive tension is subtracted out of the trace, the rapidly stretched and steady-state fibers are nearly identical.

The 5 ms experiments were done in the presence of inorganic phosphate (2 mM), so in order to assure that the presence of inorganic phosphate was not quantitatively altering the data, we performed similar experiments in the absence of phosphate. The absence of phosphate also allowed measurement of activation and relaxation kinetics, due to the slowing of cross-bridge cycling. Similar to the 5 ms data, there were no differences between steady-state force,

activation kinetics or relaxation kinetics between the rapid stretch and steady-state groups. Additionally, we performed rapid releases from a longer SL to the same SL and had very similar results. In addition to having similar steady-state force, activation kinetics and relaxation kinetics in both rapidly stretched and released myofibrils were nearly identical.

One way LDA might occur nearly instantaneously is if it results from the transduction of mechanical strain between myofilaments. As previously mentioned, the correlation between titin-based passive tension and LDA is highly reported on extensively. Consequently, we investigated the impact of titin-based strain on LDA. Previous attempts at determining the role of titin isoform length and LDA normally occurred by measuring the SL-dependence of force development in preparations that naturally expressed different titin isoform lengths (Fukuda, Wu et al. 2003; Piroddi, Belus et al. 2007). One caveat to this approach is that tissues expressing different titin isoforms also tend to express alternative isoforms of other proteins. Here, we were able to utilize a rat that was recently discovered which has a homozygous autosomal mutation (HM) causing it to preferentially express giant titin isoform (Greaser, Krzesinski et al. 2005). Out of all of the skeletal muscles in the rat, the TA undergoes the most developmental shortening, so the difference between titin isoform length it the wild-type (WT) and HM rats would be the largest in the TA (Guo, Bharmal et al. 2010).

Correspondingly, we performed chemo-mechanical experiments on TA skeletal bundles from both WT and HM rats, and also measured activation/relaxation kinetics in TA single myofibrils. Additionally, because LDA is most pronounced in the heart, we determined the force-Ca^{2+} relationship in trabeculae from both WT and HM rats (Chapter IV). The lack of major differences in other contractile proteins between WT and HM in TA muscle provided confidence that any chemo-mechanical differences between the WT and HM muscles was indeed

due to the presence of the longer titin isoform. As expected both skeletal muscle TA preparations (bundles and myofibrils) and cardiac preparations (trabeculae) exhibited a large reduction in passive tension at all SL's, which is in accordance with tissue expressing a longer isoform of titin (Greaser, Warren et al. 2008; Patel, Pleitner et al. 2011). HM tissue that expresses the longer titin isoform exhibited a reduction in maximal force development , Ca^{2+} sensitivity, maximal ATPase consumption and tension cost compared to WT tissue at both SL's. Additionally, WT tissue exhibited larger differences in these parameters following an increase in length compared to HM TA. The data suggest that in addition to being required for increases in force development and ATP consumption at a long SL compared to short, a longer titin isoform is sufficient to reduce these parameters at a short SL.

HM tissue showed a reduction in tension cost, which is the amount of ATP required for a muscle to produce a given amount of force. Because tension cost is related to *g* (Wannenburg, Heijne et al. 2000; Rundell, Manaves et al. 2005), this suggests that cross-bridge cycling is reduced in HM tissue compared to WT. Cross-bridge cycling kinetics were further examined in single TA myofibrils, which exhibited a reduction in activation kinetics following either an increase in $[Ca^{2+}]$ or a release-restretch maneuver (k_{TR}), with no effect on relaxation kinetics. The slow linear phase of relaxation (k_{LIN}) is also thought to reflect the rate of cross-bridge detachement (*g*), while there was a small trend for k_{LIN}, it was not statistically significant. The combination of a decrease in maximal force, a reduction in *g* (measured through tension cost and suggested in single myofibrils) and a reduction in *f+g* (suggested from activation kinetics in single myofibrils) suggests that the presence of a longer titin isoform in the sarcomere more strongly influences the apparent rate of cross-bridge attachment (*f*) than it does the apparent rate of detachment (*g*).

Lastly, we showed that the presence of the longer titin isoform reduced the SL-dependence of force production in trabeculae. Trabeculae from HM rats showed a reduction in both overall maximal force production and Ca^{2+} sensitivity, but also the SL-dependence of these parameters.

The final conclusions that were determined from the experiments in this thesis are as follows:

1) The transduction of the "length signal" in striated muscle and subsequent modulation of myofilament force development occurs nearly instantaneously (< 5 ms). This is true in the presence and absence of inorganic phosphate, as well as for both stretches and release.

2) Following a rapid diastolic change in SL the rate limiting factor in length dependent activation is the cross-bridge cycling rate. Force development following a step-wise increase in $[Ca^{2+}]$ is rate limited by cross-bridge cycling. The similarity between force development at steady-state SL and active force development (passive tension subtracted) following a rapid stretch suggests they are rate limited by the same process.

3) The expression of a longer titin isoform in the skeletal muscle sarcomere is associated with reduced passive tension, myofilament force development and cross-bridge cycling kinetics at both short and long SL's.

4) The extent of LDA exhibited is attenuated, but not eliminated, in skeletal and cardiac muscle preparations that preferentially express a longer titin isoform.

B. **Speculation**

The rate at which LDA is complete suggests that the length signal is a mechanical tether whereby a change in SL is transduced in a strain-dependent manner. The protein that is most

situated for this mechanical linkage is titin. Support for titin being the mechanical linker between SL and LDA comes from the data shown here that a reduction in titin-based strain reduces maximal force and Ca^{2+} sensitivity, and also the SL-dependence of those parameters.

The precise way that a change in length alters cross-bridge cycling is unknown. One possible mechanism would be that changes in titin-based strain induce compliant realignment, which would provide fine tuning of the filaments to allow optimal force generation. Originally, it was thought that both the thick and thin filaments were inextensible (Ford, Huxley et al. 1981; Bagni, Cecchi et al. 1990). This assumption allows each cross-bridge to operate independently of each other, and then the amount of force produced can be calculated by summing the average state of the pool of cross-bridges. Later data has indicated that the filaments are compliant and do extend when a muscle generates force (Huxley, Stewart et al. 1994; Wakabayashi, Sugimoto et al. 1994). It has been shown that when cross-bridges bind there is significant realignment of the myosin binding sites on actin which allows recruitment of additional cross-bridges (Daniel, Trimble et al. 1998). Also, strain-dependent changes in the geometry of the thick and thin filaments have predicted to influence the way myosin heads generate force (Williams, Regnier et al. 2010). In fact, the tension overshoots which are frequently seen during force development have been predicted to be the result of filament compliance (Campbell 2006). Tension overshoots are perfect examples of how inter-sarcomere dynamics can allow increased force production compared to steady-state situations. In addition to compliance of the filaments individually, movement of the A-band as much as 100 nm during relaxation has been shown in single cardiac myofibrils (Telley, Denoth et al. 2006). Although, the stability of the A-band in single myofibrils is most likely reduced compared to larger preparations, it still shows that both

the compliance of the thick and thin filaments as well as slight movements in respect to each other might have large consequences in cross-bridge kinetics and force production.

In addition to compliant realignment, x-ray diffraction has shown that upon lengthening a muscle there was an ordering of the thick and thin filament structures compared to slack length (Hsu, Mou et al. 2012). Possibly through a similar mechanism, titin has been shown to alter the thick filament upon increases in SL through such mechanisms as relieving cross-bridge strain (Muhle-Goll, Habeck et al. 2001) or by moving myosin heads radially inwards towards the thin filament (Farman, Gore et al. 2011). Taken together, these data provide evidence that upon lengthening and during contraction myofilaments undergo realignment which promotes force production.

An illustration depicting this increased order of thick and thin filament structures is shown in Figure 20. Going from Panel A to B there is an increase in the order of the thick and thin filaments, due to titin-based strain. A similar, yet blunted scenario happens in fibers expressing a longer titin isoform, shown in panels C and D. In these panels, there is still an increase in the order of the thick and thin filaments, but it is not nearly to the same extent as in WT muscles. Therefore, the degree of LDA exhibited is directly related to the degree of titin-based strain on a muscle for a given change in SL, which is mediated by the stiffness of the titin isoform present. Because titin mechanically tethers the filaments together, a change in SL is immediately transduced to the filaments to alter the rate of cross-bridge cycling.

Another mechanism which might enhance force production following an increase in SL has to do with differences between individual sarcomeres. Thinking that each half sarcomere is identical is a similar generalization as assuming each cross-bridge operates completely independently of each other, which I addressed previously in regards to compliant regulation.

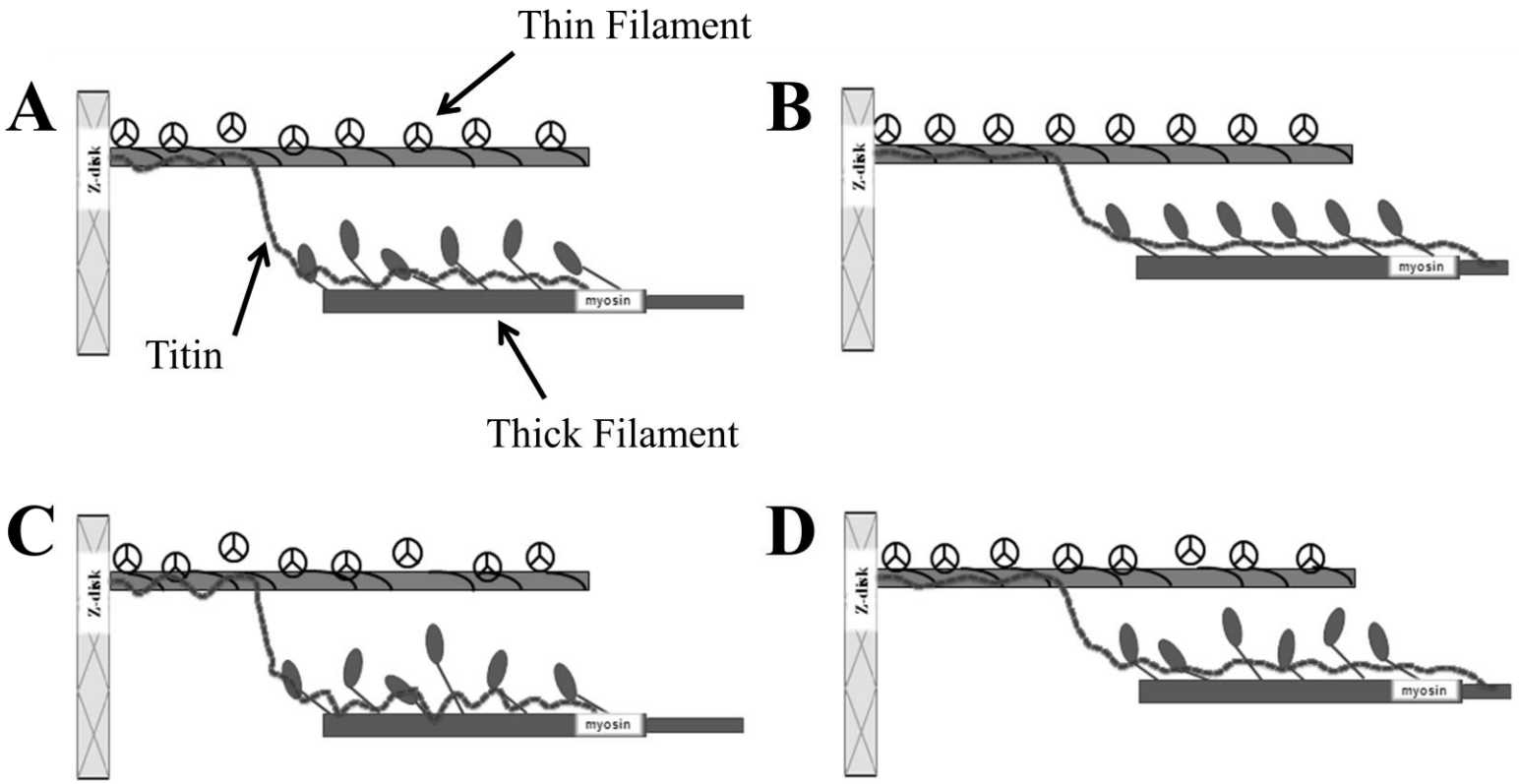

Figure 20. The mechanism of titin-based strain in LDA. Panel A and B are muscles that have a stiffer titin isoform at short and long SL, respectively. Going from short to long not only increases the ordering of the thick and thin filaments, but it also allows for increased force and Ca^{2+} sensitivity through compliant realignment. Furthermore, increased titin strain allows the cross-bridges to extend radially towards the thin filament. Panels C and D show a similar, yet blunted effect of titin-based strain in muscles which have a larger titin isoform. The reduced titin-based strain causes attenuated alterations in both thick and thin filament proteins at both SL's.

LDA allows a myofibril of sarcomeres all made up of slightly different force producing capabilities to produce the same force (Telley and Denoth 2007). Inter-sarcomere differences are accounted for when slightly stronger myofibrils can lengthen slightly weaker ones, allowing them to both produce the same force, albeit at slightly different SL's. Computer simulations of the force responses to small length perturbations fit the actual data better when individual sarcomeres are allowed to have slight variation in force, even though the sum of forces along the myofibril are not different (Campbell 2009). Therefore, it is possible that the inter-sarcomeric inhomogeneities that are naturally present not only compensate for the natural variance of biological tissue, but also synergistically allow for enhanced force production.

Titin obviously would play a very large role in these mechanisms due to extending through the entire half sarcomere and connecting the thick and thin filament. In the absence of cross-bridges, titin may be the protein that connects the thick and thin filaments and adjacent half sarcomeres allowing for inter-sarcomeric dynamics in the absence of cross-bridges. Clear evidence that titin-based strain is important for the previously mentioned mechanisms comes from chapter IV, where muscles expressing a longer isoform of titin had reduced mechanical parameters, and reduced LDA. If titin transduces strain between filaments, having a longer isoform would naturally produce less train, allowing for less LDA, which is precisely what was shown. If inter-sarcomeric effects depend on titin-based strain, the increases strain witnessed following an increase in SL might further enhance inter-sarcomeric effects.

One major contradicting idea to these conclusions which should be rectified comes from the experiments done by Cazora et al. which show that in preparations that have increased passive tension, LDA is enhanced (Cazorla, Wu et al. 2001). In the experiments completed in chapter III of this thesis, the increased passive tension witnessed upon a rapid stretch did not

contribute to altered cross-bridge kinetics or a difference in the steady-state submaximal force, as would be predicted by the conclusions of Cazorla et al 2001. One major difference between these experiments is that Cazorla et al used cardiomyocytes, which are much thicker and more stable preparation compared to the single myofibrils that were used here. A cardiomyocyte is made up of hundreds of single myofibrils, which are connected through Z-disks and M-lines and experience the strain of neighboring single myofibrils. It is possible that the adjacent myofibrils also act as a buffer, limiting the magnitude of strain a single myofibril can experience. Additionally, because inter-sarcomere strain dynamics propagate to other adjacent half sarcomeres (Telley, Denoth et al. 2006), having more of them in series and parallel might increase their duration. Single myofibrils can be thought of as the individual fibers that are woven together to form a bungee cord. Individually, while the fibers do have similar properties as the whole cord, they are mechanically weaker. When woven together though, they act synergistically to provide a very strong cord which can support much heavier weights prior to breaking than predicted by the summation of the small fibers that it consists of. Therefore, a cardiomyocyte or larger muticellular preparation might exhibit increased enhancement due to inter-sarcomeric dynamics compared to a single myofibril, in a similar fashion as many half sarcomeres have enhanced dynamics compared to a single half sarcomere. While LDA is clearly present within 5 ms in single myofibrils, larger tissue preparations may be able to experience even further fine tuning due to actomyosin realignment and inter-sarcomeric effects.

C. **Future Studies**

The results of the experiments done here provide ideas for other future studies to further clarify both the mechanism underlying LDA and the consequences of expressing a longer

titin isoform. I have suggested that a major mechanism underlying LDA involves titin-based strain. While it is known that titin binds both the thick and thin filament, the relative contribution of binding in these regions is unknown. This could be assessed by measuring the effects of both I-band and A-band binding fragments on contractile properties and extent of LDA exhibited. If one set of the fragments reduces LDA more than the other, it could be concluded that titin binding in that region is more important in the transduction of titin-bases strain on LDA. This would also allow speculation of whether LDA is more thick or thin filament based.

I have also proposed that ordering of the thick and thin filament proteins as determined by x-ray diffraction plays an important role in LDA (Hsu, Mou et al. 2012). Presumably, this reordering of the filaments is titin-based. It is not known how rapidly these structural changes take place, therefore if these structural changes occur within 5ms of a rapid stretch that would provide evidence that they are an underlying mechanism of LDA. Furthermore, if these structural changes are titin-based, they would be expected to be blunted in muscles that preferentially express a longer isoform of titin. Accordingly, the degree of thick and thin structural changes could be assessed in preparations of varying titin isoform and/or stiffness, and the degree at which they correlate would suggest their importance in LDA.

Recently, a mutation in the Rbm20 gene was identified (Guo, Bharmal et al. 2010) as the underlying cause for dysregulated titin splicing in rats hat preferentially express the longer giant titin isoform N2BA-G , which were used in Chapter IV. Interestingly, human RBM20 is preferentially expressed in the heart and mutations in RBM20 have been linked to human dilated cardiomyopathy (Brauch, Karst et al. 2009; Li, Morales et al. 2011). It is thought that RBM20 function is conserved because Rbm20 deficient rats and humans with mutations in RBM20 both exhibit similar phenotypes (Guo, Bharmal et al. 2010). Therefore, further characterization of the

contractile consequences of expression of a longer titin isoform would help elucidate the precise mechanisms by which titin isoform length contributes to dilated cardiomyopathy. Additionally, RBM20 is known to alter other molecules predicted to be involved in cardiac structure and function, ion transport and Ca^{2+} handling. Accordingly, measurement of Ca^{2+} handling in intact trabeculae would reveal if there are any compensatory mechanisms present to make up for a lack of LDA. Furthermore, experiments using skinned and intact trabeculae could differentiate between titin based and Ca^{2+} handing based contributions to dilated cardiomyopathies.

Overall, I conclude that LDA is a complex process that finely tunes force production through filament compliance and realignment of both thick and thin filament proteins. Inter-sarcomeric dynamics also allow an enhancement of force, which may be increased at longer SL's. Titin-based strain might aid in this realignment, and also might relieve cross-bridge inhibition at longer SL's. Furthermore, in order to maximize force enhancement with an increase in SL, the amount of titin-based strain a muscle experiences can be altered by preferentially altering the expression titin isoforms of varying stiffness. Finally, further analysis of the relationship between titin-bases strain and LDA along with investigation of the consequences of mutations in RBM20 will provide mechanistic insights into the pathogenesis of heart failure.

CITED LITERATURE

Adelstein, R. S. and E. Eisenberg (1980). "Regulation and kinetics of the actin-myosin-ATP interaction." Annu Rev Biochem **49**: 921-56.

Ait Mou, Y., J. Y. le Guennec, et al. (2008). "Differential contribution of cardiac sarcomeric proteins in the myofibrillar force response to stretch." Pflugers Arch **457**(1): 25-36.

Allen, D. G. and J. C. Kentish (1985). "The cellular basis of the length-tension relation in cardiac muscle." J Mol Cell Cardiol **17**(9): 821-40.

Allen, D. G. and S. Kurihara (1982). "The effects of muscle length on intracellular calcium transients in mammalian cardiac muscle." J Physiol **327**: 79-94.

Alvarez, B. V., N. G. Perez, et al. (1999). "Mechanisms underlying the increase in force and Ca(2+) transient that follow stretch of cardiac muscle: a possible explanation of the Anrep effect." Circ Res **85**(8): 716-22.

Ayittey, P. N., J. S. Walker, et al. (2009). "Glass microneedles for force measurements: a finite-element analysis model." Pflugers Arch **457**(6): 1415-22.

Babu, A., S. P. Scordilis, et al. (1987). "The control of myocardial contraction with skeletal fast muscle troponin C." J Biol Chem **262**(12): 5815-22.

Bagni, M. A., G. Cecchi, et al. (1990). "Tension and stiffness of frog muscle fibres at full filament overlap." J Muscle Res Cell Motil **11**(5): 371-7.

Blaustein, M. P. and W. J. Lederer (1999). "Sodium/calcium exchange: its physiological implications." Physiol Rev **79**(3): 763-854.

Blix, M. (1892). "Die Länge und die Spannung des Muskels." Skandinavisches Archiv Für Physiologie **3**(1): 295–318.

Brandt, P. W., R. N. Cox, et al. (1980). "Can the binding of Ca2+ to two regulatory sites on troponin C determine the steep pCa/tension relationship of skeletal muscle?" Proc Natl Acad Sci U S A **77**(8): 4717-20.

Brandt, P. W., M. S. Diamond, et al. (1987). "Co-operative interactions between troponin-tropomyosin units extend the length of the thin filament in skeletal muscle." J Mol Biol **195**(4): 885-96.

Brauch, K. M., M. L. Karst, et al. (2009). "Mutations in ribonucleic acid binding protein gene cause familial dilated cardiomyopathy." J Am Coll Cardiol **54**(10): 930-41.

Brenner, B. (1988). "Effect of Ca2+ on cross-bridge turnover kinetics in skinned single rabbit psoas fibers: implications for regulation of muscle contraction." Proc Natl Acad Sci U S A **85**(9): 3265-9.

Brenner, B., J. M. Chalovich, et al. (1986). "Stiffness of skinned rabbit psoas fibers in MgATP and MgPPi solution." Biophys J **50**(4): 685-91.

Brenner, B. and E. Eisenberg (1986). "Rate of force generation in muscle: correlation with actomyosin ATPase activity in solution." Proc Natl Acad Sci U S A **83**(10): 3542-6.

Brenner, B. and L. C. Yu (1985). "Equatorial x-ray diffraction from single skinned rabbit psoas fibers at various degrees of activation. Changes in intensities and lattice spacing." Biophys J **48**(5): 829-34.

Butters, C. A., J. B. Tobacman, et al. (1997). "Cooperative effect of calcium binding to adjacent troponin molecules on the thin filament-myosin subfragment 1 MgATPase rate." J Biol Chem **272**(20): 13196-202.

Cabral-Lilly, D., L. S. Tobacman, et al. (1997). "Molecular polarity in tropomyosin-troponin T co-crystals." Biophys J **73**(4): 1763-70.

Campbell, K. B., M. V. Razumova, et al. (2001). "Myofilament kinetics in isometric twitch dynamics." Ann Biomed Eng **29**(5): 384-405.

Campbell, K. B., H. Taheri, et al. (1993). "Similarities between dynamic elastance of left ventricular chamber and papillary muscle of rabbit heart." Am J Physiol **264**(6 Pt 2): H1926-41.

Campbell, K. S. (2006). "Filament compliance effects can explain tension overshoots during force development." Biophys J **91**(11): 4102-9.

Campbell, K. S. (2009). "Interactions between connected half-sarcomeres produce emergent mechanical behavior in a mathematical model of muscle." PLoS Comput Biol **5**(11): e1000560.

Campbell, K. S. (2011). "Impact of myocyte strain on cardiac myofilament activation." Pflugers Arch **462**(1): 3-14.

Castro-Ferreira, R., R. Fontes-Carvalho, et al. (2010). "The role of titin in the modulation of cardiac function and its pathophysiological implications." Arq Bras Cardiol **96**(4): 332-9.

Cazorla, O., A. Freiburg, et al. (2000). "Differential expression of cardiac titin isoforms and modulation of cellular stiffness." Circ Res **86**(1): 59-67.

Cazorla, O., G. Vassort, et al. (1999). "Length modulation of active force in rat cardiac myocytes: is titin the sensor?" J Mol Cell Cardiol **31**(6): 1215-27.

Cazorla, O., Y. Wu, et al. (2001). "Titin-based modulation of calcium sensitivity of active tension in mouse skinned cardiac myocytes." Circ Res **88**(10): 1028-35.

Chandra, M., D. E. Montgomery, et al. (1999). "The N-terminal region of troponin T is essential for the maximal activation of rat cardiac myofilaments." J Mol Cell Cardiol **31**(4): 867-80.

Chandra, M., M. L. Tschirgi, et al. (2006). "Troponin T modulates sarcomere length-dependent recruitment of cross-bridges in cardiac muscle." Biophys J **90**(8): 2867-76.

Colomo, F., N. Piroddi, et al. (1997). "Active and passive forces of isolated myofibrils from cardiac and fast skeletal muscle of the frog." J Physiol **500 (Pt 2)**: 535-48.

Daniel, T. L., A. C. Trimble, et al. (1998). "Compliant realignment of binding sites in muscle: transient behavior and mechanical tuning." Biophys J **74**(4): 1611-21.

de Tombe, P. P., A. Belus, et al. (2007). "Myofilament calcium sensitivity does not affect cross-bridge activation-relaxation kinetics." Am J Physiol Regul Integr Comp Physiol **292**(3): R1129-36.

de Tombe, P. P., R. D. Mateja, et al. (2010). "Myofilament length dependent activation." J Mol Cell Cardiol **48**(5): 851-8.

de Tombe, P. P. and G. J. Stienen (1995). "Protein kinase A does not alter economy of force maintenance in skinned rat cardiac trabeculae." Circ Res **76**(5): 734-41.

Dobesh, D. P., J. P. Konhilas, et al. (2002). "Cooperative activation in cardiac muscle: impact of sarcomere length." Am J Physiol Heart Circ Physiol **282**(3): H1055-62.

Eisenberg, E. and C. Moos (1968). "The adenosine triphosphatase activity of acto-heavy meromyosin. A kinetic analysis of actin activation." Biochemistry **7**(4): 1486-9.

Eisenberg, E. and C. Moos (1970). "Actin activation of heavy meromyosin adenosine triphosphatase. Dependence on adenosine triphosphate and actin concentrations." J Biol Chem **245**(9): 2451-6.

Eisenberg, E., C. R. Zobel, et al. (1968). "Subfragment 1 of myosin: adenosine triphophatase activation by actin." Biochemistry **7**(9): 3186-94.

Fabiato, A. (1983). "Calcium-induced release of calcium from the cardiac sarcoplasmic reticulum." Am J Physiol **245**(1): C1-14.

Farah, C. S. and F. C. Reinach (1995). "The troponin complex and regulation of muscle contraction." Faseb J **9**(9): 755-67.

Farman, G. P., E. J. Allen, et al. (2010). "The role of thin filament cooperativity in cardiac length-dependent calcium activation." Biophys J **99**(9): 2978-86.

Farman, G. P., Q. J. Allen, et al. (2007). "Interfilament Spacing Is Preserved during Sarcomere Length Isometric Contractions in Rat Cardiac Trabeculae." Biophys J **92**(9): L73-5.

Farman, G. P., D. Gore, et al. (2011). "Myosin head orientation: a structural determinant for the Frank-Starling relationship." Am J Physiol Heart Circ Physiol **300**(6): H2155-60.

Farman, G. P., K. Tachampa, et al. (2008). "Blebbistatin: use as inhibitor of muscle contraction." Pflugers Arch **455**(6): 995-1005.

Fenn, W. O. (1923). "A quantitative comparison between the energy liberated and the work performed by the isolated sartorius muscle of the frog." J Physiol **58**(2-3): 175-203.

Finer, J. T., R. M. Simmons, et al. (1994). "Single myosin molecule mechanics: piconewton forces and nanometre steps." Nature **368**(6467): 113-9.

Flashman, E., C. Redwood, et al. (2004). "Cardiac myosin binding protein C: its role in physiology and disease." Circ Res **94**(10): 1279-89.

Flicker, P. F., G. N. Phillips, Jr., et al. (1982). "Troponin and its interactions with tropomyosin. An electron microscope study." J Mol Biol **162**(2): 495-501.

Ford, L. E., A. F. Huxley, et al. (1981). "The relation between stiffness and filament overlap in stimulated frog muscle fibres." J Physiol **311**: 219-49.

Ford, S. J., M. Chandra, et al. (2010). "Model representation of the nonlinear step response in cardiac muscle." J Gen Physiol **136**(2): 159-77.

Frank, O. (1895). "Zur Dynamik des Herzmuskels." Z Biol **32**: 370-447.

Fuchs, F. and D. A. Martyn (2005). "Length-dependent Ca(2+) activation in cardiac muscle: some remaining questions." J Muscle Res Cell Motil **26**(4-5): 199-212.

Fuchs, F. and S. H. Smith (2001). "Calcium, cross-bridges, and the Frank-Starling relationship." News Physiol Sci **16**: 5-10.

Fukuda, N., H. L. Granzier, et al. (2008). "Physiological functions of the giant elastic protein titin in mammalian striated muscle." J Physiol Sci **58**(3): 151-9.

Fukuda, N., O. U. J, et al. (2001). "Acidosis or inorganic phosphate enhances the length dependence of tension in rat skinned cardiac muscle." J Physiol **536**(Pt 1): 153-60.

Fukuda, N., D. Sasaki, et al. (2001). "Length dependence of tension generation in rat skinned cardiac muscle: role of titin in the Frank-Starling mechanism of the heart." Circulation **104**(14): 1639-45.

Fukuda, N., Y. Wu, et al. (2003). "Titin isoform variance and length dependence of activation in skinned bovine cardiac muscle." J Physiol **553**(Pt 1): 147-54.

Fukuda, N., Y. Wu, et al. (2005). "Titin-based modulation of active tension and interfilament lattice spacing in skinned rat cardiac muscle." Pflugers Arch **449**(5): 449-57.

Gagne, S. M., S. Tsuda, et al. (1995). "Structures of the troponin C regulatory domains in the apo and calcium-saturated states." Nat Struct Biol **2**(9): 784-9.

Geeves, M. A. and S. S. Lehrer (1994). "Dynamics of the muscle thin filament regulatory switch: the size of the cooperative unit." Biophys J **67**(1): 273-82.

Godt, R. E. and D. W. Maughan (1981). "Influence of osmotic compression on calcium activation and tension in skinned muscle fibers of the rabbit." Pflugers Arch **391**(4): 334-7.

Godt, R. E. and D. W. Maughan (1988). "On the composition of the cytosol of relaxed skeletal muscle of the frog." Am J Physiol **254**(5 Pt 1): C591-604.

Gordon, A. M., E. Homsher, et al. (2000). "Regulation of contraction in striated muscle." Physiol Rev **80**(2): 853-924.

Gordon, A. M., A. F. Huxley, et al. (1966). "The variation in isometric tension with sarcomere length in vertebrate muscle fibres." J Physiol **184**(1): 170-92.

Grabarek, Z., J. Grabarek, et al. (1983). "Cooperative binding to the Ca2+-specific sites of troponin C in regulated actin and actomyosin." J Biol Chem **258**(23): 14098-102.

Granzier, H. L. and S. Labeit (2004). "The giant protein titin: a major player in myocardial mechanics, signaling, and disease." Circ Res **94**(3): 284-95.

Greaser, M. L. and J. Gergely (1971). "Reconstitution of troponin activity from three protein components." J Biol Chem **246**(13): 4226-33.

Greaser, M. L., P. R. Krzesinski, et al. (2005). "Developmental changes in rat cardiac titin/connectin: transitions in normal animals and in mutants with a delayed pattern of isoform transition." J Muscle Res Cell Motil **26**(6-8): 325-32.

Greaser, M. L., C. M. Warren, et al. (2008). "Mutation that dramatically alters rat titin isoform expression and cardiomyocyte passive tension." J Mol Cell Cardiol **44**(6): 983-91.

Guo, W., S. J. Bharmal, et al. (2010). "Titin diversity--alternative splicing gone wild." J Biomed Biotechnol **2010**: 753675.

Hellam, D. C. and R. J. Podolsky (1969). "Force measurements in skinned muscle fibres." J Physiol **200**(3): 807-19.

Helmes, M., K. Trombitas, et al. (1996). "Titin develops restoring force in rat cardiac myocytes." Circ Res **79**(3): 619-26.

Herzberg, O., J. Moult, et al. (1986). "A model for the Ca2+-induced conformational transition of troponin C. A trigger for muscle contraction." J Biol Chem **261**(6): 2638-44.

Hibberd, M. G. and B. R. Jewell (1982). "Calcium- and length-dependent force production in rat ventricular muscle." J Physiol **329**: 527-40.

Hitchcock, S. E., H. E. Huxley, et al. (1973). "Calcium sensitive binding of troponin to actin-tropomyosin: a two-site model for troponin action." J Mol Biol **80**(4): 825-36.

Hofmann, P. A. and F. Fuchs (1987). "Effect of length and cross-bridge attachment on Ca2+ binding to cardiac troponin C." Am J Physiol **253**(1 Pt 1): C90-6.

Holmes, K. C. (1995). "The actomyosin interaction and its control by tropomyosin." Biophys J **68**(4 Suppl): 2S-5S; discussion 6S-7S.

Holmes, K. C., M. Tirion, et al. (1993). "A comparison of the atomic model of F-actin with cryo-electron micrographs of actin and decorated actin." Adv Exp Med Biol **332**: 15-22; discussion 22-4.

Horowits, R., E. S. Kempner, et al. (1986). "A physiological role for titin and nebulin in skeletal muscle." Nature **323**(6084): 160-4.

Hsu, H., Y. A. Mou, et al. (2012). Structural changes in both the troponin complexand the thick filament may underlie myofilament length dependent activation. 56th Annual Biophysical Meeting. San Diego, California.

Huxley, A. (1988). "Muscular contraction." Annu Rev Physiol **50**: 1-16.

Huxley, A. F. (1957). "Muscle structure and theories of contraction." Prog Biophys Biophys Chem **7**: 255-318.

Huxley, A. F. (2000). "Cross-bridge action: present views, prospects, and unknowns." J Biomech **33**(10): 1189-95.

Huxley, A. F. and R. Niedergerke (1954). "Structural changes in muscle during contraction; interference microscopy of living muscle fibres." Nature **173**(4412): 971-3.

Huxley, A. F. and R. M. Simmons (1971). "Proposed mechanism of force generation in striated muscle." Nature **233**(5321): 533-8.

Huxley, H. and J. Hanson (1954). "Changes in the cross-striations of muscle during contraction and stretch and their structural interpretation." Nature **173**(4412): 973-6.

Huxley, H. E. (1953). "Electron microscope studies of the organisation of the filaments in striated muscle." Biochim Biophys Acta **12**(3): 387-94.

Huxley, H. E. (1953). "X-ray analysis and the problem of muscle." Proc R Soc Lond B Biol Sci **141**(902): 59-62.

Huxley, H. E. (1957). "The double array of filaments in cross-striated muscle." J Biophys Biochem Cytol **3**(5): 631-48.

Huxley, H. E. (1963). "Electron Microscope Studies on the Structure of Natural and Synthetic Protein Filaments from Striated Muscle." J Mol Biol **7**: 281-308.

Huxley, H. E., A. Stewart, et al. (1994). "X-ray diffraction measurements of the extensibility of actin and myosin filaments in contracting muscle." Biophys J **67**(6): 2411-21.

Irving, T. C., J. Konhilas, et al. (2000). "Myofilament lattice spacing as a function of sarcomere length in isolated rat myocardium." Am J Physiol Heart Circ Physiol **279**(5): H2568-73.

Jelicks, L. A. and R. K. Gupta (1991). "Intracellular free magnesium and high energy phosphates in the perfused normotensive and spontaneously hypertensive rat heart. A 31P NMR study." Am J Hypertens **4**(2 Pt 1): 131-6.

Johnson, G. J. (2008). The ten most beautiful experiments / George Johnson. London :, Bodley Head.

Julian, F. J. (1969). "Activation in a skeletal muscle contraction model with a modification for insect fibrillar muscle." Biophys J **9**(4): 547-70.

Kabsch, W., H. G. Mannherz, et al. (1990). "Atomic structure of the actin:DNase I complex." Nature **347**(6288): 37-44.

Katz, A. M. and B. H. Lorell (2000). "Regulation of cardiac contraction and relaxation." Circulation **102**(20 Suppl 4): IV69-74.

Kawai, M., J. S. Wray, et al. (1993). "The effect of lattice spacing change on cross-bridge kinetics in chemically skinned rabbit psoas muscle fibers. I. Proportionality between the lattice spacing and the fiber width." Biophys J **64**(1): 187-96.

Kentish, J. C., H. E. ter Keurs, et al. (1986). "Comparison between the sarcomere length-force relations of intact and skinned trabeculae from rat right ventricle. Influence of calcium concentrations on these relations." Circ Res **58**(6): 755-68.

Kobayashi, T., L. Jin, et al. (2008). "Cardiac thin filament regulation." Pflugers Arch **457**(1): 37-46.

Konhilas, J. P., T. C. Irving, et al. (2002). "Frank-Starling law of the heart and the cellular mechanisms of length-dependent activation." Pflugers Arch **445**(3): 305-10.

Konhilas, J. P., T. C. Irving, et al. (2002). "Length-dependent activation in three striated muscle types of the rat." J Physiol **544**(Pt 1): 225-36.

Konhilas, J. P., T. C. Irving, et al. (2002). "Myofilament calcium sensitivity in skinned rat cardiac trabeculae: role of interfilament spacing." Circ Res **90**(1): 59-65.

Konhilas, J. P., T. C. Irving, et al. (2003). "Troponin I in the murine myocardium: influence on length-dependent activation and interfilament spacing." J Physiol **547**(Pt 3): 951-61.

Kruger, M., T. Kohl, et al. (2006). "Developmental changes in passive stiffness and myofilament Ca2+ sensitivity due to titin and troponin-I isoform switching are not critically triggered by birth." Am J Physiol Heart Circ Physiol **291**(2): H496-506.

Kruger, M. and W. A. Linke (2010). "The giant protein titin: a regulatory node that integrates myocyte signaling pathways." J Biol Chem **286**(12): 9905-12.

Labeit, S. and B. Kolmerer (1995). "Titins: giant proteins in charge of muscle ultrastructure and elasticity." Science **270**(5234): 293-6.

Lee, E. J., J. Peng, et al. (2010). "Calcium sensitivity and the Frank-Starling mechanism of the heart are increased in titin N2B region-deficient mice." J Mol Cell Cardiol **49**(3): 449-58.

Levine, R., A. Weisberg, et al. (2001). "Multiple structures of thick filaments in resting cardiac muscle and their influence on cross-bridge interactions." Biophys J **81**(2): 1070-82.

LeWinter, M. M. and H. Granzier (2010). "Cardiac titin: a multifunctional giant." Circulation **121**(19): 2137-45.

Li, D., A. Morales, et al. (2011). "Identification of novel mutations in RBM20 in patients with dilated cardiomyopathy." Clin Transl Sci **3**(3): 90-7.

Li, S., W. Guo, et al. (2011). "Comprehensive analysis of titin protein isoform and alternative splicing in normal and mutant rats." J Cell Biochem.

Linke, W. A. (2008). "Sense and stretchability: the role of titin and titin-associated proteins in myocardial stress-sensing and mechanical dysfunction." Cardiovasc Res **77**(4): 637-48.

Lymn, R. W. and E. W. Taylor (1971). "Mechanism of adenosine triphosphate hydrolysis by actomyosin." Biochemistry **10**(25): 4617-24.

Mak, A. S. and L. B. Smillie (1981). "Non-polymerizable tropomyosin: preparation, some properties and F-actin binding." Biochem Biophys Res Commun **101**(1): 208-14.

Malnic, B. and F. C. Reinach (1994). "Assembly of functional skeletal muscle troponin complex in Escherichia coli." Eur J Biochem **222**(1): 49-54.

Martyn, D. A., M. Regnier, et al. (2001). "Ca2+ - and cross-bridge-dependent changes in N- and C-terminal structure of troponin C in rat cardiac muscle." Biophys J **80**(1): 360-70.

McClellan, G., I. Kulikovskaya, et al. (2001). "Changes in cardiac contractility related to calcium-mediated changes in phosphorylation of myosin-binding protein C." Biophys J **81**(2): 1083-92.

McCray, J. A., L. Herbette, et al. (1980). "A new approach to time-resolved studies of ATP-requiring biological systems; laser flash photolysis of caged ATP." Proc Natl Acad Sci U S A **77**(12): 7237-41.

McDonald, K. S. and R. L. Moss (1995). "Osmotic compression of single cardiac myocytes eliminates the reduction in Ca2+ sensitivity of tension at short sarcomere length." Circ Res **77**(1): 199-205.

McKillop, D. F. and M. A. Geeves (1993). "Regulation of the interaction between actin and myosin subfragment 1: evidence for three states of the thin filament." Biophys J **65**(2): 693-701.

Metzger, J. M. (1995). "Myosin binding-induced cooperative activation of the thin filament in cardiac myocytes and skeletal muscle fibers." Biophys J **68**(4): 1430-42.

Millman, B. M. (1998). "The filament lattice of striated muscle." Physiol Rev **78**(2): 359-91.

Moss, R. L., L. O. Nwoye, et al. (1991). "Substitution of cardiac troponin C into rabbit muscle does not alter the length dependence of Ca2+ sensitivity of tension." J Physiol **440**: 273-89.

Muhle-Goll, C., M. Habeck, et al. (2001). "Structural and functional studies of titin's fn3 modules reveal conserved surface patterns and binding to myosin S1--a possible role in the Frank-Starling mechanism of the heart." J Mol Biol **313**(2): 431-47.

Neagoe, C., C. A. Opitz, et al. (2003). "Gigantic variety: expression patterns of titin isoforms in striated muscles and consequences for myofibrillar passive stiffness." J Muscle Res Cell Motil **24**(2-3): 175-89.

Needham, D. M. (1971). Machina carnis : the biochemistry of muscular contraction in its historical development / by Dorothy M. Needham. Cambridge [Eng.] :, University Press.

Obermann, W. M., M. Gautel, et al. (1996). "The structure of the sarcomeric M band: localization of defined domains of myomesin, M-protein, and the 250-kD carboxy-terminal region of titin by immunoelectron microscopy." J Cell Biol **134**(6): 1441-53.

Palmer, S. and J. C. Kentish (1998). "Roles of Ca2+ and crossbridge kinetics in determining the maximum rates of Ca2+ activation and relaxation in rat and guinea pig skinned trabeculae." Circ Res **83**(2): 179-86.

Pan, B. S., A. M. Gordon, et al. (1989). "Removal of tropomyosin overlap modifies cooperative binding of myosin S-1 to reconstituted thin filaments of rabbit striated muscle." J Biol Chem **264**(15): 8495-8.

Parmley, W. W. and L. Chuck (1973). "Length-dependent changes in myocardial contractile state." Am J Physiol **224**(5): 1195-9.

Patel, J. R., J. M. Pleitner, et al. (2011). "Magnitude of length-dependent changes in contractile properties varies with titin isoform in rat ventricles." Am J Physiol Heart Circ Physiol **302**(3): H697-708.

Petroff, M. G., S. H. Kim, et al. (2001). "Endogenous nitric oxide mechanisms mediate the stretch dependence of Ca2+ release in cardiomyocytes." Nat Cell Biol **3**(10): 867-73.

Pieples, K. and D. F. Wieczorek (2000). "Tropomyosin 3 increases striated muscle isoform diversity." Biochemistry **39**(28): 8291-7.

Piroddi, N., A. Belus, et al. (2007). "Tension generation and relaxation in single myofibrils from human atrial and ventricular myocardium." Pflugers Arch **454**(1): 63-73.

Piroddi, N., C. Tesi, et al. (2003). "Contractile effects of the exchange of cardiac troponin for fast skeletal troponin in rabbit psoas single myofibrils." J Physiol **552**(Pt 3): 917-31.

Prado, L. G., I. Makarenko, et al. (2005). "Isoform diversity of giant proteins in relation to passive and active contractile properties of rabbit skeletal muscles." J Gen Physiol **126**(5): 461-80.

Rassier, D. E., W. Herzog, et al. (2003). "Stretch-induced, steady-state force enhancement in single skeletal muscle fibers exceeds the isometric force at optimum fiber length." J Biomech **36**(9): 1309-16.

Rayment, I. (1996). "The structural basis of the myosin ATPase activity." J Biol Chem **271**(27): 15850-3.

Rayment, I., H. M. Holden, et al. (1993). "Structure of the actin-myosin complex and its implications for muscle contraction." Science **261**(5117): 58-65.

Regnier, M., H. Martin, et al. (2004). "Cross-bridge versus thin filament contributions to the level and rate of force development in cardiac muscle." Biophys J **87**(3): 1815-24.

Richard P, V. E., Charron P, Isnard R. (2006). "The Genetic Bases of Cardiomyopathies." J Am Coll Cardiol. **48**: A79-A89.

Rome, E. (1968). "X-ray diffraction studies of the filament lattice of striated muscle in various bathing media." J Mol Biol **37**(2): 331-44.

Rundell, V. L., V. Manaves, et al. (2005). "Impact of beta-myosin heavy chain isoform expression on cross-bridge cycling kinetics." Am J Physiol Heart Circ Physiol **288**(2): H896-903.

Sadayappan, S., J. Gulick, et al. (2005). "Cardiac myosin-binding protein-C phosphorylation and cardiac function." Circ Res **97**(11): 1156-63.

Sandow, A. (1952). "Excitation-contraction coupling in muscular response." Yale J Biol Med **25**(3): 176-201.

Schaub, M. C., M. A. Hefti, et al. (1998). "Modulation of contractility in human cardiac hypertrophy by myosin essential light chain isoforms." Cardiovasc Res **37**(2): 381-404.

Sivaramakrishnan, M. and M. Burke (1982). "The free heavy chain of vertebrate skeletal myosin subfragment 1 shows full enzymatic activity." J Biol Chem **257**(2): 1102-5.

Sonnenblick, E. H. and C. L. Skelton (1974). "Reconsideration of the ultrastructural basis of cardiac length-tension relations." Circ Res **35**(4): 517-26.

Sorenson, M. M., A. C. da Silva, et al. (1995). "Concerted action of the high affinity calcium binding sites in skeletal muscle troponin C." J Biol Chem **270**(17): 9770-7.

Starling, E. H. (1918). Linacre Lecture on the law of the Heart, London, UK
Longmans, Green & Co.

Stehle, R., M. Kruger, et al. (2002). "Force kinetics and individual sarcomere dynamics in cardiac myofibrils after rapid ca(2+) changes." Biophys J **83**(4): 2152-61.

Stehle, R., M. Kruger, et al. (2002). "Isometric force kinetics upon rapid activation and relaxation of mouse, guinea pig and human heart muscle studied on the subcellular myofibrillar level." Basic Res Cardiol **97 Suppl 1**: I127-35.

Stehle, R., J. Solzin, et al. (2009). "Insights into the kinetics of Ca2+-regulated contraction and relaxation from myofibril studies." Pflugers Arch **458**(2): 337-57.

Stelzer, J. E., J. R. Patel, et al. (2006). "Protein kinase A-mediated acceleration of the stretch activation response in murine skinned myocardium is eliminated by ablation of cMyBP-C." Circ Res **99**(8): 884-90.

Sumandea, M. P., E. M. Burkart, et al. (2004). "Molecular and integrated biology of thin filament protein phosphorylation in heart muscle." Ann N Y Acad Sci **1015**: 39-52.

Sumandea, M. P., W. G. Pyle, et al. (2003). "Identification of a functionally critical protein kinase C phosphorylation residue of cardiac troponin T." J Biol Chem **278**(37): 35135-44.

Sun, Y. B. and M. Irving (2010). "The molecular basis of the steep force-calcium relation in heart muscle." J Mol Cell Cardiol **48**(5): 859-65.

Sun, Y. B., F. Lou, et al. (2009). "Calcium- and myosin-dependent changes in troponin structure during activation of heart muscle." J Physiol **587**(Pt 1): 155-63.

Swartz, D. R. and R. L. Moss (1992). "Influence of a strong-binding myosin analogue on calcium-sensitive mechanical properties of skinned skeletal muscle fibers." J Biol Chem **267**(28): 20497-506.

Syska, H., J. M. Wilkinson, et al. (1976). "The relationship between biological activity and primary structure of troponin I from white skeletal muscle of the rabbit." Biochem J **153**(2): 375-87.

Tachampa, K., T. Kobayashi, et al. (2008). "Increased cross-bridge cycling kinetics after exchange of C-terminal truncated troponin I in skinned rat cardiac muscle." J Biol Chem **283**(22): 15114-21.

Tachampa, K., H. Wang, et al. (2007). "Cardiac troponin I threonine 144: role in myofilament length dependent activation." Circ Res **101**(11): 1081-3.

Telley, I. A. and J. Denoth (2007). "Sarcomere dynamics during muscular contraction and their implications to muscle function." J Muscle Res Cell Motil **28**(1): 89-104.

Telley, I. A., J. Denoth, et al. (2006). "Half-sarcomere dynamics in myofibrils during activation and relaxation studied by tracking fluorescent markers." Biophys J **90**(2): 514-30.

ter Keurs, H. E., W. H. Rijnsburger, et al. (1980). "Tension development and sarcomere length in rat cardiac trabeculae. Evidence of length-dependent activation." Circ Res **46**(5): 703-14.

Terui, T., M. Sodnomtseren, et al. (2008). "Troponin and titin coordinately regulate length-dependent activation in skinned porcine ventricular muscle." J Gen Physiol **131**(3): 275-83.

Tesi, C., F. Colomo, et al. (2000). "The effect of inorganic phosphate on force generation in single myofibrils from rabbit skeletal muscle." Biophys J **78**(6): 3081-92.

Tesi, C., F. Colomo, et al. (2002). "Characterization of the cross-bridge force-generating step using inorganic phosphate and BDM in myofibrils from rabbit skeletal muscles." J Physiol **541**(Pt 1): 187-99.

Tesi, C., N. Piroddi, et al. (2002). "Relaxation kinetics following sudden Ca(2+) reduction in single myofibrils from skeletal muscle." Biophys J **83**(4): 2142-51.

Tobacman, L. S. (1996). "Thin filament-mediated regulation of cardiac contraction." Annu Rev Physiol **58**: 447-81.

Tobacman, L. S. and D. Sawyer (1990). "Calcium binds cooperatively to the regulatory sites of the cardiac thin filament." J Biol Chem **265**(2): 931-9.

Tskhovrebova, L. and J. Trinick (2003). "Titin: properties and family relationships." Nat Rev Mol Cell Biol **4**(9): 679-89.

Van Eyk, J. E. and R. S. Hodges (1988). "The biological importance of each amino acid residue of the troponin I inhibitory sequence 104-115 in the interaction with troponin C and tropomyosin-actin." J Biol Chem **263**(4): 1726-32.

Vibert, P., R. Craig, et al. (1997). "Steric-model for activation of muscle thin filaments." J Mol Biol **266**(1): 8-14.

Wagner, P. D. and E. Giniger (1981). "Hydrolysis of ATP and reversible binding to F-actin by myosin heavy chains free of all light chains." Nature **292**(5823): 560-2.

Wakabayashi, K., Y. Sugimoto, et al. (1994). "X-ray diffraction evidence for the extensibility of actin and myosin filaments during muscle contraction." Biophys J **67**(6): 2422-35.

Wannenburg, T., G. H. Heijne, et al. (2000). "Cross-bridge kinetics in rat myocardium: effect of sarcomere length and calcium activation." Am J Physiol Heart Circ Physiol **279**(2): H779-90.

Wannenburg, T., P. M. Janssen, et al. (1997). "The Frank-Starling mechanism is not mediated by changes in rate of cross-bridge detachment." Am J Physiol **273**(5 Pt 2): H2428-35.

Warren, C. M., P. R. Krzesinski, et al. (2004). "Titin isoform changes in rat myocardium during development." Mech Dev **121**(11): 1301-12.

Warren, C. M., P. R. Krzesinski, et al. (2003). "Vertical agarose gel electrophoresis and electroblotting of high-molecular-weight proteins." Electrophoresis **24**(11): 1695-702.

Weber, E. (1846). "Muskelbewegung." Handwörterbuch der Physiologie mit Rücksicht auf physiologische Pathologie. **3**(2): 1-122.

Williams, C. D., M. Regnier, et al. (2010). "Axial and radial forces of cross-bridges depend on lattice spacing." PLoS Comput Biol **6**(12): e1001018.

Wolska, B. M. and D. M. Wieczorek (2003). "The role of tropomyosin in the regulation of myocardial contraction and relaxation." Pflugers Arch **446**(1): 1-8.

Xu, C., R. Craig, et al. (1999). "Tropomyosin positions in regulated thin filaments revealed by cryoelectron microscopy." Biophys J **77**(2): 985-92.

Yu, L. C., A. C. Steven, et al. (1985). "Distribution of mass in relaxed frog skeletal muscle and its redistribution upon activation." Biophys J **47**(3): 311-21.

Zhao, Y. and M. Kawai (1994). "Kinetic and thermodynamic studies of the cross-bridge cycle in rabbit psoas muscle fibers." Biophys J **67**(4): 1655-68.

Zimmer, H. G. (2002). "Who discovered the Frank-Starling mechanism?" News Physiol Sci **17**: 181-4.

Zot, H. G. and J. D. Potter (1982). "A structural role for the Ca2+-Mg2+ sites on troponin C in the regulation of muscle contraction. Preparation and properties of troponin C depleted myofibrils." J Biol Chem **257**(13): 7678-83.

VITA

NAME: Ryan Daniel Mateja

EDUCATION: B.S., Kinesiology, University of Illinois at Chicago, Chicago IL, 2005

Ph.D., Physiology and Biophysics, University of Illinois at Chicago, Chicago IL, 2013

PROFESSIONAL MEMBERSHIP: Biophysical Society

ABSTRACTS: Mateja RD, de Tombe PP. Length dependent activation develops virtually instantaneously (<5ms) in Guinea pig myocardium Biophysical Journal, Feb 2011 Poster presented at the 2011 Annual Biophysical Society meeting, Baltimore MD.

Mateja RD, de Tombe PP. Rate of Myofilament Length Dependent Activation in Guinea-Pig Single Myofibrils Biophysical Journal, Feb 2010 Poster presented at the 2010 Annual Biophysical Society meeting, San Francisco, CA

Mateja RD, de Tombe PP. Activation and Relaxation Kinetics in Isolated Guinea-Pig Myofibrils: Impact of Sarcomere Length Biophysical Journal, Volume 96, Issue 3, Supplement 1, February 2009 - Poster presented at the 2009 Annual Biophysical Society meeting, Boston MA

PUBLICATIONS: Mateja, RD and de Tombe PP (2012). Impact of titin isoform on length dependent activation and cross-bridge cycling kinetics in rat skeletal muscle. *BBA- Molecular Cell Research*. In Press

Mateja, RD and de Tombe PP. Myofilament Length-Dependent Activation Develops within 5 ms in Guinea-Pig Myocardium. *Biophysical journal* 103(1): L13-L15.

de Tombe PP, Mateja RD, Tachampa K, Mou YA, Farman GP, Irving TC. Myofilament length dependent activation. *Journal of Molecular and Cellular Cardiology*. 48(5):851-8, 2010

Farman GP, Tachampa K, Mateja R, Cazorla O, Lacampagne A, de Tombe PP. Blebbistatin: use as inhibitor of muscle contraction. *Pflügers Archiv*. 455(6):995-1005, 2008

Hornberger TA, Mateja RD, Chin ER, Andrews JL, Esser KA. Aging does not alter the mechanosensitivity of the p38, p70S6k, and JNK2 signaling pathways in skeletal muscle. *Journal of Applied Physiology*. 98(4):1562-6, 2005